

UNIVERSITÉ DE MONTRÉAL

**RETINAL OPTICAL IMAGING OF INTRINSIC  
SIGNALS**

AZADEH NADERIAN

INSTITUT DE GÉNIE BIOMÉDICAL

DÉPARTEMENT DE PHARMACOLOGIE ET PHYSIOLOGIE

FACULTÉ DE MÉDECINE

UNIVERSITÉ DE MONTRÉAL

THÈSE PRÉSENTÉE EN VUE DE L'OBTENTION

DU DIPLÔME DE PHILOSOPHIÆ DOCTOR

(GÉNIE BIOMÉDICAL)

NOVEMBRE 2017

## **DEDICATION**

To my lovely Maman, Baba, Ghazal & Majid ...

## **ACKNOWLEDGMENTS**

I would like to express my sincere gratitude to my Ph.D. advisor professor, Dr. Christian Casanova for his patience, guidance, and support. I appreciate your understanding and considerations. With your busy schedule as the director of the school, you have put the time to listen to me with patience and understanding whenever I have needed. I would also like to express my appreciation and thanks to my co-advisor professor, Dr. Frederic Lesage. Your motivation, calmness and positive personality not only helped me a lot during my research but also inspired me as a person. I have learned a lot from the positive and supportive ambiance of your laboratory in the months that I had the chance to work at Polytechnique.

My sincere thanks to Dr. Sébastien Thomas for his supervision, help, advice and prompt corrections.

I would especially like to thank Dr. Samuel Bélanger for his help and many insightful discussions and suggestions. Special thanks to Bruno Oliveira for all his help in the lab as well as his motivation, enthusiasm, and patience in trying new things. My appreciation to Genviève Cyr, for her valuable technical assistance.

I would also like to sincerely thank all my labmates of my both labs in UdeM and Polytechnique who ease the difficulties of research by their support and scientific discussions. I wish you all the best.

I gratefully thank all of my friends in the student office who made the bureau my second home, especially Robyn who with her presence brought color and energy to our office. I also appreciate her language corrections for my thesis.

The most important of all in the world I thank my parents. Whatever I have in my life is because of their unconditional love and support. Your prayer for me was what sustained me thus far. And all my efforts in life is because of your love and happiness.

The greatest thanks to my dearest sister and best friend, Ghazal. You have supported me through many ups and downs during last three years. Your kind and helpful hand always brought me out of all the difficulties.

The best thing that happened to me during my study was to get to know my beloved husband, Majid during my stay in Polytechnique. Your presence, love, and support during the last year of my study gave me lots of motivation to continue.

## Résumé

**Mots-clés:** rétine, imagerie intrinsèque, modèle animal, conception d'appareillage, système imagerie, électrorétinogramme, photorécepteurs, cellules bipolaires, cellules ganglionnaires.

Une méthode relativement récente qui est utilisée pour étudier l'activité neuronale de façon indirecte désigne l'imagerie optique des signaux intrinsèques. Cette méthode a d'abord été utilisée afin de visualiser l'activité corticale. L'imagerie optique intrinsèque mesure les variations de réflectance de la lumière associées à l'activité du tissu nerveux. Les études au niveau cérébral ont montré que ces changements de réflectance sont attribuables à des changements de volume et de flot sanguin, du niveau d'oxygénation de sang (oxymétrie), et de la dispersion de la lumière. Similairement, les études sur l'application de cette méthode d'imagerie au niveau de la rétine montrent la présence de signaux intrinsèques pendant l'activité rétinienne. Cependant, il apparaît que les signaux intrinsèques observés dans la rétine ont leurs propres caractéristiques, étant donné la structure particulière de la rétine. L'origine anatomique de ces signaux intrinsèques est donc encore incertaine. L'imagerie optique intrinsèque rétinienne pourrait présenter un avenir prometteur pour le diagnostic de pathologies oculaires lors de tests cliniques. Toutefois, avant que cette technique puisse être utilisée en clinique, une connaissance détaillée des propriétés et de l'origine des signaux intrinsèques rétiniens est nécessaire.

Le premier but de ce projet est d'étudier les réponses intrinsèques rétiniennes pour déterminer les caractéristiques ainsi que l'origine anatomique. Afin d'atteindre cet

objectif un système imagerie rétinien (RFI), conçu pour l'œil humain est utilisé. Pour ce système, nous utiliserons le lapin comme modèle animal, car il a des yeux de grandeur comparable aux yeux humains. Plusieurs agents pharmacologiques ont été utilisés pour bloquer les différentes cellules de la rétine afin de déterminer l'origine du signal cellulaire intrinsèque dans lapin.

Le deuxième but de ce projet est de développer un système d'imagerie optique des signaux intrinsèques. Ce système est développé pour le modèle de rat. Un agent pharmacologique (Aspartate) est utilisé chez le rat afin de valider ce système imagerie.

Nos résultats indiquent que dans la rétine du lapin les cellules bipolaires sont les principales cellules à l'origine des signaux intrinsèques rétiniens. De plus environ 20% des cellules ganglionnaires jouent un rôle dans la genèse des signaux intrinsèques. Nos résultats indiquent aussi qu'il est possible de construire un système d'imagerie efficace pour des petits animaux comme le rat. Les données obtenues avec ce nouveau système confirment que la rétine interne est à l'origine des signaux intrinsèques rétiniens.

## **Abstract**

**Keywords:** retina, intrinsic imaging, animal model, equipment design, imaging system, electroretinogram, photoreceptors, bipolar cells, ganglion cells.

A relatively new method to study neural activity indirectly is optical imaging of intrinsic signals. This method was first used to visualize cortical activity. The intrinsic optical imaging measures the reflectance variations of light associated with the activity of nervous tissue. Brain studies have shown that these changes in reflectance are attributable to changes in volume, blood flow, blood oxygenation level (oximetry), and light scattering. Similarly, studies on the application of this imaging method to the retina show the presence of intrinsic signals during retinal activity. It appears that the intrinsic signals observed in the retina have their own characteristics, given the particular structure of the retina. The anatomical origins of these intrinsic signals are still uncertain. Retinal intrinsic optical imaging may provide a promising future for the diagnosis of eye diseases in clinical trials. Thus, before this technique can be used clinically, a detailed knowledge of the properties and origin of intrinsic signals are needed.

The first goal of this project is to study the retinal intrinsic responses to determine the characteristics and its anatomic origin. To achieve this aim, the retinal imaging system (RFI), designed for the human eye is used. For this system, we used the rabbit as the animal model because the size of their eyes is comparable to that of human. Several pharmacological agents have been used to block the different cells of the retina and to determine the origin of the intrinsic cellular signal in rabbits.

The second goal of this project is to develop an optical imaging system of intrinsic signals. This system was designed for the rat animal model. A pharmacological agent (Aspartate) is used to validate this imaging system on rats.

Our results indicate that in rabbit bipolar cells are the main cells responsible for the intrinsic retinal signals. Also, approximately 20% of the Ganglion cells also show that 20% play a role in the genesis of intrinsic signals. Our results also indicate that it is possible to construct an efficient imaging system for small animals such as rats. The data obtained with this new retinal imager confirm that the inner retina is at the origin of intrinsic retinal signals.

# Table of contents

DEDICATION .....	II
ACKNOWLEDGMENTS .....	III
RÉSUMÉ .....	V
ABSTRACT.....	VII
TABLE OF CONTENTS.....	IX
LIST OF TABLES .....	XII
LIST OF FIGURES.....	I
LIST OF ACRONYMS AND ABBREVIATIONS .....	II
CHAPTER 1.....	1
INTRODUCTION.....	1
<b>1. THE RETINA.....</b>	<b>3</b>
1.1 PHOTORECEPTORS .....	5
1.1.1 <i>Rods and cones</i> .....	6
1.2 BIPOLAR CELLS.....	8
1.3 HORIZONTAL CELLS.....	10
1.4 AMACRINE CELLS.....	10
1.5 INTERPLEXIFORM CELLS.....	11
1.6 GANGLION CELLS.....	11
<b>2. THE NEUROTRANSMITTERS OF THE RETINA .....</b>	<b>14</b>
<b>3. PHARMACOLOGICAL DISSECTION OF RETINAL PATHWAYS .....</b>	<b>16</b>
<b>4. ANIMAL MODELS USED IN THIS STUDY .....</b>	<b>18</b>
4.1 THE RETINA OF RABBIT .....	18
4.2 THE RETINA OF THE RAT.....	20
<b>5. ELECTRORETINOGRAM (ERG).....</b>	<b>22</b>
5.1 ORIGIN OF FLASH ERG COMPONENTS .....	24
<b>6. RETINAL IMAGING.....</b>	<b>27</b>
6.1 RETINAL VASCULATURE .....	27
6.2 OPTICAL IMAGING OF INTRINSIC SIGNALS.....	29
6.2.1 <i>The mechanism underneath the origin of intrinsic signals</i> .....	30
6.2.2 <i>The neurovascular coupling</i> .....	31
6.2.3 <i>The sources of intrinsic signal</i> .....	32
6.2.4 <i>The shape and time course of each signal</i> .....	34
6.2.5 <i>Spatial characteristic of intrinsic signals</i> .....	35
6.2.6 <i>The application of optical imaging of intrinsic signals</i> .....	35
6.3 RETINAL OPTICAL IMAGING OF INTRINSIC SIGNALS.....	37
<b>7. AIMS OF THE STUDY .....</b>	<b>39</b>

<b>CHAPTER 2 .....</b>	<b>41</b>
<b>ARTICLE 1: CELLULAR ORIGIN OF INTRINSIC OPTICAL SIGNALS IN THE RABBIT RETINA.....</b>	<b>41</b>
<b>ABSTRACT.....</b>	<b>42</b>
<b>1. INTRODUCTION .....</b>	<b>43</b>
<b>2. MATERIAL AND METHODS .....</b>	<b>45</b>
2.1 RETINAL INTRINSIC IMAGING AND STIMULUS PARAMETERS .....	46
2.2 EXPERIMENTAL PROTOCOL.....	47
2.3 IMAGE AND DATA ANALYSIS.....	48
2.4 ELECTRORETINOGRAM (ERG).....	48
2.5 INTRAVITREAL INJECTION.....	49
<b>3. RESULTS.....</b>	<b>50</b>
3.1 RIS BASIC CHARACTERISTICS .....	50
3.2 COMPARISON BETWEEN RIS AND ERG SIGNALS.....	51
3.3 ANATOMICAL ORIGIN OF RIS.....	52
3.3.1 <i>Control for intravitreal injections.....</i>	<i>52</i>
3.3.2 <i>Isolation of photoreceptor's activity.....</i>	<i>52</i>
3.3.3 <i>Injection of TTX, APB and PDA.....</i>	<i>53</i>
<b>4. DISCUSSION.....</b>	<b>55</b>
4.1 ON THE RELATION BETWEEN RIS AND ERG.....	55
4.2 INTERSPECIES DIFFERENCES IN RIS .....	57
<b>REFERENCES .....</b>	<b>61</b>
<b>FIGURES LEGENDS.....</b>	<b>65</b>
<b>SUPPLEMENTARY FIGURES.....</b>	<b>68</b>
<b>CHAPTER 3.....</b>	<b>80</b>
<b>ARTICLE 2: RETINAL OPTICAL IMAGING USING INTRINSIC SIGNALS IN RAT'S RETINA .....</b>	<b>80</b>
<b>ABSTRACT.....</b>	<b>81</b>
<b>1. INTRODUCTION .....</b>	<b>81</b>
<b>2. RESULTS .....</b>	<b>84</b>
<b>2.1 PART 1: OPTICAL DESIGN OF THE FUNDUS OPTICAL IMAGER OF INTRINSIC SIGNALS .....</b>	<b>84</b>
2.1.1 ZEMAX SIMULATION .....	85
2.1.2 OPTICAL SYSTEM ASSEMBLY .....	87
2.1.3 OPTICAL SYSTEM CHARACTERIZATION .....	88
<b>2.2 PART 2: VALIDATION OF THE OPTICAL SYSTEM .....</b>	<b>89</b>
2.2.1 EXPERIMENTAL SETUPS AND PROCEDURE .....	90
2.2.2 ANIMAL PREPARATION FOR IN-VIVO IMAGING.....	90
2.2.3 INTRAVITREAL INJECTION .....	91
2.2.4 ELECTRORETINOGRAMS (ERGs) RECORDINGS.....	92
2.2.5 IMAGING PROTOCOL.....	92
2.2.6 IMAGING RESULTS AND ANALYSES.....	93

2.2.7 IMAGING OF CONTROL RETINA AND ASPARTATE INJECTED RETINA WITH THE RETINAL FUNCTIONAL IMAGER .....	94
<b>3. DISCUSSION .....</b>	<b>96</b>
<b>REFERENCES .....</b>	<b>100</b>
<b>FIGURES .....</b>	<b>104</b>
<b>CHAPTER 4.....</b>	<b>110</b>
<b>1. DISCUSSION.....</b>	<b>110</b>
1.1 SUMMARY OF RESULTS .....	111
1.2 COMPARE & CONTRAST .....	112
1.3 TECHNICAL DIFFICULTIES .....	118
<b>2. PROSPECTIVE.....</b>	<b>121</b>
<b>REFERENCES .....</b>	<b>123</b>

## **List of tables**

Table 1-1: The various neurotransmitters found in mammalian retina (Kolb, 1995b). ....15

## List of figures

Figure 1-1: The structure of the retina. The image shows the arrangement of the retinal neuronal cells. The image is retrieved from: <a href="http://163.178.103.176/Fisiologia/neurofisiologia/Objetivo_3/Album/pages/7_09_jpg.htm">http://163.178.103.176/Fisiologia/neurofisiologia/Objetivo_3/Album/pages/7_09_jpg.htm</a> .....	4
Figure 2-1: The photoreceptors: Rods and cones: the 3 segment of the receptors (outer segment, inner segment and synaptic segment) is indicated in Rods and Cones. <a href="http://thebrain.mcgill.ca/flash/d/d_02/d_02_m/d_02_m_vis/d_02_m_vis.html">http://thebrain.mcgill.ca/flash/d/d_02/d_02_m/d_02_m_vis/d_02_m_vis.html</a> .....	5
Figure 3-1: Phototransduction. The process of phototransduction is shown in this figure in order from 1 to 4. Image from: <a href="http://openwetware.org/wiki/BIO254:Phototransduction">http://openwetware.org/wiki/BIO254:Phototransduction</a> .....	7
Figure 4-1: The ON and OFF pathway: The post-photoreceptor process is shown in the picture. The image is retrieved from: <a href="http://courses.washington.edu/psych333/handouts/coursepack/ch13Information_processing_in_retina">http://courses.washington.edu/psych333/handouts/coursepack/ch13Information_processing_in_retina</a> .....	9
Figure 5-1: The production of the action potential in the ganglion cells. Changes in glutamate release from bipolars cause changes in the membrane potential of the GCs and so it produce the action potential. The image is retrieved from: <a href="http://courses.washington.edu/psych333/handouts/coursepack/ch13-Information_processing_in_retina.pdf">http://courses.washington.edu/psych333/handouts/coursepack/ch13-Information_processing_in_retina.pdf</a> .....	13
Figure 6-1: The fundus image of (A) human (the image adapted from: <a href="https://en.wikipedia.org/wiki/Fundus">https://en.wikipedia.org/wiki/Fundus</a> (eye)), (B) rabbit (the image adapted from: <a href="http://www.medirabbit.com/EN/Eye_diseases/Clinical/Eye_diseases.htm">http://www.medirabbit.com/EN/Eye_diseases/Clinical/Eye_diseases.htm</a> ), and (C) rat (the image dapted from: <a href="https://www.youtube.com/watch?v=17HB50oHebk">https://www.youtube.com/watch?v=17HB50oHebk</a> ). ..	21
Figure 7-1: The ERG of the cat in response to the flash stimulus of 2 sec, modified from (I. Perlman, 1995). .....	23
Figure 8-1: The human ERG recording in scotopic and photopic condition using short stimuli of 10 microseconds. The a-wave and b-wave are illustrated in each condition. In photopic condition a flash of 2 db is used in the background of 30 cd/mm, and in the scotopic condition a flash of -4 db is used. ....	24
Figure 9-1: the optical absorption spectra of oxyhemoglobin in blue and deoxyhemoglobin in red. The figure adapted from: <a href="http://omlc.org/spectra/hemoglobin/">http://omlc.org/spectra/hemoglobin/</a> .....	33

## LIST OF ACRONYMS AND ABBREVIATIONS

This list presents in alphabetical order the abbreviations and acronyms used in the thesis as well as their meanings.

2-DG - 2-deoxyglucose

AMPA -  $\alpha$ -amino-3-hydroxy-5-methyl-4-isoxazolepropionic acid

APB - 2-amino-4-phosphonobutyrate

ATP - Adenosine triphosphate

CDEA - Comité de déontologie de l'expérimentation sur les animaux

cGMP - cyclic guanosine monophosphate

CW - corneal window

DBs - diffuse cone bipolar cells

DTLs - Dawson, Trick and Litzkow

ERG - electroretinogram

FWHM - full-width at half maximum

GABA - Gamma aminobutyric acid

GCs - Ganglion cells

HBR - deoxyhemoglobin

HCs - Horizontal cells

iGluR - ionotropic glutamate receptors

INL - inner nuclear layer

IPL - inner plexiform layer

ISCEV - The International Society for Clinical Electrophysiology of Vision

LED - light-emitting diode

LGN - lateral geniculate nucleus

mGluR6 - metabotropic glutamate receptors

OCT - optical coherent tomography

ONL - outer nuclear layer

OPL - outer plexiform layer

PDA - cis-2,3-piperidinedicarboxylic acid

PDE - phosphodiesterase

PhNR - photopic negative response

RIS - Retinal intrinsic signals

SEM - standard error by the mean

SLO - scanning laser ophthalmoscope

SNR - signal-to-noise ratio

TTX - tetrodotoxin

USAF - United States Air Force

# Chapter 1

## Introduction

The retina is a part of the central nervous system, and thus its mechanisms can serve as a model for neuronal mechanisms and interactions throughout the nervous system. It is accessible by different imaging methods through the transparent media of the eye. Having accurate methods to study the retina is of great importance for clinical studies either towards detecting retinal diseases or follow up of treatment methods. So, in general, understanding the functions and cellular mechanism of the retina is of great importance for neuroscientists, vision scientists, and clinicians.

Different methods are used to study the structure of the retina (for example through imaging techniques such as scanning laser ophthalmoscopy (SLO) (Sharp & Manivannan, 1997; Yannuzzi et al., 2004) and optical coherence tomography (OCT) (Chen et al., 2005; Costa et al., 2006; Kiernan, Mieler, & Hariprasad, 2010)), as well as to study the function of the retina (by electroretinogram recordings (Frishman, 2006; Hood et al., 2012; McCulloch et al., 2015)). Having high-resolution imaging of retinal function is desirable.

Optical imaging of intrinsic signals is a non-invasive method for assessing retinal function. Use of this imaging technique for the retina is relatively new, and it needs to be studied and characterized before being ready to be used in clinics and laboratories.

The present thesis aims to investigate and characterize retinal optical imaging of intrinsic signals via two independent studies. The first study had the aim to find the cellular origin

of intrinsic signals in the rabbit retina while the second study aimed to develop an optical imaging system adapted for small size eyes, namely the rat.

This thesis comprises four chapters. The first chapter will introduce the basic knowledge needed to understand and follow the study. To understand and characterize the retinal intrinsic signal accurately, revealed with optical imaging, we first need to know about the anatomy and physiology of the retina. The first part of the first chapter will cover this subject. Then in this chapter, the neurotransmitters of the retina will be presented. Knowing the neurotransmitters help us to choose more appropriately the pharmacological agents that we will use later during this study. These pharmacological agents will also be presented in this chapter. This chapter will also cover the basic knowledge about the optical imaging of the intrinsic signals, its principle, and its potential applications. Parallel to the optical imaging method I will always use ERG as a control method for measuring retinal activity during the study. Consequently, the ERG will also be presented in this chapter. The latter will end by introducing the aims of my study and the hypothesis for each aim.

The second chapter is the article written on the cellular origin of intrinsic signals in rabbit retina. It contains the methods used in the first study and the results obtained. The third chapter presents the second study, which is the development of an optical imaging system. This chapter will be presented as a methodological article. It explains in detail the method of constructing an optical imaging system adapted for the rat's eye. It also shows the result of using this optical retinal imager on the rat's retina. The fourth chapter contains the general discussion about the two studies of this thesis.

## **1. The Retina**

Once passing the different optical parts of the eye, the light encounters the retina where it is converted into neural signals.

The retina consists of three cellular layers: The outer nuclear layer (ONL) which includes the photoreceptors, the inner nuclear layer (INL) which contains bipolar cells, horizontal cells, amacrine cells and interplexiform cells, and the ganglion cells layer. Between these nuclear layers exist two synaptic layers: the outer plexiform layer (OPL) and the inner plexiform layer (IPL). Figure 1-1 shows the structure of the retina and the arrangement of the retinal neuronal cells. Each neuronal cell type is discussed in more details in the following section.

The human retina contains an avascular area in its central zone, called macula in which the fovea can be found in the center of this area. The fovea is highly concentrated in cone photoreceptors and is responsible for human's visual acuity and detailed vision (Yamada, 1969). In some other mammalian retinas, there is also a similar specialized region such as the area centralis in cats and visual streak, which is a long horizontal strip area, in rabbits (J. H. Prince, 1964; Yu & Cringle, 2004).

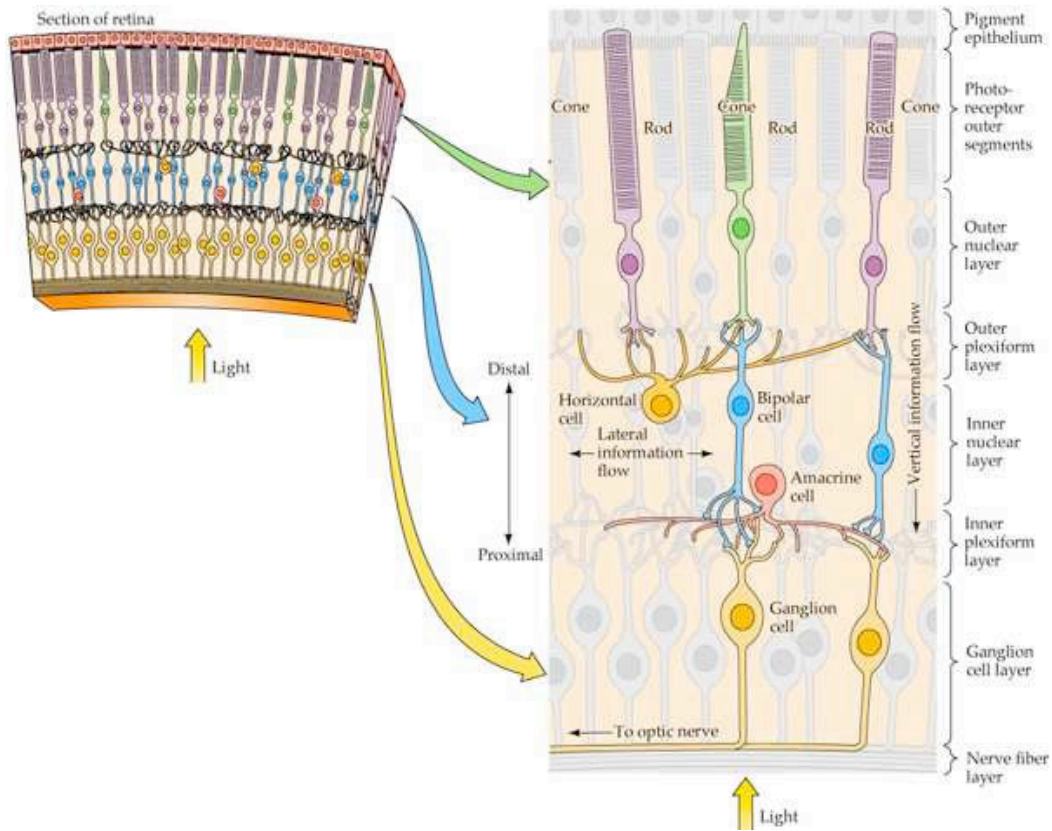


Figure 1-1: The structure of the retina. The image shows the arrangement of the retinal neuronal cells. The image is retrieved from: [http://163.178.103.176/Fisiologia/neurofisiologia/Objetivo\\_3/Album/pages/7\\_09\\_jpg.htm](http://163.178.103.176/Fisiologia/neurofisiologia/Objetivo_3/Album/pages/7_09_jpg.htm)

## 1.1 Photoreceptors

There are two types of photoreceptors: rods and cones. Traditionally, the shape of their outer segment differentiated each photoreceptor, but this criterion is not always reliable. The photoreceptors have various morphologies in different species. But, they are all composed of three separate segments. An outer segment which contains the visual pigments, an inner segment which contains the cell body, and a terminal which contains the synaptic ends and by which the photoreceptors connect to the bipolar cells and horizontal cells in the outer plexiform layer as shown in the figure 2-1.

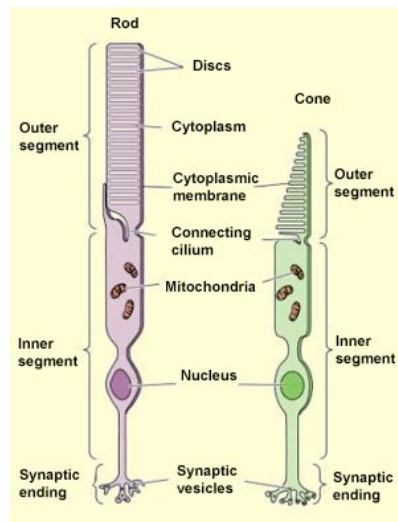


Figure 2-1: The photoreceptors: Rods and cones: the 3 segment of the receptors (outer segment, inner segment and synaptic segment) is indicated in Rods and Cones. [http://thebrain.mcgill.ca/flash/d/d\\_02/d\\_02\\_m/d\\_02\\_m\\_vis/d\\_02\\_m\\_vis.html](http://thebrain.mcgill.ca/flash/d/d_02/d_02_m/d_02_m_vis/d_02_m_vis.html)

### **1.1.1 Rods and cones**

Cones and rods operate at two different intensity levels. The cones are working under most conditions, or more precisely under any level of illumination where we can see distinct colors. Cones are responding fast, property, which becomes necessary where fast reactions are needed to survive. Also, they are sensitive to small changes in illumination (about 0.5 %) and can detect a contrast (Lamb, 2003). Cones need hundreds of photon hit per cone to be stimulated whereas rods are so sensitive that they can be stimulated by one or just a few photon. But they will be saturated in intense illumination, and it will take time for rods to recover after exposure to extremely intense illumination (Lamb, 2003).

Unlike rods, which contain a single photopigment, cones have three different photopigments that are present in the outer segment of the photoreceptors and have a different sensitivity to light of different wavelengths. There are three types of cones, responding to the blue (420nm), green (531nm) and red (588nm) regions of the spectrum (Purves D, 2001).

Phototransduction is the first essential step in vision. This process, which is done by photoreceptors, converts light into a neuronal signal. The activation of the photosensitive pigment activates the transducins which, through the activation of phosphodiesterases, hydrolyze the cGMP molecules, close the sodium channels, and hyperpolarize the photoreceptors. Figure 3-1 demonstrates the process of phototransduction in a rod photoreceptor (Kolb, 1995c; Lamb, 2003). The activation of a single rhodopsin molecule by a single photon is sufficient to cause a significant change in the membrane conductance due to amplifications present during the transduction cascade. A single

activated rhodopsin can cause the hydrolysis of more than 100,000 molecules of cGMP per second (Fu, 1995; Lamb, 2003).

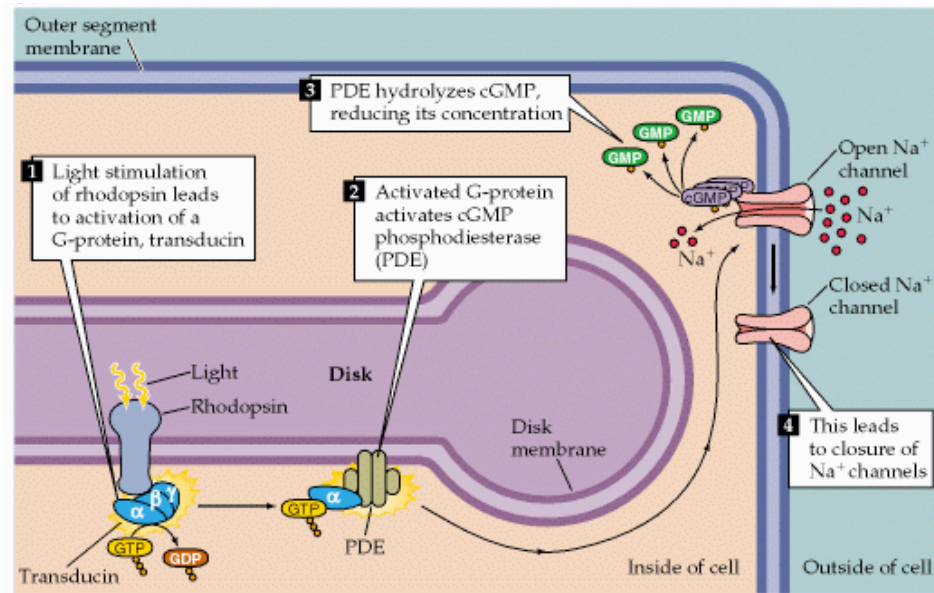


Figure 3-1: Phototransduction. The process of phototransduction is shown in this figure in order from 1 to 4. Image from: <http://openwetware.org/wiki/BIO254:Phototransduction>

In the dark, a steady current of mostly Na<sup>+</sup> (about 80%, also includes an approximately 15 % of Ca<sup>+</sup> and 5% of Mg<sup>+</sup>), called ‘dark current’, depolarizes the photoreceptors (Kolb, 1995c). The depolarized photoreceptors release the neurotransmitter, glutamate, to the second order neurons (bipolar cells and horizontal cells). In bright conditions, photoreceptors are hyperpolarized and therefore inhibit the release of glutamate.

After reaching photoreceptors in the outer plexiform layer, the visual signal splits into two pathways via the bipolar cells: ON, which detects objects lighter than the background and OFF, which detects objects darker than the background. These two pathways are shown in figure 4-1. The function of the bipolar ON and OFF are discussed in more detail in the following section.

## 1.2 Bipolar cells

In mammals, there are different types of bipolar cells (9 to 11 have been distinguished), which among them there are cells that connect to cones and others that connect to rods mariani

(Kolb, 1970; Mariani, 1984). The dendritic arbor of rod-related bipolars are usually larger than that of the cone-related bipolars since a single rod-bipolar may connect to as many as 30 to 50 rod terminals and a single cone-bipolar may connect to one or more (between five to seven) cone terminals (Dowling & Boycott, 1966; R. Nelson & Connaughton, 1995).

In the primate retina, different types of bipolar cells are present. The diffuse cone bipolar cells (DBs) receive the information from multiple cones and converge the information. The degree of converges ranges from 5 to 7 cones in the central retina to 14 to 20 in the peripheral retina (Mariani, 1981). Another type of bipolar cells, which are known as midget bipolar cells, is connected only to one cone. This kind of bipolar cell is found mostly in the central part of the retina (fovea). There are only cones present in this area, and a single cone in the fovea connects to both on and off bipolar cells (Dowling & Boycott, 1966). Another type of the bipolar cell known in primates is a blue-cone-specific type, which connects only to blue sensitive cones (Kolb, 1970; R. Nelson & Connaughton, 1995).

The bipolar cells respond in two different manners to the presence of light, depending on the type of glutamate receptors that they have. They are bipolar cells, similar to photoreceptors, which hyperpolarize in the light. These are OFF-center cells and are the

start of the off-center channel in the retina and then the visual pathways. These cells are driven via ionotropic (iGluR) AMPA-Kainate glutamate in their synapses with photoreceptors. The other group of the bipolar cell has metabotropic glutamate receptors (mGluR6). These cells depolarize in light, contrary to the photoreceptors, and are on the basis of the ON-center channel in the visual pathway (R. Nelson & Connaughton, 1995).

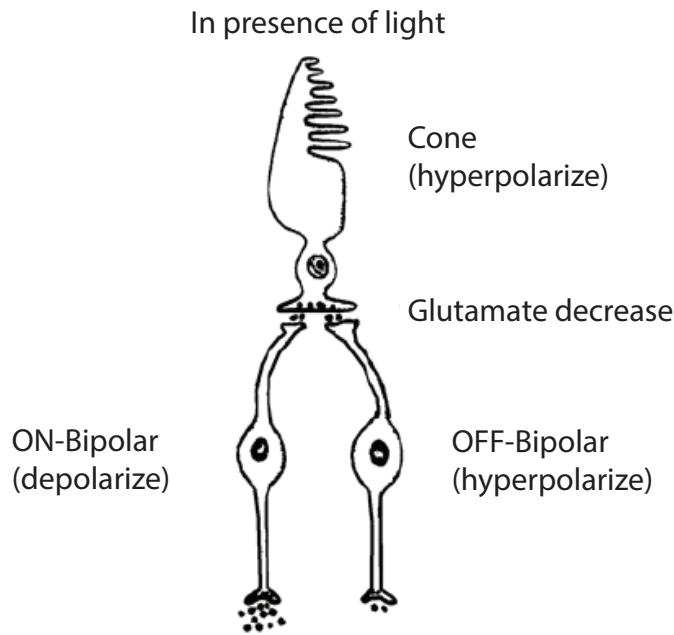


Figure 4-1: The ON and OFF pathway: The post-photoreceptor process is shown in the picture. The image is retrieved from: [http://courses.washington.edu/psych333/handouts/coursepack/ch13Information\\_processing\\_in\\_retina](http://courses.washington.edu/psych333/handouts/coursepack/ch13Information_processing_in_retina).

### **1.3 Horizontal cells**

There are two basic types of horizontal cells known in mammals: the A-type, which is an axonless cell, and the B-type, which is a cell containing an axon. In the presence of light, they hyperpolarize like photoreceptors, causing a feedback inhibitory signal to occur. This feedback signal provides a sum of information from a wide spatial area of the outer plexiform layer. Horizontal cells (HCs) receive their input from many photoreceptors cells, cones, and rods. They transmit a feedback signal, which alters the release of neurotransmitters from photoreceptors. This feedback organizes the center-surround receptive field of bipolar cells (Ido Perlman, Kolb, & Nelson, 2003). The horizontal cells have AMPA receptors. When in darkness, there is a continuous release of glutamate, which ultimately depolarizes these cells and renders them into an active state. In light conditions, the AMPA receptors deactivate, and the HCs hyperpolarize (Ido Perlman et al., 2003).

### **1.4 Amacrine cells**

This name was given by Cajal to signify that these cells have no axon. They are the most diverse of all the retinal cells. In mammals, there are 20 to 30 different types of amacrine cells (Masland, 2012). The two principal types of amacrine cell are diffuse and stratified. The diffuse cells process through the whole thickness of the inner plexiform layer, whereas the stratified amacrine cells process in one or few strata of the inner plexiform layer. There were also other classifications done after Cajal, based on the dendritic spread of the cells in one or several levels in the inner plexiform layer such as mono-, bi-, and

multistratified amacrine cells. Some amacrine cells are named based on the shape of their dendrite tree such as starburst, while others are named based on their neuroactive substance such as dopaminergic amacrine cells. Some cells are also appointed by non-descriptive titles such as A1, AII, and A17.

Amacrine cells are known to have also diversity in their functional role. It is thus difficult to name a general role for all the amacrine cells since each of the cells can have a different transmission of information through the retina.

One of the roles of amacrine cells is that they make a feedback connection to the bipolar cells in IPL. Thus, another center-surround mechanism is occurring in the IPL with the role of amacrine cells being somehow similar to that of horizontal cells in OPL. Most of the amacrine cells in mammals have inhibitory neurotransmitters GABA or Glycine (Kolb, 1995a, 1995d; MacNeil & Masland, 1998).

### **1.5 Interplexiform cells**

Interplexiform cells are believed to extend processes into both inner and outer plexiform layers of the retina. They also appear to carry information from inner to outer plexiform layers (Gallego, 1971). These cells were initially considered amacrine cells, however later they were found unique cells given their differences.

### **1.6 Ganglion cells**

Ganglion cells are post-synaptic to bipolar cells and amacrine cells. Similar to the amacrine cells, the ganglion cells can also be classified into two major groups based on

the morphology of their dendrites: stratified or diffuse and can be further sub-divided into small- and large-field, mono-, bi, and multistratified (Grunert, 2003; R. Nelson, 1995).

The ganglion cells can be divided into two major functional groups namely ON and OFF, which transfer the information about the light increment and decrement, as it is the case for bipolar cells. They also exhibit antagonistic surrounds. The ON ganglion cells and OFF ganglion cells are determined by the bipolar cells that contact with them (Kolb, 1995a).

The ON and OFF class of ganglion cells can be each divided into two main morphological type. In primates, those are the parvo (P) and magno (M) classes. The parvo cells (P-cells) are midget ganglion cells, and they project to the parvocellular layer of the lateral geniculate nucleus (LGN). They are known to transfer the visual information about form and color. The magno cells (M-cells) are parasol ganglion cells and project to the magnocellular layer of the LGN. They transmit visual information about motion and spatial relationship (Botir T. Sagdullaev, 2008).

In the central retina, the midget GCs are the major type of ganglion cells (about 70%). In the central retina which has the high resolution, a cone connects to two separate midget ganglion cells via an ON-bipolar cell and an OFF-bipolar cell (Boycott & Wassle, 1974; Kolb, Nelson, & Mariani, 1981).

About 10 % of the retinal ganglion cells are parasols and are receiving inputs from many bipolar cells (Dacey, 1993).

Ganglion cells produce action potentials and are the only cells in the retina that are doing so (apart from a few amacrine cells). However, they produce action potentials only when they receive sufficient glutamate from the bipolar cells. Changes in glutamate release

from bipolar cells cause changes in the membrane potential of the GCs and produce an action potential only when this change is enough to depolarize the ganglion cells to threshold (Dacey, 1993; Kolb, 1995a). The action potential is then transmitted to the brain by the axons of the optic nerve as is shown in figure 5-1.

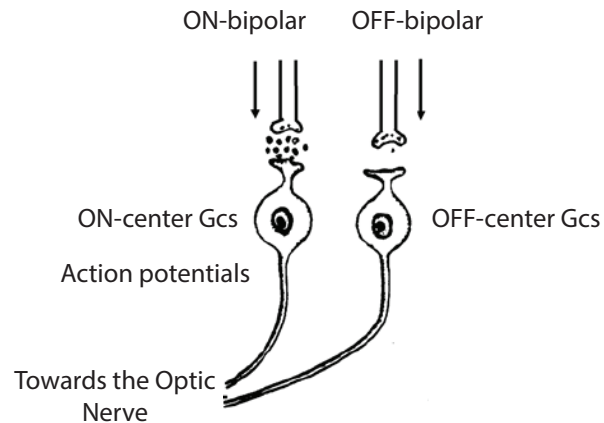


Figure 5-1: The production of the action potential in the ganglion cells. Changes in glutamate release from bipolars cause changes in the membrane potential of the GCs and so it produce the action potential. The image is retrieved from: [http://courses.washington.edu/psych333/handouts/coursepack/ch13-Information\\_processing\\_in\\_retina.pdf](http://courses.washington.edu/psych333/handouts/coursepack/ch13-Information_processing_in_retina.pdf)

## **2. The neurotransmitters of the retina**

The neurochemistry of the retina is complex and reflects the diversity of its cell constituents. The various neurotransmitters found in the mammalian retina are listed in Table 1 (Kolb, 1995b). As categorized earlier, the visual information is transferred to the brain through three major cells in the vertical pathway of the retina: photoreceptors, bipolar cells, and ganglion cells. The visual signals of the vertical pathway can then be altered by the cells in horizontal pathways at two levels: the outer plexiform layer via horizontal cells and the inner plexiform layer via amacrine and inner plexiform cells. All of these cells use different neurotransmitters (excitatory and inhibitory) to transfer visual information.

The major neurotransmitter of neurons in the vertical pathway is the excitatory amino acid glutamate (Connaughton, 1995; Thoreson & Witkovsky, 1999). The photoreceptors (rods and cones) release glutamate to transmit the signal to the second order neurons (bipolar cells and horizontal cells). In the second order neurons, this signal passes through two different types of sensory channels. One type of post synaptic receptor is the metabotropic glutamate channel (mGluR6) in ON- bipolar cells, and the other type is ionotropic in the OFF-bipolar cells via at least two types of AMPA receptors and Na ions (Connaughton, 1995; Thoreson & Witkovsky, 1999).

Glutamate is also known to be the neurotransmitter of the bipolar cells to transfer the visual signal to the third order neurons (Ganglion cells and amacrine cells) in the inner plexiform layer.

The two major inhibitory neurotransmitters in the retina are Gamma aminobutyric acid (GABA) and Glycine. Bipolar cells have receptors for GABA (A, B, and C type), dopamine (D1) and Glycine in the IPL. GABA is associated with many large field amacrine cells, and Glycine is associated in most of the small-field types of amacrine cells (Kolb, 1995b). There are also other neurotransmitter substances in the mammalian retina as shown in table 1.

Neurotransmitter	Amacrine cell type		
	rabbit	cat	primate
GABA		A2, A10, A13, A17, A19, A22, A20	same as cat
glycine	All DAPI-3	A3, A4 All A8	same as cat
acetylcholine	“starburst” Ca, Cb	“starburst” a-type, b-type	“starburst” a-type, b-type
dopamine	Toh-IR CA1, CA2, CA3	A18	CA-type1 CA-type2
serotonin	S1, S2	A20 and A22	A17
substance P	tri-stratified	A22	thomy 2
VIP	Tri-stratified		
somatostatin	association neuron long axon-like processes		
nitric oxide	NADPH-diaphorase cell		multiaxonal spiny

Table 1-1: The various neurotransmitters found in mammalian retina (Kolb, 1995b).

### **3. Pharmacological dissection of retinal pathways**

In our study, we will use different pharmacological agents to block the activity of various retinal cells and to explore the role of that particular cell type on the intrinsic signal captured in optical retinal imaging. So, in this section, I will present the pharmacological agents that will be used later in the study.

Since it is known that the neurotransmitter of the photoreceptors is L-Glutamate, using the agonists or antagonists of the L-glutamate can block the synaptic transmission from the photoreceptors and isolate the photoreceptors. Aspartate is an excitatory amino acid like glutamate, that when present in excess, can be toxic to retinal neurons. Aspartate can block the uptake of glutamate, thus saturate the synapses (Bloomfield & Dowling, 1985; Mosinger & Altschuler, 1985). It can be used to isolate the photoreceptors from other retinal cells.

2-amino-4-phosphonobutyrate (APB) is a glutamatergic receptor agonist. This agonist is shown to selectively block the transmission from photoreceptors to depolarizing bipolar cells (ON bipolars) while not affecting any other retinal neurons (Knapp & Schiller, 1984; Massey, Redburn, & Crawford, 1983; Slaughter & Miller, 1981).

To prevent the activity of the OFF pathway a glutamatergic receptor antagonist called PDA (cis-2,3-piperidinedicarboxylic acid) is used (Hare & Ton, 2002). Application of it blocks the transmission from photoreceptors to OFF bipolar cells and horizontal cells. In IPL it also blocks the transmission of both ON and OFF bipolar cells to amacrine cells

and ganglion cells (Massey & Miller, 1988). So the application of PDA results in the isolation of photoreceptors and ON bipolar cells.

Retinal ganglion cells generate action potentials in response to light stimuli. To block the voltage-gated sodium channel a highly specific blocker can be used called tetrodotoxin (TTX) (Narahashi, Moore, & Scott, 1964).

## **4. Animal models used in this study**

Choosing the animal species for retinal studies depends on several factors including similarity of the ocular structures to those of humans, availability, cost, simplicity for experimentation, and prior knowledge about retinal structure and function (A.Tsonics, 2008). Rabbits and rats are two animal models used in the present study.

In our first study, we used the rabbit as the animal model. Rabbits have big eyes, similar in size to the human eye and can easily be used for ophthalmic research. Although the rabbit eye has a poorly developed retinal vascular system, the structure of the retina is similar to that of other mammals and primates (A.Tsonics, 2008; Hughes, 1971).

For the second study, we used the rat as our animal model. Rats have a well-developed retinal vascular system, as with humans, with arteries and veins emerging radially from the optic disc. The retinal structure is also similar to humans, composed of three layers of nuclei, and two synaptic layers (A.Tsonics, 2008; Hughes, 1979).

In the following section, I will present the retinal structure of these two animal models in more details.

### **4.1 The retina of rabbit**

There is a lot of resemblance between the retinal elements of the rabbit and that of a rat or human. The rabbit retina also contains three nuclear layers: outer nuclear layer, inner nuclear layer and ganglion cells and two plexiform layers (inner and outer). The primary difference of the rabbit retina is the visual streak in the rabbit retina (Hughes, 1971).

The visual streak is the horizontal region parallel to the blood vessels and perpendicular to the fibers. The origin of the term visual streak is apparent from the band of high ganglion cell count running under the retinal blood vessels for most of the length of the retina. Although there is a change of the density of the ganglion cells along the length of the visual streak itself, the decline in density is most immediately noticeable in comparing the streak to the retina above or below of the streak (Caldwell & Daw, 1978; Hughes, 1971).

The number of the receptors also reveals the existence of a high density of photoreceptors in the area of visual streak. The slight excess of inner layer nuclei (bipolar cells, horizontal cells, and amacrine cells) over photoreceptors in this area indicates a lesser degree of convergence in the connection of the photoreceptors to the post-photoreceptors cells (Caldwell & Daw, 1978; Hughes, 1971). In the inner retina, the count ratio of the inner nuclear layer to the ganglion cells changes from a value of five at the streak to one of about 95 in the peripheral retina. All these cell connections and ratios reflect a different organization at the visual streak (J. H. Prince, 1964).

Another difference of the rabbit retina to the human retina is its vasculature. The retinal vasculature supplied by the central retinal artery and drained by several veins confines itself to a pair of wing shape areas that extend from the optic nerve head both medially and laterally (De Schaepdrijver, Simoens, Lauwers, & De Geest, 1989; Sugiyama, Bacon, Morrison, & Van Buskirk, 1992).

## **4.2 The retina of the rat**

The retina of the rat also consists of three nuclear layers. (1) Outer nuclear layer, which contains rod and cone photoreceptors. (2) Inner nuclear layer, which contains horizontal cells, bipolar cells, and amacrine cells. (3) Ganglion cells, and two plexiform layers: outer plexiform layer and inner plexiform layer (LeVere, 1978).

Analogous to the human retina, there is a vertical and horizontal organization within these retinal layers. The vertical organization involves the photoreceptors, which synapse with bipolar cells, and in turn synapse with ganglion cells. In the rat retina, there are two types of bipolar cells: I, and II. The Type I bipolar cells synapse with rod-type receptors and the Type II bipolar cells synapse with cone-type receptors (Leure-Dupree, 1974). There are four general types of ganglion cells observed in the rat retina, within the inner nuclear layer and the ganglion cell layer.

The horizontal organization of the rat retina is at two levels and involves the horizontal cells at the outer plexiform layer and the amacrine cells at the inner plexiform layer (Leure-Dupree, 1974). The horizontal cells provide a linkage between individual receptor units and the amacrine cells provide a similar function concerning bipolar cells and ganglion cells (Leure-Dupree, 1974; LeVere, 1978).

In the rat retina, the optic disk in which the optic nerve is formed is approximately 6.5 % of the diameter of the retina, and the blood vessels radiate equally from the optic disk. A fundus image of human, rabbit, and rat is shown in the figure 6-1.

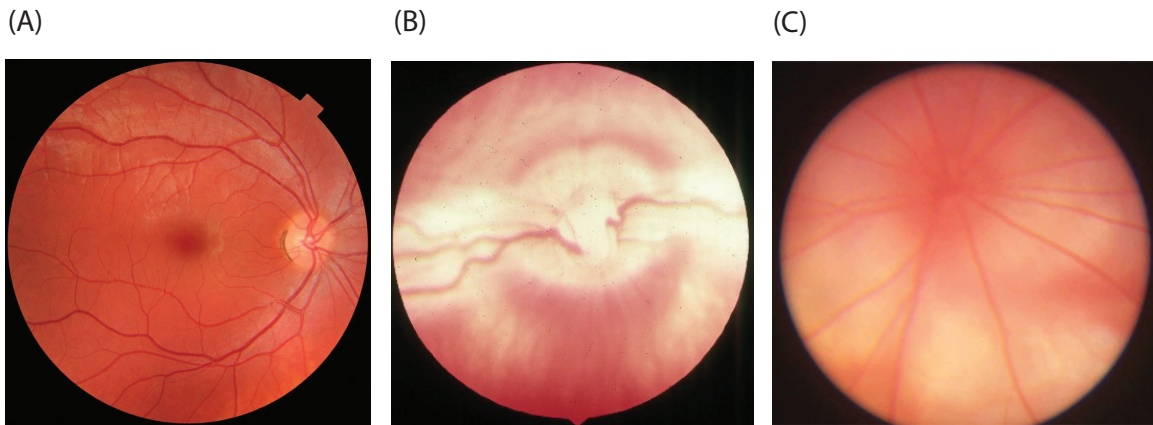


Figure 6-1: The fundus image of (A) human (the image adapted from: <https://en.wikipedia.org/wiki/Fundus> (eye)), (B) rabbit (the image adapted from: [http://www.medirabbit.com/EN/Eye\\_diseases/Clinical/Eye\\_diseases.htm](http://www.medirabbit.com/EN/Eye_diseases/Clinical/Eye_diseases.htm)), and (C) rat (the image daped from: <https://www.youtube.com/watch?v=17HB50oHebk>).

## **5. Electroretinogram (ERG)**

The electroretinogram (ERG) is a technique used to study the function of retinal cells in a clinic and laboratory setting. In our study, we have used ERG as a standard method to verify the activity of the retina in control retinas as well as in pharmacological injected retinas. So in this section, I will present the ERG waves and their cellular origins so that the result that will be present later become clearer.

Different types of ERGs test the function of the retina using the different stimuli such as full-field ERG, multifocal ERG or pattern ERG (Heckenlively & Arden, 2006), revealing the role of various cells and neurons in the retina.

The first published human ERG goes back to 1924 by Kahn and Löwentein, but it was not until almost a decade later that the improved techniques led to investigations about the components of the ERG by Granit (DeRouck, 2006). The synchronized activity of retinal cells, together with their structured organization creates currents large enough to be recorded from a distance at the cornea. One would expect that such currents reveal the activity of all retinal cells, but it is thought that the radial oriented cells such as photoreceptors, bipolar cells, and glial cells contribute predominantly to the ERG than the cells with a horizontal orientation such as horizontal cells and amacrine cells (Frishman, 2006).

Granit explained the appearance of different components in ERG as the results of three processes (or potentials): PI, PII, and PIII named by order of disappearance under anesthesia, these waves are shown in the figure 7-1. Granit indicated that the fast developing component PIII forms the a-wave. He also reported that the PII originate in

the second order neurons and probably by bipolar cells (DeRouck, 2006; I. Perlman, 1995). The cellular and neuronal origins of these potentials are explained further in this chapter.

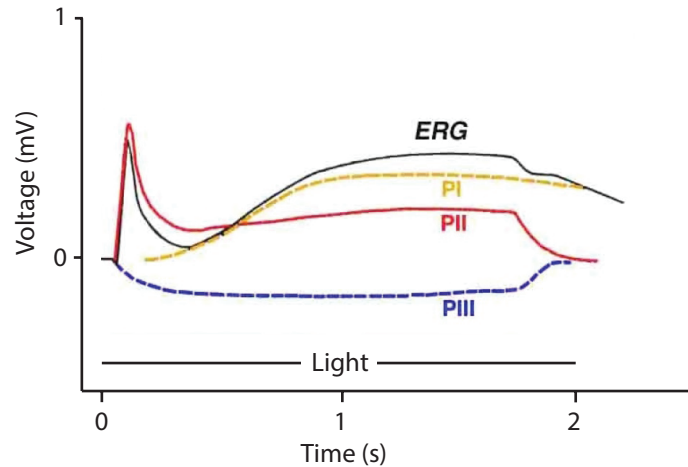


Figure 7-1: The ERG of the cat in response to the flash stimulus of 2 sec, modified from (I. Perlman, 1995).

The magnitude of the electrical signals in the ERG is influenced by stimulus condition and recording condition. In this regard, the ISCEV standards are internationally used to have comparable ERG recordings (Hood et al., 2012; McCulloch et al., 2015).

To register the electrical signal of the retina three electrodes are usually used: 1) The active electrode, that makes contact with the eye, and it exists in different forms such as contact lens with an integrated silver or gold disc electrodes or the microfiber electrodes, DTLs. 2) The reference electrode and 3) The ground electrode.

Different approaches such as intraretinal depth recording, site-specific lesion, pathology or targeted mutation and pharmacological dissection have been used over the years to determine the neuronal origin and cellular mechanism generating the ERG. In recent years, as more knowledge has been obtained about the retinal neurotransmitters and

microcircuitry, better pharmacological agents can be used to isolate different cell types and study their specific roles using ERG components.

### 5.1 Origin of flash ERG components

The ERG response to a flash of light includes positive and negative components originating from different stages of retinal processing. The ERG can be used to study the activity of cones and rods in different light conditions. In well-lit condition (photopic condition), to show cone dominated activities. In dark-adapted retina (in scotopic condition), to indicate rod-dominated activities. In low lighting (mesopic condition), which is a combination of photopic and scotopic condition to demonstrate the activities of a mixture of rods and cones. Figure 8-1 shows an example of the human ERG in photopic and scotopic conditions.

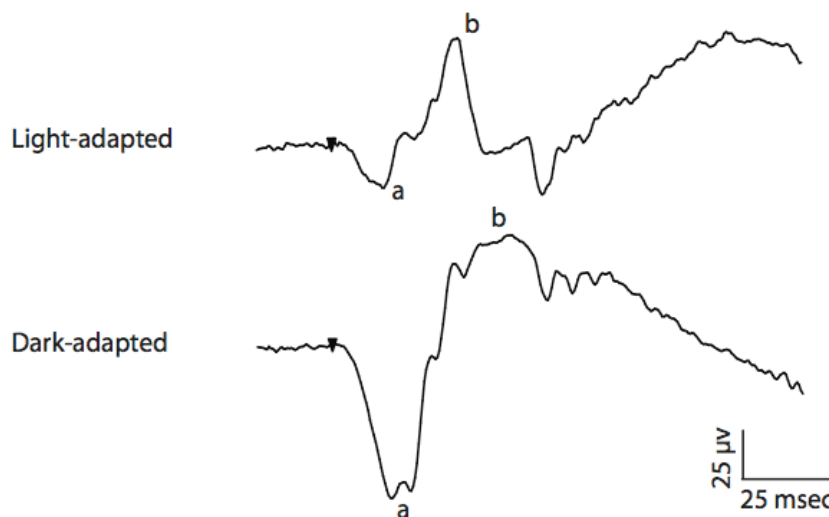


Figure 8-1: The human ERG recording in scotopic and photopic condition using short stimuli of 10 microseconds. The a-wave and b-wave are illustrated in each condition. In

photopic condition a flash of 2 db is used in the background of 30 cd/mm, and in the scotopic condition a flash of -4 db is used.

As it is shown in figure 8-1, the components of the photopic ERG are named as a- wave, b-wave. In the presence of longer stimuli another wave also appears, the d-wave (Sieving, 2006).

The a-wave is the leading part of the Granit's PIII. The studies using microelectrodes and also pharmacological dissection showed that the photoreceptors are at the origin of the a-waves in ERG (I. Perlman, 1995).

The b-wave is the largest component of the diffuse flash ERG, initially identified as the PII by Granit (Falk & Shiells, 2006; Frishman, 2006). Pharmacological studies showed that the b-wave is diminished by agents that interfere with the synaptic transmission from the photoreceptor to the second order neurons (Sillman, Ito, & Tomita, 1969). Also, the b-wave was observed to be intact in the ERG of patients or animal models experiencing degeneration of ganglion cells (Noell, 1954). Granit has suggested that the b-wave is caused by membrane depolarization (DeRouck, 2006) and this idea was supported by other studies (Falk & Shiells, 2006; Frishman, 2006). In the retina, the cell postsynaptic to the photoreceptors that are radially oriented and also depolarizes in the presence of a flash of light is the ON-bipolar cell. Although there is a contribution of the Müller cells in the b-wave, the pharmacological dissections by blocking ON bipolar cells indicate that the b-wave shows to a large degree the currents of the ON-bipolar cells (Knapp & Schiller, 1984; Massey et al., 1983).

The d-wave, which is observable during the long stimuli and at the time the stimulus turns OFF, reflects the transient depolarization of the hyperpolarizing cone bipolar cells

(the OFF-bipolar cells). The pharmacological studies that block the OFF pathway show the disappearance of the d-wave in the ERG (Hare & Ton, 2002; Horiguchi, Suzuki, Kondo, Tanikawa, & Miyake, 1998).

In the photopic ERG, there is also another component, which appears as a negative going wave after the b-wave and also after the d-wave for the long flashes, which is called, the photopic negative response (PhNR) (Frishman, 2006). The pharmacological studies that block the spiking activity of retinal ganglion cells show the disappearance of this negative wave and therefore prove that the activity of ganglion cells is at the origin of PhNR (Frishman, 2006; Hanazono, Tsunoda, Kazato, Tsubota, & Tanifuji, 2008; Hare & Ton, 2002).

## **6. Retinal imaging**

Retinal imaging can provide valuable data towards understanding how the eye and the visual system function. It also plays a significant role in the diagnosis of various medical conditions. Nowadays, there are different methods of ophthalmic and retinal imaging that are routinely used in clinics or laboratories such as optical coherent tomography (OCT), fluorescein angiography using either the fundus camera or the scanning laser ophthalmoscope (SLO).

Using the optical imaging of a retinal intrinsic signal is a relatively new method, which has a significant potential as a non-invasive method for assessing retinal functions in the human and in animals for clinics as well as in laboratories. The optical imaging of intrinsic signal is developed in brain imaging, and the precise and detailed description of it is highlighted in the following section.

### **6.1 Retinal vasculature**

We will see in the next section about the optical imaging of intrinsic signal that there is a vascular component considered as a source of the intrinsic signals. Before discussing optical imaging, some knowledge about the vasculature of the retina is required.

The retina is one of the most metabolically active tissue, consuming O<sub>2</sub> more rapidly than any other tissues, including the brain (Ames, 1992). It can vary according to the animal model, but generally, there are two separate vascular systems that bring oxygen and essential nutrients to the retina: retinal circulation and choroidal circulation. These two

networks of blood vessels have distinct physical and functional characteristics (Delaey & Van De Voorde, 2000; Wangsa-Wirawan & Linsenmeier, 2003).

The retinal circulation provides the oxygen of the inner retina and the choroidal circulation to the outer retina. Retinal circulation is characterized by low blood flow and high level of oxygen extraction (the artery-vein pO<sub>2</sub> difference is about 40%). In contrast, the choroidal circulation has very high blood flow but has a small capacity for extraction of oxygen (the artery-vein pO<sub>2</sub> difference is about 3%) (Alm & Bill, 1973; Tornquist & Alm, 1979). The choroidal circulation is controlled primarily by a sympathetic innervation and is not autoregulated. The retinal circulation, meanwhile, has no independent innervation. Thus, the arterial tone of the retina is influenced only by local factors such as changes in perfusion pressure, pO<sub>2</sub>, pCO<sub>2</sub> and pH (Delaey & Van De Voorde, 2000).

Another feature in the retinal circulation is the self-regulatory capacity that provides constant blood flow despite perfusion pressure changes (Dumskyj, Eriksen, Dore, & Kohner, 1996). This self-regulation is produced by metabolic mechanisms. Self-regulation can be described as the adaptation of the blood flow to the metabolic demands of the cells of the retina (Delaey & Van De Voorde, 2000; Dumskyj et al., 1996).

Studies in hypoxemia show that the retinal circulatory can increase blood flow by more than a factor of three during hypoxemia. In the outer retina, hypoxemia leads to a steep decrease in choroidal PO<sub>2</sub>. It occurs because the choroidal blood flow does not increase in hypoxemia (Wangsa-Wirawan & Linsenmeier, 2003).

## **6.2 Optical imaging of intrinsic signals**

Optical imaging of an intrinsic signal is one of the newest techniques for retinal imaging as it was first used for the imaging of cortical activity. The optical imaging of intrinsic signals was first developed by Grinvald et al. for mapping the cortical activity (Grinvald, Lieke, Frostig, Gilbert, & Wiesel, 1986). This technique measures the activity of the neurons indirectly, through activity-dependent changes in the optical property of tissues. By illumination of the exposed tissue (cortex, or retina) to a monochromatic light, optical imaging of the intrinsic signal detects the changes in light reflectance from the metabolically active tissue. The light reflection changes during neuronal activation due to changes in oxygen delivery and consumption in the active tissue as well as changes in the scattering property of the tissue. Although the changes of the optical properties of the brain tissue during neuronal activation has been known for many years (Cohen, 1973), it took about a decade until these features were used for imaging brain activity (Grinvald et al., 1986). Before the advent of optical imaging, the cortical function was studied mainly with electrophysiological techniques by using single or multi-units extracellular electrodes and through 2-deoxyglucose (2-DG) labeling (Zepeda, Arias, & Sengpiel, 2004). These techniques have limitations as being invasive and limited in space. For example, in the case of inserting electrodes in electrophysiology, we are spatially limited to the zone registered by the electrodes. Another example is in the 2-DG labeling that we are confined to the time that we have the glucose molecule in the imaging area. Intrinsic imaging does not use extrinsic substances like dyes, electrodes or radioactively labeled substances, which could damage the brain. Therefore this technique of imaging can

repeatedly be used on the same tissue. Optical imaging of intrinsic signals offers a high spatial resolution of the functional organization at the cortical level (Frostig, Lieke, Ts'o, & Grinvald, 1990). Optical imaging by the intrinsic signal can fill the gap between the single cell electrophysiology testing and the anatomical and histological methods of imaging.

Optical imaging can be used in different ways to visualize the tissue, to detect diseases at an early stage when they are still treatable. The advantage of being non-invasive makes this kind of optical imaging easy to use with a wide variety of experimental paradigms and stimulus configurations.

### **6.2.1 The mechanism underneath the origin of intrinsic signals**

To use optical imaging as a functional method of imaging, it is necessary to understand the mechanisms underlying the intrinsic signals and their relationship to the activation of the neurons. As mentioned earlier, the source of the intrinsic signals is composed of several activation processes correlated with the neuronal firing. These processes cause the change in optical property of the tissue, so they cause a change in light reflectance comparing to the not active state. At least three physiological parameters affect light reflection during neuronal activity: 1) Change in blood volume 2) The oximetry component (change in oxy/ deoxy-hemoglobin ratio) and 3) Light scattering (Frostig et al., 1990; Malonek et al., 1997; Malonek & Grinvald, 1996). The first two factors rely on the increase in metabolic demand of the active tissue. Modern imaging techniques have demonstrated that there is a strong coupling between neuronal activity, local metabolic activity and blood flow (Vanzetta & Grinvald, 2008). The third factor determines the

surface reflectance changes due to ionic and/ or water movement due to membrane conformation changes during neuronal activation (D. Ts'o et al., 2009; Zepeda et al., 2004).

### **6.2.2 The neurovascular coupling**

To sustain neuronal function the brain has evolved neurovascular mechanisms to provide the energy needed following neuronal activation. This mechanism causes changes in blood flow and volume in the regions where the neurons are active. This relationship between vascular changes and neuronal activity is known as neurovascular coupling (Vanzetta & Grinvald, 2008).

The neuronal activity uses energy and thus causes the hydrolysis of ATP. ATP is provided by the metabolism of glucose, which requires oxygen. The first studies to understand the mechanism of neurovascular coupling considered the primary source of oxygen as the oxy-hemoglobin molecules in the blood carried by capillaries to the active tissue. Therefore, during neuronal activation, there is a high demand for oxygen. In response to that demand, there is a flux of oxygen from the capillaries to the active tissue, which causes a highly localized increase in deoxy-hemoglobin concentration very early after the neuronal activity. This local rise in deoxy-hemoglobin leads to an increase in local blood flow and volume to bring more oxygen to the tissue, which is depleted from oxy-hemoglobin. This increase in oxyhemoglobin is usually less co-localized with the area of initial oxygen consumption (Vanzetta & Grinvald, 2008; Zepeda et al., 2004).

Besides the classical hypothesis that suggests a close relationship between neuronal activity and local hemodynamic responses (Vanzetta & Grinvald, 2008; Zepeda et al.,

2004), more recent studies suggest that the origin of the changes in blood flow and hemodynamic is not, at least initially, only dependent on local metabolic need due to neuronal activity (Hillman, 2014). This new hypothesis suggests that the neurovascular coupling is not just a supply to the demand during neuronal metabolism (Lindauer et al., 2010). A supporting statement for this theory is that the changes of blood flow generate excess in local oxygen, which is much more than the demand; therefore it suggests an indirect relationship between oxygen supply and demand. The other supporting statement is the time delay of the increased blood flow peak (about 3-5 seconds after stimulus onset) compared to neuronal activity. This time delay also confirms that the neurons do not rely on functional hyperemia for their initial needs in oxygen and glucose (Lindauer et al., 2010).

### **6.2.3 The sources of intrinsic signal**

One of the sources of the intrinsic signal as mentioned earlier is the oximetry component (change in oxy/ deoxyhemoglobin ratio). Light absorption and reflection are different in oxygenated and deoxygenated hemoglobin. So the change of the oxygen level in hemoglobin during neuronal activity can be monitored considering this characteristic. In the figure 9-1, the optical absorption of hemoglobin is shown.

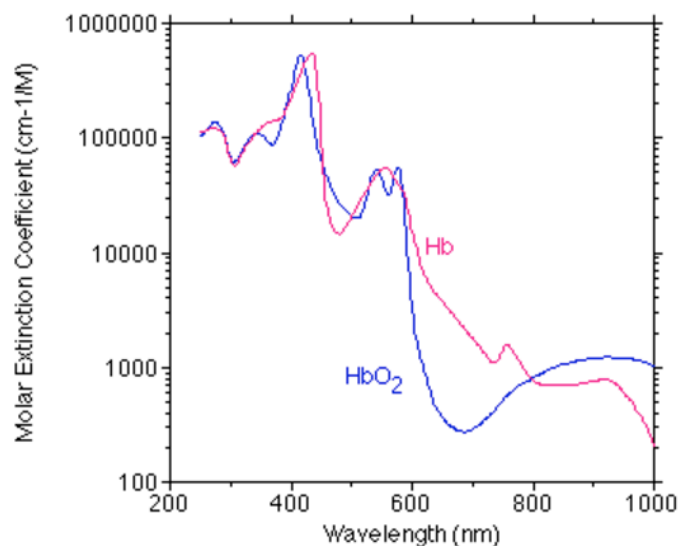


Figure 9-1: the optical absorption spectra of oxyhemoglobin in blue and deoxyhemoglobin in red. The figure adapted from: <http://omlc.org/spectra/hemoglobin/>.

As it is shown in figure 9-1, the absorption spectrum of hemoglobin has useful characteristics for functional imaging. There is a difference in absorption of light between oxygenated hemoglobin and deoxygenated hemoglobin in near-infrared wavelengths (between 600 nm and 800 nm). In this range of the spectrum, the deoxy-hemoglobin absorbs more and reflects less of the incident light. On the contrary, the oxy-hemoglobin absorbs less light. So this range of the spectrum is used for detection of oximetry change.

In the green wavelength (around 570 nm), the absorption of the oxy/deoxyhemoglobin is the same (termed isosbestic wavelength) and is therefore useful for detection of blood volume change. Frostig et al. have proved the dominance of blood volume change for the signals captured in 570 nm by injecting a fluorescent dye into the bloodstream of an animal, and compared the changes in the fluorescence signal excited at the hemoglobin isosbestic wavelength to the reflection signal in this wavelength range (Frostig et al.,

1990). Their experiment demonstrated that the blood volume changes following neuronal activation could yield a high-resolution functional map.

The light scattering component of the intrinsic signal comes from the scattering properties of the tissue. The presence of this signal following neuronal activity is due to the ion and water movement, expansion and contraction of the extracellular spaces, capillary expansion, or neurotransmitter release that together cause changes to the scattering properties of the tissue (Cohen, 1973). The light scattering signal can be obtained at any wavelength, although it is more pronounced in the near infrared range where the light penetration in the tissue is the greatest. So, for the wavelengths more than 630 nm, scattering becomes one of the significant sources of the intrinsic signal, and in the near-infrared region above 800 nm, it dominates the other sources of the intrinsic signals (Frostig et al., 1990).

#### **6.2.4 The shape and time course of each signal**

In summary, each mechanism at the origin of intrinsic signals have a distinct time course and can be isolated using an appropriate illumination wavelength. Light scattering is the first component that happens in the time since it is related to the activities associated with the changes in membrane potential (Stepnoski et al., 1991). The increase in light scattering reaches its maximum in 2-3 s of stimulus onset. The deoxy-hemoglobin component (the use of oxygen by the active tissue) is the next element, which peaks within 4-6 s after the stimulus onset. Oxyhemoglobin provided by an increase in blood volume rises even more slowly (Frostig et al., 1990; Zepeda et al., 2004).

Different sources of the intrinsic signal also create different shapes for the signal. At near infrared-light (600-800 nm), as explained earlier, the oxyhemoglobin is dominant, and the shape of the signal is biphasic. Following the activation, there is a decrease in reflection and an initial dip due to the high absorption of deoxyhemoglobin. It is followed by an increase in the reflection due to the increase in blood flow and a significant amount of oxygenated hemoglobin.

### **6.2.5 Spatial characteristic of intrinsic signals**

The intrinsic signal can be used for functional mapping of the cortex using different wavelengths. Although using different wavelength for imaging gives us different spatial resolution (Frostig et al., 1990; Malonek et al., 1997). The higher spatial resolution is obtained with a wavelength of 600-630 nm, which is the first vascular response, considering the initial phase (usually the negative phase) of the intrinsic response (Malonek & Grinvald, 1996). The secondary vascular response (such as the increase in blood flow and blood volume) offers a lower spatial resolution comparing to the HbR component. Scattering reflects changes at the cell level, so it is more localized to the cell origin of the activation than the hemoglobin molecules. However, this signal has a relatively small amplitude compared to the other components of the intrinsic signals.

### **6.2.6 The application of optical imaging of intrinsic signals**

The first application of the optical imaging of intrinsic signals was to understand the functional architecture of the visual cortex (of rat and monkey) (Frostig et al., 1990;

Grinvald et al., 1986; D. Y. Ts'o, Frostig, Lieke, & Grinvald, 1990). Now, this method of imaging has an important role in studying the functional activity of other areas of the brain such as the motor, somatosensory, auditory cortices and the olfactory bulb. Also, this method of imaging is used to investigate the functional cortical development under normal and pathological conditions (Grinvald, Frostig, Siegel, & Bartfeld, 1991; Martin, Martindale, Berwick, & Mayhew, 2006; Roe, 2007).

Optical imaging of intrinsic signals using infrared light is also used to study the neuronal function of the retina (Hanazono et al., 2007; J. Schallek, Li, et al., 2009; Tsunoda et al., 2009).

The optical imaging of intrinsic signals as a technique provides functional information within cortical areas and retina. The other advantages of this technology are its relatively high spatial resolution, its affordability, and its flexibility, including the ease of incorporation into a wide variety of experimental paradigms and stimulus configurations.

### **6.3 Retinal optical imaging of intrinsic signals**

Several groups have studied the origins and characteristics of retinal intrinsic signals (RIS) in both in-vivo (Hanazono et al., 2008; Hanazono et al., 2007; Inomata et al., 2008; Mihashi et al., 2011; J. B. Schallek, McLellan, Viswanathan, & Ts'o, 2012; J. Schallek, Li, et al., 2009; J. Schallek & Ts'o, 2011; D. Ts'o et al., 2009; Tsunoda, Oguchi, Hanazono, & Tanifuji, 2004) and in-vitro experiments (Y. C. Li et al., 2010). Two collective conclusions can be drawn from these studies. First, there is a high spatial correspondence between the localization of intrinsic signals and stimulation loci, suggesting that they reflect the activity of retinal neurons. Second, RIS is constituted of distinct temporal components that are cell-type and topographically precise. For example in non-human primates (Tsunoda et al., 2009), RIS result from the combination of both fast and slow kinetics components. Further, the RIS time course, shape, and origin vary according to the portion of the retina that is stimulated. Studies have suggested that the photoreceptors are responsible for the fast component and that the slow component arises from the inner retina, mostly from ganglion cells (Y. C. Li et al., 2010; Tsunoda et al., 2009).

In the cat, by examining RIS in response to stimuli of different spatial frequencies, it was demonstrated that RIS reflect not only the activity of the photoreceptors but also the activity of the inner part of the retina (Hirohara et al., 2013). However, in the same animal species, Schallek et al. (J. Schallek, Kardon, et al., 2009) investigated the cellular origin of RIS through the use of pharmacological agents and, contrary to what was

reported in other species (Hanazono et al., 2007; Tsunoda et al., 2009; Zhang et al., 2012) they concluded that photoreceptors were the only cells responsible for RIS.

Notwithstanding the numerous studies on RIS, there is yet no consensus regarding the anatomical origins of these signals.

## **7. Aims of the study**

In this study, we followed two distinct aims in retinal optical imaging of intrinsic signals: The first objective is to characterize the intrinsic optical signals in the retina of rabbit and to understand the anatomical origin of these intrinsic signals. I hypothesize that the intrinsic signals are dynamic and depend on the stimulation condition. Also, I have the hypothesis that the anatomical origin of retinal intrinsic signals is in the outer retina as Schalleck et al. found in the cat (J. Schalleck, Kardon, et al., 2009). To achieve this aim, we use a retinal functional imager with illumination light in near-infrared light. The rabbit will be utilized as the animal model since it has big eyes comparable to the size of the human's eyes, and so we can use the camera designed for human, for the rabbit's eyes. Specific pharmacological agents will be used to block the activity of each cell type in the retina of the rabbit to reveal their contribution to the intrinsic signal and so to find out the anatomical origin of the retinal intrinsic signals in the rabbit. The complete method, as well as the results obtained, are presented in detail in the first article presented in the next chapter.

Our focus in the second part of the study is on the development of a retinal functional imager adapted for animals with small eyes; we chose rat for this objective. In this regard, we have the aim to simulate the optical pathway of the optical imager and verify different part of it. Once the proper optical elements are chosen, we have the aim to provide the selected items to build the functional imager. We have the idea that this optical imager system using near-infrared light can capture the intrinsic signals from the rat retina and so

can be used further for the functional studies of the rat's retina. The details of the optical design and the results of imaging with this system are presented in the second article in chapter 3.

## Chapter 2

### **Article 1: Cellular Origin of Intrinsic Optical Signals in the Rabbit Retina**

A. Naderian<sup>1</sup>, L. Bussi eres<sup>1</sup>, S. Thomas<sup>1</sup>, F. Lesage<sup>2</sup>, C. Casanova<sup>1\*</sup>

<sup>1</sup>School of Optometry, Universit e de Montr al, CP 6128 succursale centre-ville, Montreal, Quebec, Canada

<sup>2</sup>Department of Electrical Engineering,  cole Polytechnique, CP 6079 succursale centre-ville, Montreal, Quebec, Canada

**Running title:** Intrinsic signals in the rabbit retina

**Keywords:** imaging, bipolar cells, photoreceptors, ganglion cells, electroretinogram.

\* Corresponding author:  
Christian Casanova  
School of Optometry  
Universit e de Montr al  
CP 6128, Succ Centre-Ville  
Montr al, Qu bec  
Canada, H3C-3J7

Tel: (514)-343-6948  
Fax: (514)-343-2382  
e-mail : [christian.casanova@umontreal.ca](mailto:christian.casanova@umontreal.ca)

## **Abstract**

Optical imaging of retinal intrinsic signals is a relatively new method that provides spatiotemporal patterns of retinal activity through activity-dependent changes in light reflectance of the retina. The exact physiological mechanisms at the origin of retinal intrinsic signals are poorly understood and there are significant inter-species differences in their characteristics and cellular origins. In this study, we re-examined this issue through pharmacological dissection of retinal intrinsic signals in the rabbit with simultaneous ERG recordings. Retinal intrinsic signals faithfully reflected retinal activity as their amplitude was strongly associated with stimulation intensity ( $r^2=0.85$ ). Further, a strong linear relation was found using linear regression ( $r^2=0.98$ ) between retinal intrinsic signal amplitude and the ERG b wave, which suggests common cellular origins. Intravitreal injections of pharmacological agents were performed to isolate the activity of the retina's major cell types. Retinal intrinsic signals were abolished when the photoreceptors' activity was isolated with aspartate, indicative that they are not at the origin of this signal. A small but significant decrease in intrinsic response (20%) was observed when ganglion and amacrine cells' activity was inhibited by TTX injections. The remaining intrinsic responses were abolished in a dose-dependent manner through the inhibition of ON-bipolar cells by APB. Our results indicate that, in rabbits, retinal intrinsic signals reflect stimulation intensity and originate from the inner retina with a major contribution of bipolar cells and a minor one from ganglion or amacrine cells.

## **1. Introduction**

Recent advances in imaging techniques; such as scanning laser ophthalmoscopy (SLO) (Sharp & Manivannan, 1997; Yannuzzi et al., 2004) and optical coherent tomography (OCT) (Chen et al., 2005; Costa et al., 2006; Kiernan et al., 2010) have provided clinicians and researchers the means to reveal the structure of the retina at a very high spatial resolution. While these techniques have the potential to detect anatomical changes associated with retinal diseases, they do not provide functional assessments of retinal activity. Therefore, medical investigation of retinal integrity often requires the use of complementary functional techniques. As such, the electroretinogram (ERG) is the most frequently employed method to study retinal function, both in clinical settings and research laboratories (Heckenlively & Arden, 2006). However, ERG recordings typically reflect the activity of relatively large volumes of retinal cells and are thus characterized by a coarse spatial resolution. Hence, both the clinical and research communities could potentially benefit from the development of higher resolution retinal functional assessment techniques.

Optical imaging of intrinsic signals is a technique that measures activity-dependent changes in intrinsic optical properties of a tissue (Grinvald et al., 2004; Grinvald et al., 1986) and it has been successfully used to reveal anatomo-functional maps of the cortex (Grinvald et al., 1986; Zepeda et al., 2004). Pioneering experiments have demonstrated that intrinsic signals can also be captured in the retina and generated hope that this non-invasive technique may be used as an anatomo-functional diagnosis tool in the near future

(Hanazono et al., 2008; Hanazono et al., 2007; Inomata et al., 2008; J. B. Schallek et al., 2012; J. Schallek, Li, et al., 2009; J. Schallek & Ts'o, 2011; D. Ts'o et al., 2009; Tsunoda et al., 2004). Indeed, optical imaging of retinal intrinsic signals (RIS) may enable the detection of functional disorders before the emergence of symptomatic or anatomical changes in the retina.

Several groups have studied the origins and characteristics of intrinsic signals in the retina in both *in vivo* (Hanazono et al., 2008; Hanazono et al., 2007; Inomata et al., 2008; Mihashi et al., 2011; J. B. Schallek et al., 2012; J. Schallek, Li, et al., 2009; J. Schallek & Ts'o, 2011; D. Ts'o et al., 2009; Tsunoda et al., 2004) and *in vitro* experiments (Y. C. Li et al., 2010). Two collective conclusions can be drawn from these studies. First, there is high spatial correspondence between the localization of intrinsic signals and stimulation loci, suggesting that they reflect the activity of retinal neurons. Second, RIS are constituted of distinct temporal components that are cell-type and topographically specific. For example, in non-human primates (Ivo Vanzetta, 2014; Tsunoda et al., 2009), RIS result from the combination of both fast and slow kinetics components. Further, the RIS time course, shape and origin vary according to the portion of the retina that is stimulated. Studies have suggested that the photoreceptors are responsible for the fast component and that the slow component arises from the inner retina, mostly from ganglion cells (Y. C. Li et al., 2010; Tsunoda et al., 2009).

In the cat, by examining RIS in response to stimuli of different spatial frequencies, it was demonstrated that RIS reflect not only the activity of the photoreceptors but also the activity of the inner part of the retina (Hirohara et al., 2013). However, in the same animal species, Schallek et al. (J. Schallek, Kardon, et al., 2009) investigated the cellular

origin of RIS through the use of pharmacological agents and, contrary to what was reported in other species (Hanazono et al., 2007; Tsunoda et al., 2009; Zhang et al., 2012), concluded that photoreceptors were the sole cells responsible for RIS.

Notwithstanding the numerous studies on RIS, there is yet no consensus regarding the anatomical origins of these signals. In this study, we re-examined this issue through the pharmacological dissection of RIS and simultaneous ERG recordings in the rabbit. This animal model was chosen for both phylogeny and practical reasons. Practically, the size of the rabbit eye is comparable to the human eye, thus facilitating experimental manipulations and enabling the use of equipment calibrated for human eye imaging. In addition, data on RIS from the lagomorph order would supplement the available data from primates and carnivores and further highlight the differences and similitudes in RIS among mammals.

Our results indicate that retinal intrinsic signals are activity-dependent signals. Concomitant ERG recordings showed that RIS amplitude tightly co-varied with the b-wave amplitude. Through sequential intravitreal injections of cell-type specific inhibitors, we observed a dominant impact of the activity of bipolar cells and a minimal influence of ganglion cells and/ or amacrine cells on the generation of RIS in the rabbit.

## **2. Material and Methods**

Experiments were performed on Dutch Belt (n=34, 1-2.5 kg, Covance, NJ, United States) and Polish Dwarf hutch rabbits (n=7, 1-2.5 kg, Aubin, QC, Canada). Data from both breeds were pooled together since the two samples were not statistically different.

Seventeen animals were used to study the effects of stimulus intensity and 22 animals were used for pharmacological experiments (see below). The animals were treated according to the guidelines of the Canadian Council on Animal Care and in accordance with the Code of Ethics of the World Medical Association. The experimental protocol was accepted by the Animal Ethics Committee of the Université de Montréal. All efforts were made to minimize any discomfort of the animals.

Animals were pre-medicated by the subcutaneous injection of glycopyrolate (0.1 mg/kg) to reduce tracheal secretions, and Atravet (0.5 mg/kg), a muscle relaxant. Thirty minutes later, animals were anesthetized by an intramuscular injection of a mix of ketamine (30 mg/kg) and xylazine (5 mg/kg). After tracheotomy, animals were transferred into a stereotaxic apparatus, immobilized by a gallamine perfusion (10 mg/kg/h for a solution of 2%) and artificially ventilated by a respiratory pump. During the experiments, anesthesia was maintained under isoflurane (1%) in a mixture of O<sub>2</sub> (30%) and N<sub>2</sub>O (70%). Pupils were dilated with eye drops of 1% tropicamide and 2.5% phenylephrine hydrochloride. Corneas were protected against dryness by contact lenses and periodic applications of artificial tears. Body temperature was maintained between 37-39 °C using a feedback-controlled heating blanket (Homeothermic Blanket, Harvard Apparatus Ltd., England, UK). Electrocardiograms (ECG) and expired CO<sub>2</sub> levels were monitored throughout the experiments.

## **2.1 Retinal intrinsic imaging and stimulus parameters**

Retinal intrinsic signals (RIS) were acquired with the retinal functional imager (RFI, Optical Imaging Ltd, Rehovot, Israel), a system based on a modified fundus camera (Retinal Imager-functional Topcon TRC-50DX) (Izhaky, Nelson, Burgansky-Eliash, &

Grinvald, 2009; D. A. Nelson et al., 2005). The camera was focused on the eye fundus and positioned to record from the same retinal region across animals. This region included part of the retinal blind spot as shown in Fig 1 (see also Fig 3, dotted red square).

Illumination was provided by a 12 V, 100 W halogen lamp, whose light was band-pass filtered in the near-infrared range ( $750 \pm 20$  nm, flux/power of  $-1.4 \log \text{ cd.s.m}^{-2}$ ). Visual stimulation was performed using a 120 W mercury lamp (X-Cite series 120, Photonic Solution Inc., Canada), passing through a UV filter and a green filter ( $564 \pm 40$  nm). The reported stimulus intensity values were calculated with a photometer (Sekonic L-608), with its detector placed at the same distance from the camera lens as the rabbit eye cornea during the experiments. Stimulus duration was controlled by a shutter (Uniblitz, Model VCM-D1 shutter drive, Vincent Associates, NY), synchronized with the data acquisition software (Metabrowse, Optical Imaging Ltd., Rehovot, Israel). For all recordings (except those shown in Fig 1), the camera angle of view was 50 degrees while the emitted light used for stimulation activated a retinal area of approximately  $16 \text{ mm}^2$ . This stimulus profile was kept constant for all animals in order to minimize data variability. The optical signals presented here were based on the analysis of a circumscribed ROI within this area of stimulation.

## **2.2 Experimental protocol**

All experiments were performed in the dark. At experiment onset, a 1-second saturation flash ( $35 \text{ cd.m}^{-2}$  intensity) was projected onto the imaged part of the retina and was followed by 60 minutes of dark adaptation. Experiments consisted in imaging trials of 24 seconds (10 Hz,  $512 \times 512$  pixels) with inter-trial intervals of 90 seconds. Stimuli (200 ms)

were delivered 3 s after trial onset. In order to improve the signal-to-noise ratio (SNR), data was averaged over 10 consecutive trials.

### **2.3 Image and data analysis**

Raw images (binary files) were converted into matrices for data analysis using Matlab scripts (The Mathworks Inc., MA, USA). Intrinsic changes in light reflection ( $\Delta R/R$ ) were calculated as follow: individual data frames (R) were first subtracted, pixel by pixel, with the average image from the pre-stimulus period ( $R_{baseline}$ ) and further normalized by  $R_{baseline}$  to measure percent-change, as shown in following equation:

$$\Delta R/R\% = (R - R_{baseline}) / R_{baseline} \times 100$$

Error bars in figures represent the standard error by the mean (SEM).

### **2.4 Electroretinogram (ERG)**

Concurrently with RIS imaging, ERGs were recorded using DTL electrodes positioned onto the cornea. The reference electrode was placed under the tongue and the ground electrode in the forelimb. The ERG signal was amplified 10,000 times and band-pass filtered between 1 and 1000 Hz using an AC amplifier (P511 series AC amplifier, GRASS, Astro-Med, Inc.). The amplified signal was recorded with a data acquisition interface (CED 1401), controlled by Signal 3.10 software (Cambridge Electronic Design, Cambridge, UK). The a-wave and b-wave amplitudes were measured according to ISCEV standards (McCulloch et al., 2015): The a-wave was measured from the baseline and the b-wave was measured from the a-wave minimum to the b-wave peak.

For the assessment of OFF bipolar cells pathway (see below), specific ERG recordings (interleaved with RIS imaging trials) were made to obtain the d-wave. During these recordings, a longer stimulus was used (1 s flash) (Heckenlively & Arden, 2006).

Otherwise, the ERG recordings were obtained from the stimuli used to generate RIS responses.

## **2.5 Intravitreal injection**

To selectively block the activity of the different retinal cells, pharmacological agents were administered by intravitreal injections. The injection needle (30-G) was inserted perpendicular to the eye surface, posterior to the limbus. Once inserted, it was angled toward the center of the vitreous humor to ensure the delivery of the drug as close as possible to the retina while avoiding the lens. The procedure was validated by *post hoc* visual inspection of the lens integrity. In all cases reported here, no lens injury was found. After a slow and controlled delivery of the injection volume (50  $\mu$ L), the needle was kept in place for about 20-30 seconds before its removal. To estimate the final drug concentrations, the vitreous volume was established at 1.2 mL (Kiernan et al., 2010). In agreement with previously studies, all pharmacological agents were dissolved in saline solution (Dong, Agey, & Hare, 2004; Levinger, Zemel, & Perlman, 2012). The following drugs, at their final vitreous concentrations, were used: TTX (100 nM), APB (2-10 mM), PDA (5-10 mM) and aspartate (25 mM). Prior to each injection, control levels of RIS were acquired for 2 hours. Subsequently, the injection was performed and the imaging resumed shortly afterward (approximately 5 min) for about 3 hours, on average, after injection.

### 3. Results

In a first step, the basic characteristics of retinal intrinsic signals were studied. Hence, RIS were measured using different stimulus conditions and were compared with ERG recordings, an established functional assay of retinal activity.

*Fig 2  
near here*

#### 3.1 RIS basic characteristics

Fundamentals of rabbit RIS are shown in Fig 1. In this example, the eye was stimulated with a discrete circular visual stimulus of 14 degrees at an intensity of 16 cd.m<sup>-2</sup> (panel A). As seen in the differential images and the reflectance time course, RIS are biphasic in nature (Fig 1, B-D). One to two seconds following stimulation a relatively short-lasting decrease in light reflection (or increase in light absorption by the active tissue) is observed (panel B). This negative phase of the retinal signal is followed by a long-lasting positive phase that lasts 60 seconds on average. This waveform pattern was observed for all effective stimulus intensities and was consistent across all animals tested with this protocol (n=22). Hence, our data indicate that intrinsic retinal signals are spatially restricted to the stimulated retinal segments and, similar to other studies in primates and cats (Hanazono et al., 2007; D. Ts'o et al., 2009; Tsunoda et al., 2009), are composed of both fast and slow components.

*Fig 1  
near here*

We next examined the stimulus-dependency of the intrinsic signals. The amplitude of the RIS components was measured in response to stimuli of increasing intensity, ranging between 5 and 35 cd.m<sup>-2</sup>. No reliable optical intrinsic signals were observed at intensities below 12 cd.m<sup>-2</sup> (see supplementary Figure 1 (S1 Fig)) while response saturation occurred near 25 cd.m<sup>-2</sup>. A result from a typical experiment is shown in panel A of Fig 2

for intensity values within this range. In all animals tested (n=10), RIS increased as a function of light intensity, irrespective of the RIS amplitude metric selected (negative or positive peaks, peak to peak). Data from all animals were normalized to the response amplitude of the smallest stimulus (12 cd.m<sup>-2</sup>), pooled and subject to regression analysis. The relation between stimulus intensity and RIS amplitude was best fitted with an exponential model (see panels B-C), independent of whether the negative (r<sup>2</sup>=0.74), the positive (r<sup>2</sup>=0.95) or the peak-to-peak (r<sup>2</sup>=0.85) amplitudes were considered. Thus, our results indicate that the retinal intrinsic signal reflects the intensity of the stimulus.

*Fig 4  
near here*

We further observed that responses could not be evoked throughout the whole retina. Figure 3 shows a schematic of the rabbit retina and the location of RIS recordings (squares 1 to 5) made in various areas (see Fig 3). Data indicate that RIS was not detected at the optic nerve head (panel 1), at the myelinated region of the nerve fibers (panel 2) or in the vascular part of the retina (panel 4). On the other hand, strong responses were always recorded in the visual streak (panels 3 and 5).

*Fig 3  
near here*

### **3.2 Comparison between RIS and ERG signals**

In all our experiments, ERG signals were recorded along with the RIS imaging, allowing a direct comparison between the two recordings. An analysis investigating the relation between RIS amplitude and ERG's a- and b-wave components was done (Fig 4). While the a-wave is considered to mainly reveal the activity of photoreceptors, the b-wave is thought to mostly reflect the activity of bipolar cells (Heckenlively & Arden, 2006). The raw values of a and b waves as a function of stimulus intensities are shown in panels A and B. As shown in panel C, the relation between RIS and a-wave amplitude is not linear reaching a plateau at intensities near 21 cd.m<sup>-2</sup>. From this point, the dynamic range of the

Fig 5  
near here

a-wave signal starts to exceed the one from RIS, which has saturated. The relation between the a-wave and RIS amplitudes was best fitted with an exponential model ( $r^2=0.87$ ,  $p<0.001$ ,  $n=8$ ). On the other hand, while both RIS (Fig 2, D) and b-wave amplitudes (Fig 4, B) showed signs of saturation in their responses, they were strongly linearly correlated (Fig 4, D:  $r^2=0.98$ ,  $n=8$ ). Identical results were obtained when considering only the positive or negative peaks of RIS. Thus, for the remaining parts of the paper, RIS amplitude will correspond to the absolute sum of both negative and positive components' peak.

### **3.3 Anatomical origin of RIS**

Intravitreal injections of selective pharmacological agents were made to determine the contribution of the different retinal cells in the genesis of RIS.

#### **3.3.1 Control for intravitreal injections**

Control experiments were performed to test for non-specific effects on RIS arising from the injection procedure. In four experiments, injections of the vehicle solution (saline) were administered. A representative example is shown in Fig 5. In all experiments, RIS amplitude remained stable following intravitreal saline injections ( $p = 0.85$ , Student's paired *t*-test).

#### **3.3.2 Isolation of photoreceptor's activity**

A first set of pharmacological experiments was carried out with aspartate, an excitatory amino acid, which is effective in blocking synaptic transmission in the OPL, thereby isolating the photoreceptor from other retinal cells (Yannuzzi et al., 2004).

Characteristic individual results and population data are shown in Fig 6. Intrinsic signals, together with the ERG b wave, were completely eliminated following aspartate injection (mean RIS amplitude ( $\% \Delta R/R$ ): control:  $1.1 \pm 0.07$ , aspartate:  $0.07 \pm 0.02$ ,  $p < 0.001$ ,  $n=6$ ). The time course of the effects of aspartate injection on ERG recordings is included in supplementary Fig 2 (S2 Fig). As expected, the ERG a-wave was preserved. Hence, no retinal intrinsic signal was observed when the photoreceptors' activity was isolated with aspartate.

### 3.3.3 Injection of TTX, APB and PDA

*Fig 6  
near here*

A second set of experiments involved a sequence of two intravitreal injections. First, tetrodotoxin (TTX) was injected in order to study the role of the activity of the inner retina on RIS (Fig 7, A). TTX is a blocker of voltage-sensitive sodium channels and inhibits the generation of action potentials in ganglion cells (GCs) as well as in some amacrine cells (Trenholm et al., 2012). RIS amplitude was significantly reduced following the injection of TTX (24% decrease in response amplitude,  $p = 0.017$ , paired  $t$ -test,  $n=16$ ). The effect of TTX was controlled by the absence of consensual pupillary light reflex in the fellow eye. Additionally, dedicated experiments run in photopic conditions

*Fig 7  
near here*

( $n=2$ ,  $20 \text{ cd.m}^{-2}$  of ambient light, stimulus of  $35 \text{ cd.m}^{-2}$ ) indicated that the b wave and the photopic negative response (PhNR) were reduced by TTX at this concentration (100 nM,

S3 Fig). As shown by others (Hanazono et al., 2008), the effects of TTX were irreversible, lasting for as long we could collect data. Hence, the effects of a second injection could be measured, with confidence that the effects of TTX were stable throughout our recordings (Hanazono et al., 2008).

Following the inhibition of ganglion and/or amacrine cells with TTX, the role of the activity of bipolar cells was investigated by injection of cis-2,3-piperidinedicarboxylic acid (PDA) and 2-amino-4-phosphonobutyric acid (APB).

PDA is an antagonist for iGluRs receptors, and is expected to block the activity of OFF-bipolar cells without interfering with the activity of the ON-bipolar cells (Hare & Ton, 2002; Massey et al., 1983; Slaughter & Miller, 1981). As shown in the example presented in panel B of Fig 7, RIS amplitude was not affected by PDA injections ( $p = 0.88$ , Student's paired  $t$ -test). In contrast, the ERG d-wave was eliminated following PDA injections (traces 3 and 4, panel B) as expected (Heckenlively & Arden, 2006; Horiguchi et al., 1998), demonstrating the efficacy of the drug injection.

APB is an mGluR agonist that blocks the activity of ON-bipolar cells without interfering with the activity of OFF-bipolar cells (Knapp & Schiller, 1984; Massey et al., 1983; Slaughter & Miller, 1981). As shown in panel C, APB decreased RIS and ERG b-wave amplitudes, in a dose-dependent manner. ERG b waves were eliminated using both 2 and 10 mM concentrations but the latter was associated with a quicker inhibition (S4 Fig). These concentrations were comparable to the ones used in previous studies (Guite & Lachapelle, 1990; Schiller, Sandell, & Maunsell, 1986) and proved efficient and toxicity-free. While a 2 mM concentration caused a 23% decrease in RIS amplitude ( $p=0.2207$ ,

Student's paired *t*-test, *n*= 6), a 10 mM concentration completely eliminated RIS ( $p < 0.001$ , Student's *t*-test, *n*=6) (see panel c of Fig 7).

## **4. Discussion**

In this study, retinal intrinsic signals (RIS) were described for the first time in the rabbit. RIS amplitude was proportional to stimulus intensity and was also correlated with the ERG b-wave amplitude. Our results demonstrate that rabbit RIS originate from the inner retina, with a dominant contribution from ON bipolar cells.

### **4.1 On the relation between RIS and ERG**

ERG recordings and RIS imaging were performed simultaneously, allowing direct comparisons between these two functional measurement methods. One obvious fundamental difference between the two methods lies in the kinetics of both signal types. While ERG signal components can have time-course scale on the order of milliseconds, RIS have much slower kinetics (see Fig 1). The kinetics of RIS responses in rabbits is comparable to the ones reported in cat and primate models (D. Ts'o et al., 2009; Tsunoda et al., 2009). A second difference pertains to the biophysical nature of both signals. ERG recordings represent the spatial and temporal integration of graded electrical currents in the retina. The exact biophysical mechanism behind retinal intrinsic signals is much less understood: potential mechanisms include changes in local hemoglobin concentration or oxidation states, osmotic cell swelling and light scattering (Grinvald, Frostig, Lieke, & Hildesheim, 1988; Malonek et al., 1997; Vanzetta & Grinvald, 2008). Irrespective of the

exact mechanism at their origin, RIS responses occur several milliseconds after the end of retinal electrical responses and thus provide an indirect measure of cellular activity.

A third difference between RIS and ERG techniques resides in their spatial resolution. In ERG recordings, the DTL electrode integrates the electric activity of the retina as a whole. Hence, unless focal stimuli are used as in multi-focal ERG experiments (Hood et al., 2012; Hood, Odel, Chen, & Winn, 2003), this technique does not provide spatial information from the physiology of the retina. In the case of RIS the spatial resolution of the response is theoretically fixed at half of the illumination wavelength and further shaped by optic magnification and camera resolution. While this theoretical optical resolution is further reduced by both physical processes (e.g. light scattering) and vascular anatomy underlying the hemodynamic processes, it remains that RIS can yield spatially distinct signals in the retina as demonstrated here by the use of regions of interest. Further, the resolution of this technique does not depend on the stimulus size, i.e., one can deliver a full-field stimulus and probe regional retinal physiology through the selection of regions of interest. Thus, when compared to ERG recordings, RIS has the potential to provide data with significantly higher spatial resolution.

In this study, the strong linear relation between b-wave and RIS' amplitude led us to hypothesize that they shared similar cellular origins (see Fig 4, panel D). The ERG b-wave is known to originate mostly from the activity of bipolar cells (Heckenlively & Arden, 2006) and our hypothesis was verified when we performed pharmacological injections targeting these cells. Probably because experiments were done in mesopic conditions, RIS and ERG b-waves were mostly dependent on the activity of ON bipolar cells. Thus, the fact that PDA did not affect RIS amplitude in our experimental conditions

does not rule out that OFF bipolar cells may also contribute to RIS genesis in other illumination conditions. Our results also showed that TTX yielded a decrease of about 20 % of the RIS amplitude. This suggests that there is a contribution of either ganglion cells or some amacrine cells. Given the modest impact of TTX, amacrine cells are more likely to be involved than ganglion cells.

## **4.2 Interspecies differences in RIS**

Throughout the scope of available literature on RIS, their kinetics, waveform, local characteristics and their cellular origins are subject to significant inter-species differences.

Our results demonstrate that rabbit RIS are biphasic and that both phases of the signal (negative and positive) are co-localized and reflect with high spatial fidelity the retinal stimulation site. The negative peak of RIS rose very quickly, within a second of stimulation onset, whereas the positive peak reached its maximum approximately 10 seconds after stimulus onset, only to get back to baseline levels after 60 seconds.

In contrast, negative and positive phases of cat RIS are spatially separated. The RIS negative phase is confined to the stimulated retinal region, whereas signals with a positive phase are only found on the periphery of the stimulation site (J. Schallek, Li, et al., 2009; D. Ts'o et al., 2009). In primates, RIS signals are mainly negative and their kinetics depend on the retinal region being stimulated (Hanazono et al., 2007; Ivo Vanzetta, 2014). In our data, when images were divided into multiple ROIs, we did not find any regional specificity in RIS waveforms but we have not done a systematic study on this. What we found, however, is that optical signals were absent at the optic nerve

head (ONH) location, in the nearby myelinated optic fibers, and on the vascularized regions. The strong and robust responses were always located along the visual streak area, i.e. the avascular part of the retina. This is at odds with results described in the monkey where functional responses are also observed in the blood-vessel-rich optic nerve (Ivo Vanzetta, 2014). The absence of response in vascular regions of the rabbit retina may indicate that optical signals are not driven by hemodynamics (see below). This assumption is, however, difficult to reconcile with the biphasic profile of the optical intrinsic response.

In this study, rabbit RIS time course was comparable to the slow RIS signals described in cats and primates (Hanazono et al., 2007; D. Ts'o et al., 2009; Tsunoda et al., 2009). As discussed above, the exact cellular mechanism at the origin of retinal intrinsic signals is poorly understood. In primates, slow RIS are thought to be controlled by retinal ganglion cells that trigger blood flow changes in vessels and capillaries (Tsunoda et al., 2009). While we cannot rule out the contribution of ganglion cells in rabbits, we suggest, based on the weak effect of the TTX injections, that part of RIS originated from the activity of retinal amacrine cells. However, because of the rabbit retina's poor irrigation (Yu & Cringle, 2004) and the major role played by bipolar cells in RIS generation, the mechanism at the origin of rabbit RIS likely consists of cellular mechanisms such as hyperpolarisation-induced changes in light scattering or osmotic changes in cytoplasmic volume (Zepeda et al., 2004).

In concordance with the strong correlation between RIS and ERG b wave that suggested common cellular origins, pharmacological experiments discard a role for

photoreceptors in the genesis of intrinsic signals which is in contrast to the cat findings (J. Schallek, Kardon, et al., 2009; D. Ts'o et al., 2009). Consequently, our data suggest that, in rabbits, RIS arise from the activity of the inner retina. Our data also indicate that ON bipolar cells' activity plays an important role in RIS under mesopic conditions in rabbits, with a possible small contribution of amacrine cells.

**Acknowledgments:** This work was supported by an NSERC grant to CC (2014-06503). AN received scholarships from EOUM-FESP and IGB-FESP. We thank Geneviève Cyr for her technical help.

## References

- Chen, T. C., Cense, B., Pierce, M. C., Nassif, N., Park, B. H., Yun, S. H., . . . de Boer, J. F. (2005). Spectral domain optical coherence tomography: ultra-high speed, ultra-high resolution ophthalmic imaging. *Arch Ophthalmol*, *123*(12), 1715-1720. doi: 10.1001/archophth.123.12.1715
- Costa, R. A., Skaf, M., Melo, L. A., Jr., Calucci, D., Cardillo, J. A., Castro, J. C., . . . Wojtkowski, M. (2006). Retinal assessment using optical coherence tomography. *Prog Retin Eye Res*, *25*(3), 325-353. doi: 10.1016/j.preteyeres.2006.03.001
- Dong, C. J., Agey, P., & Hare, W. A. (2004). Origins of the electroretinogram oscillatory potentials in the rabbit retina. *Vis Neurosci*, *21*(4), 533-543. doi: 10.1017/S0952523804214043
- Grinvald, A., Bonhoeffer, T., Vanzetta, I., Pollack, A., Aloni, E., Ofri, R., & Nelson, D. (2004). High-resolution functional optical imaging: from the neocortex to the eye. *Ophthalmol Clin North Am*, *17*(1), 53-67. doi: 10.1016/j.ohc.2003.12.003
- Grinvald, A., Frostig, R. D., Lieke, E., & Hildesheim, R. (1988). Optical imaging of neuronal activity. *Physiol Rev*, *68*(4), 1285-1366.
- Grinvald, A., Lieke, E., Frostig, R. D., Gilbert, C. D., & Wiesel, T. N. (1986). Functional architecture of cortex revealed by optical imaging of intrinsic signals. *Nature*, *324*(6095), 361-364. doi: 10.1038/324361a0
- Guite, P., & Lachapelle, P. (1990). The effect of 2-amino-4-phosphonobutyric acid on the oscillatory potentials of the electroretinogram. *Doc Ophthalmol*, *75*(2), 125-133.
- Hanazono, G., Tsunoda, K., Kazato, Y., Tsubota, K., & Tanifuji, M. (2008). Evaluating neural activity of retinal ganglion cells by flash-evoked intrinsic signal imaging in macaque retina. *Invest Ophthalmol Vis Sci*, *49*(10), 4655-4663. doi: 10.1167/iovs.08-1936
- Hanazono, G., Tsunoda, K., Shinoda, K., Tsubota, K., Miyake, Y., & Tanifuji, M. (2007). Intrinsic signal imaging in macaque retina reveals different types of flash-induced light reflectance changes of different origins. *Invest Ophthalmol Vis Sci*, *48*(6), 2903-2912. doi: 10.1167/iovs.06-1294
- Hare, W. A., & Ton, H. (2002). Effects of APB, PDA, and TTX on ERG responses recorded using both multifocal and conventional methods in monkey. Effects of APB, PDA, and TTX on monkey ERG responses. *Doc Ophthalmol*, *105*(2), 189-222.
- Heckenlively, John R., & Arden, Geoffrey B. (2006). Origins of slow electrophysiological components *Principle and practice of clinical electrophysiology of vision* (pp. 121-234): MIT press.
- Hirohara, Y., Mihashi, T., Kanda, H., Morimoto, T., Miyoshi, T., Wolffsohn, J. S., & Fujikado, T. (2013). Optical imaging of retina in response to grating stimuli in cats. *Exp Eye Res*, *109*, 1-7. doi: 10.1016/j.exer.2013.01.007

- Hood, D. C., Bach, M., Brigell, M., Keating, D., Kondo, M., Lyons, J. S., . . . International Society For Clinical Electrophysiology of Vision. (2012). ISCEV standard for clinical multifocal electroretinography (mfERG) (2011 edition). *Doc Ophthalmol*, 124(1), 1-13. doi: 10.1007/s10633-011-9296-8
- Hood, D. C., Odel, J. G., Chen, C. S., & Winn, B. J. (2003). The multifocal electroretinogram. *J Neuroophthalmol*, 23(3), 225-235.
- Horiguchi, M., Suzuki, S., Kondo, M., Tanikawa, A., & Miyake, Y. (1998). Effect of glutamate analogues and inhibitory neurotransmitters on the electroretinograms elicited by random sequence stimuli in rabbits. *Invest Ophthalmol Vis Sci*, 39(11), 2171-2176.
- Inomata, K., Tsunoda, K., Hanazono, G., Kazato, Y., Shinoda, K., Yuzawa, M., . . . Miyake, Y. (2008). Distribution of retinal responses evoked by transscleral electrical stimulation detected by intrinsic signal imaging in macaque monkeys. *Invest Ophthalmol Vis Sci*, 49(5), 2193-2200. doi: 10.1167/iovs.07-0727
- Ivo Vanzetta, Thomas Deneux, Amiram Grinvald. (2014). High-Resolution Wide-Field Optical Imaging of Microvascular Characteristics: From the Neocortex to the Eye. In H. M. Mingrui Zhao, Theodore H. Schwartz (Ed.), *Neurovascular Coupling Methods* (Vol. 88, pp. 123-159): Springer New York.
- Izhaky, D., Nelson, D. A., Burgansky-Eliash, Z., & Grinvald, A. (2009). Functional imaging using the retinal function imager: direct imaging of blood velocity, achieving fluorescein angiography-like images without any contrast agent, qualitative oximetry, and functional metabolic signals. *Jpn J Ophthalmol*, 53(4), 345-351. doi: 10.1007/s10384-009-0689-0
- Kiernan, D. F., Mieler, W. F., & Hariprasad, S. M. (2010). Spectral-domain optical coherence tomography: a comparison of modern high-resolution retinal imaging systems. *Am J Ophthalmol*, 149(1), 18-31. doi: 10.1016/j.ajo.2009.08.037
- Knapp, A. G., & Schiller, P. H. (1984). The contribution of on-bipolar cells to the electroretinogram of rabbits and monkeys. A study using 2-amino-4-phosphonobutyrate (APB). *Vision Res*, 24(12), 1841-1846.
- Levinger, E., Zemel, E., & Perlman, I. (2012). The effects of excitatory amino acids and their transporters on function and structure of the distal retina in albino rabbits. *Doc Ophthalmol*. doi: 10.1007/s10633-012-9354-x
- Li, Y. C., Strang, C., Amthor, F. R., Liu, L., Li, Y. G., Zhang, Q. X., . . . Yao, X. C. (2010). Parallel optical monitoring of visual signal propagation from the photoreceptors to the inner retina layers. *Opt Lett*, 35(11), 1810-1812. doi: 10.1364/OL.35.001810
- Malonek, D., Dirnagl, U., Lindauer, U., Yamada, K., Kanno, I., & Grinvald, A. (1997). Vascular imprints of neuronal activity: relationships between the dynamics of cortical blood flow, oxygenation, and volume changes following sensory stimulation. *Proc Natl Acad Sci U S A*, 94(26), 14826-14831.
- Massey, S. C., Redburn, D. A., & Crawford, M. L. (1983). The effects of 2-amino-4-phosphonobutyric acid (APB) on the ERG and ganglion cell discharge of rabbit retina. *Vision Res*, 23(12), 1607-1613.

- McCulloch, D. L., Marmor, M. F., Brigell, M. G., Hamilton, R., Holder, G. E., Tzekov, R., & Bach, M. (2015). ISCEV Standard for full-field clinical electroretinography (2015 update). *Doc Ophthalmol*, *130*(1), 1-12. doi: 10.1007/s10633-014-9473-7
- Mihashi, T., Okawa, Y., Miyoshi, T., Kitaguchi, Y., Hirohara, Y., & Fujikado, T. (2011). Comparing retinal reflectance changes elicited by transcorneal electrical retinal stimulation with those of optic chiasma stimulation in cats. *Jpn J Ophthalmol*, *55*(1), 49-56. doi: 10.1007/s10384-010-0906-x
- Nelson, D. A., Krupsky, S., Pollack, A., Aloni, E., Belkin, M., Vanzetta, I., . . . Grinvald, A. (2005). Special report: Noninvasive multi-parameter functional optical imaging of the eye. *Ophthalmic Surg Lasers Imaging*, *36*(1), 57-66.
- Schallek, J. B., McLellan, G. J., Viswanathan, S., & Ts'o, D. Y. (2012). Retinal intrinsic optical signals in a cat model of primary congenital glaucoma. *Invest Ophthalmol Vis Sci*, *53*(4), 1971-1981. doi: 10.1167/iops.11-8299
- Schallek, J., Kardon, R., Kwon, Y., Abramoff, M., Soliz, P., & Ts'o, D. (2009). Stimulus-evoked intrinsic optical signals in the retina: pharmacologic dissection reveals outer retinal origins. *Invest Ophthalmol Vis Sci*, *50*(10), 4873-4880. doi: 10.1167/iops.08-3291
- Schallek, J., Li, H., Kardon, R., Kwon, Y., Abramoff, M., Soliz, P., & Ts'o, D. (2009). Stimulus-evoked intrinsic optical signals in the retina: spatial and temporal characteristics. *Invest Ophthalmol Vis Sci*, *50*(10), 4865-4872. doi: 10.1167/iops.08-3290
- Schallek, J., & Ts'o, D. (2011). Blood contrast agents enhance intrinsic signals in the retina: evidence for an underlying blood volume component. *Invest Ophthalmol Vis Sci*, *52*(3), 1325-1335. doi: 10.1167/iops.10-5215
- Schiller, P. H., Sandell, J. H., & Maunsell, J. H. (1986). Functions of the ON and OFF channels of the visual system. *Nature*, *322*(6082), 824-825. doi: 10.1038/322824a0
- Sharp, P. F., & Manivannan, A. (1997). The scanning laser ophthalmoscope. *Phys Med Biol*, *42*(5), 951-966.
- Slaughter, M. M., & Miller, R. F. (1981). 2-amino-4-phosphonobutyric acid: a new pharmacological tool for retina research. *Science*, *211*(4478), 182-185.
- Trenholm, S., Borowska, J., Zhang, J., Hoggarth, A., Johnson, K., Barnes, S., . . . Awatramani, G. B. (2012). Intrinsic oscillatory activity arising within the electrically coupled AII amacrine-ON cone bipolar cell network is driven by voltage-gated Na<sup>+</sup> channels. *J Physiol*, *590*(10), 2501-2517. doi: 10.1113/jphysiol.2011.225060
- Ts'o, D., Schallek, J., Kwon, Y., Kardon, R., Abramoff, M., & Soliz, P. (2009). Noninvasive functional imaging of the retina reveals outer retinal and hemodynamic intrinsic optical signal origins. *Jpn J Ophthalmol*, *53*(4), 334-344. doi: 10.1007/s10384-009-0687-2
- Tsunoda, K., Hanazono, G., Inomata, K., Kazato, Y., Suzuki, W., & Tanifuji, M. (2009). Origins of retinal intrinsic signals: a series of experiments on retinas of macaque monkeys. *Jpn J Ophthalmol*, *53*(4), 297-314. doi: 10.1007/s10384-009-0686-3

- Tsunoda, K., Oguchi, Y., Hanazono, G., & Tanifuji, M. (2004). Mapping cone- and rod-induced retinal responsiveness in macaque retina by optical imaging. *Invest Ophthalmol Vis Sci*, 45(10), 3820-3826. doi: 10.1167/iovs.04-0394
- Vanzetta, I., & Grinvald, A. (2008). Coupling between neuronal activity and microcirculation: implications for functional brain imaging. *HFSP J*, 2(2), 79-98. doi: 10.2976/1.2889618
- Yannuzzi, L. A., Ober, M. D., Slakter, J. S., Spaide, R. F., Fisher, Y. L., Flower, R. W., & Rosen, R. (2004). Ophthalmic fundus imaging: today and beyond. *Am J Ophthalmol*, 137(3), 511-524. doi: 10.1016/j.ajo.2003.12.035
- Yu, D. Y., & Cringle, S. J. (2004). Low oxygen consumption in the inner retina of the visual streak of the rabbit. *Am J Physiol Heart Circ Physiol*, 286(1), H419-423. doi: 10.1152/ajpheart.00643.2003
- Zepeda, A., Arias, C., & Sengpiel, F. (2004). Optical imaging of intrinsic signals: recent developments in the methodology and its applications. *J Neurosci Methods*, 136(1), 1-21. doi: 10.1016/j.jneumeth.2004.02.025
- Zhang, Q. X., Zhang, Y., Lu, R. W., Li, Y. C., Pittler, S. J., Kraft, T. W., & Yao, X. C. (2012). Comparative intrinsic optical signal imaging of wild-type and mutant mouse retinas. *Opt Express*, 20(7), 7646-7654. doi: 10.1364/OE.20.007646

## Figures legends

**Figure 1: Retinal intrinsic responses in rabbits.** (A) Image of the fundus, under near infrared illumination. The arrowhead points to the retinal blind spot. The circle represents the retinal surface stimulated by a 200 ms flash of green light at an intensity of  $16 \text{ cd.m}^{-2}$  and the square indicates the region of interest for quantification. In this control experiment, the area stimulated covered 14 degrees. (B)-(C) Differential images obtained at different times following stimulation. (D) Retinal intrinsic responses are biphasic, with an initial drop in light reflectance (negative peak, see B), followed by an increase in light reflectance (positive peak, see C). The two vertical lines indicate the time and duration of stimulation.

**Figure 2: Relation between stimulus intensity and RIS amplitude.** A) RIS time course at different stimulus intensities. B-D) Scatter plots of RIS waveform components as a function of stimulus intensity. Solid lines represent the fitted non-linear regressions and the corresponding confidence bounds are illustrated by dotted lines.

**Figure 3: Regional differences of the RIS.** A schematic of the rabbit retina is shown at the top of the figure (modified from Hughes, 1971). The horizontal lines below the optic nerve head and blood vessels represent the visual streak. The red dotted line shows the imaging frame. Optical intrinsic signals were acquired from five different zones (green squares) and the responses are shown in panels 1 to 5: 1) optical nerve head (ONH), 2) myelinated fiber optics, 3) visual streak, 4) retinal vessels, and 5) visual streak. The

intrinsic signals of these five areas of the retina are shown below the retinal map. Red squares represent the ROIs. N: nasal, T: temporal.

**Figure 4: Relationship between RIS and ERG waves amplitude.** (A, B) Amplitude of ERG a-wave and b-wave as a function of stimulus intensities used (12-25 cd.m<sup>-2</sup>). (C) Normalized RIS amplitude plotted as a function of the normalized ERG a-wave. The relationship between IS and the a-wave quickly reached a plateau. The data were best fitted with an exponential model ( $r^2=0.87$ ). (D) Normalized RIS amplitude, plotted as a function of the normalized ERG b-wave. This time, the data were best fitted with a linear regression ( $r^2= 0.98$ ).

**Figure 5: Control intravitreal injections.** A-B Examples of RIS before (A) and after (B) injection of saline. C. Histogram of RIS amplitude before and after saline injection.

**Figure 6: Role of the photoreceptors in the genesis of RIS.** 1-2: Time course of RIS prior to (1) and following (2) the injection of aspartate. Note the disappearance of RIS. 3-4: ERG recordings made in parallel with the data presented in 1-2. On the right, the bar graph illustrates the normalized RIS response before (control) and after aspartate injection. (\*\*\*)= $p<0.001$ ).

**Figure 7: Role of inner retinal cells in the genesis of RIS.** A) RIS and ERG signals prior to and following the injection of TTX (\*:  $p<0.05$ , Student's paired *t*-test). (B) From eyes previously injected with TTX, RIS and ERG signals prior to and following the

injection of PDA. ERG traces were obtained separately, using a stimulus allowing the measurement of the d-wave, indicated by an arrow. Note that while PDA abolished the d-wave, it did not affect RIS amplitude. C) From eyes previously injected with TTX, RIS and ERG signals prior to and following the injection of APB at two different concentrations (\*\*\*:  $p < 0.001$ , Student's paired  $t$ -test).

## Supplementary figures

**S1 Fig:** RIS amplitude as a function of stimulus intensity (5 to 35  $\text{cd.m}^{-2}$ ). The optical responses are not visible at low intensities.

**S2 Fig: Effects of aspartate on ERG.** ERG traces obtained at numerous time points following the injection of aspartate (25 mM). Note that the b wave was eliminated after 30 minutes and that the a-wave gradually increased.

**S3 Fig: PhNR ERG component is reduced by TTX.** Average ERG traces before (blue) and after (red) the injection of TTX (100 nM). ERG was performed under photopic conditions (20  $\text{cd.m}^{-2}$ ), with the use of 50-degree, 35  $\text{cd.m}^{-2}$  stimulation. The arrowhead indicates the PhNR that was decreased by the injection of TTX.

**S4 Fig: Dose-dependent effects of APB on ERG.** ERG traces obtained at numerous time points following the injection of APB, shown for two different concentrations (2 and 10 mM).

Figure 1

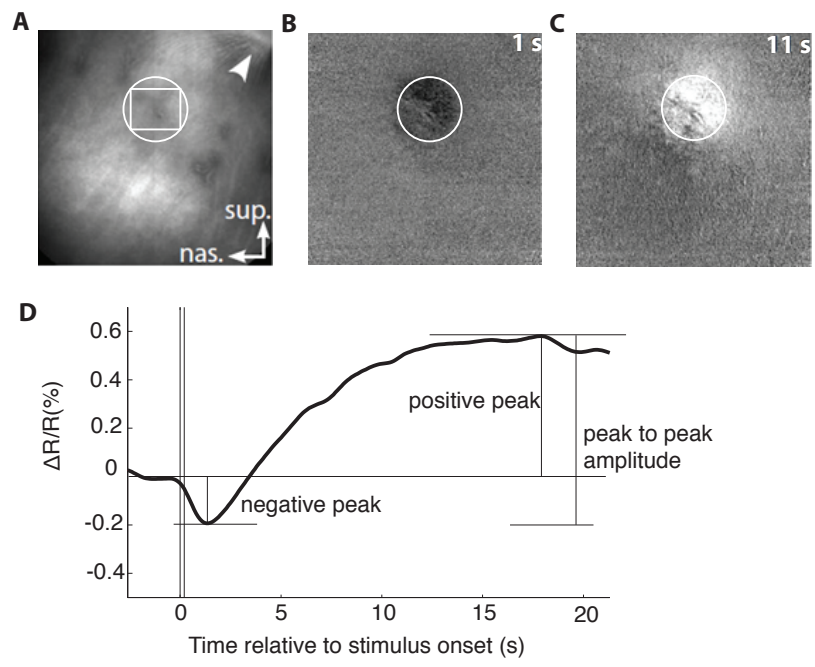
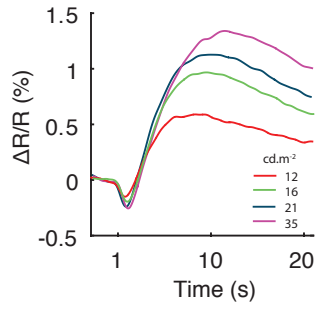
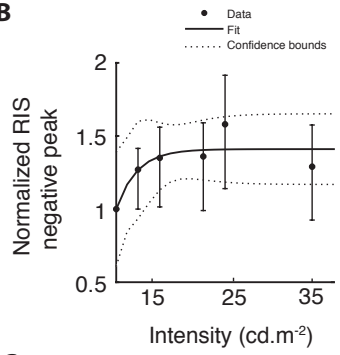


Figure 2

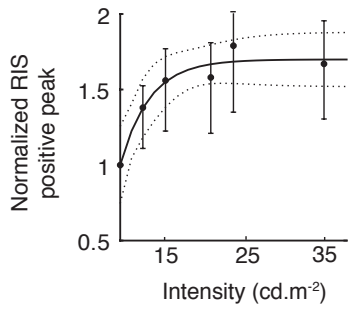
**A**



**B**



**C**



**D**

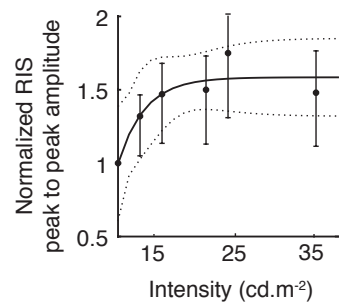


Figure 3

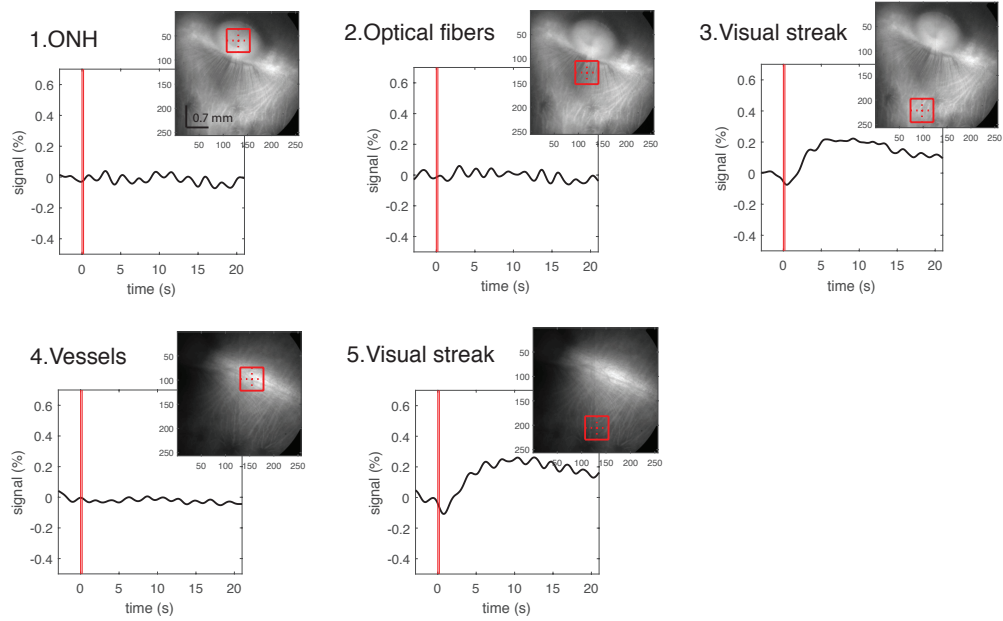
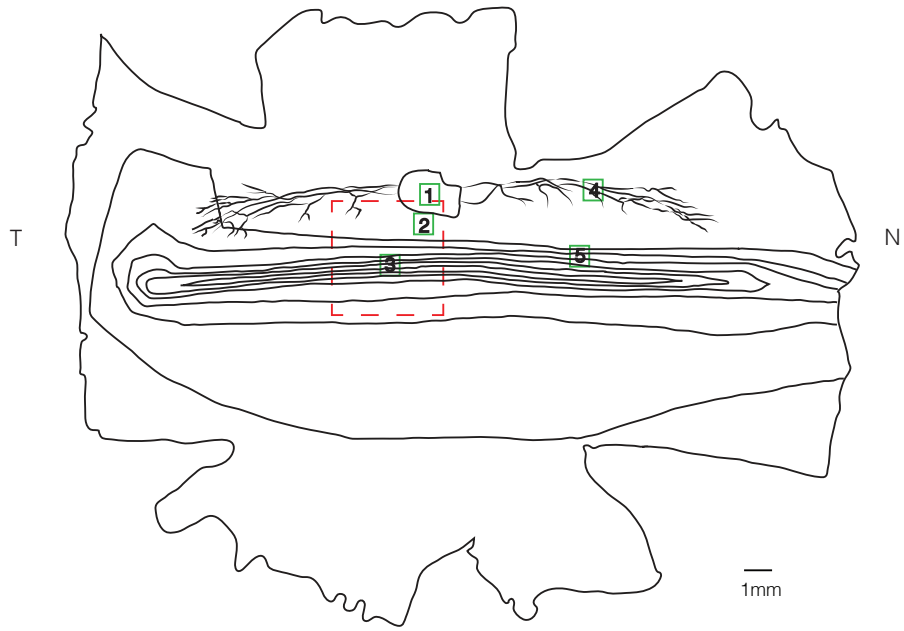


Figure 4

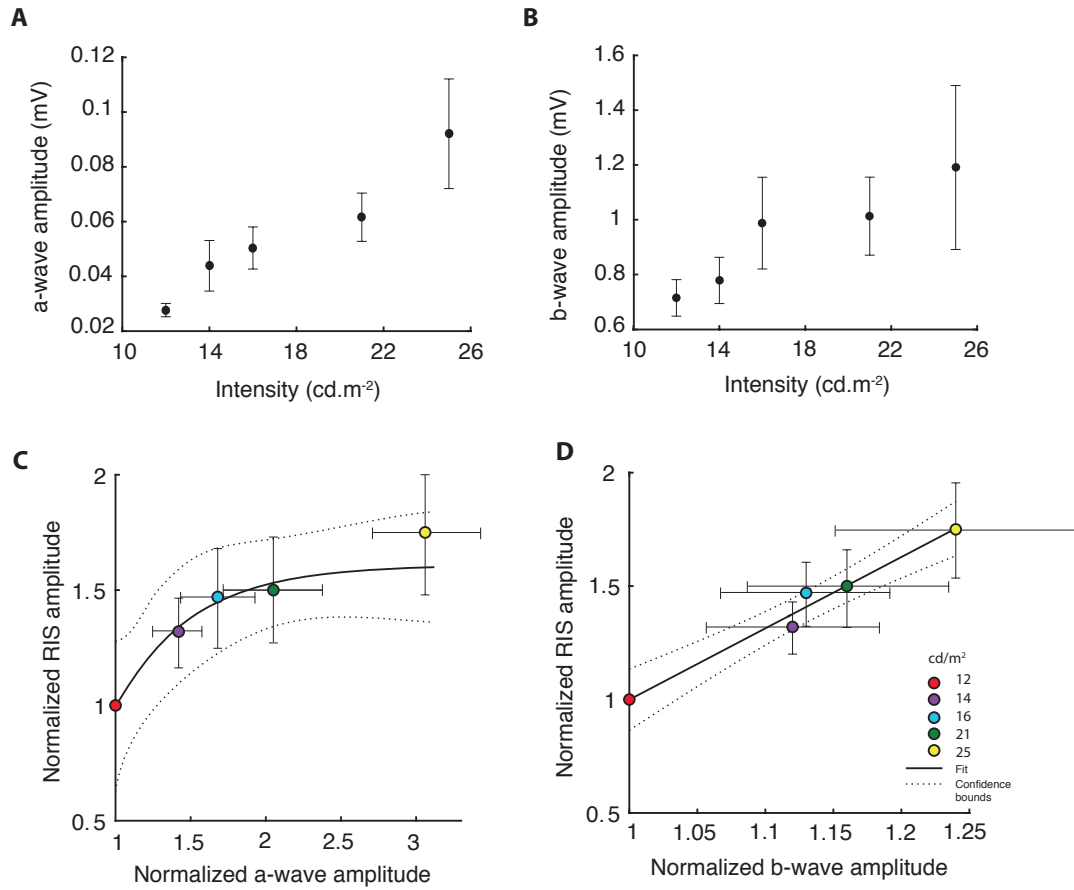


Figure 5

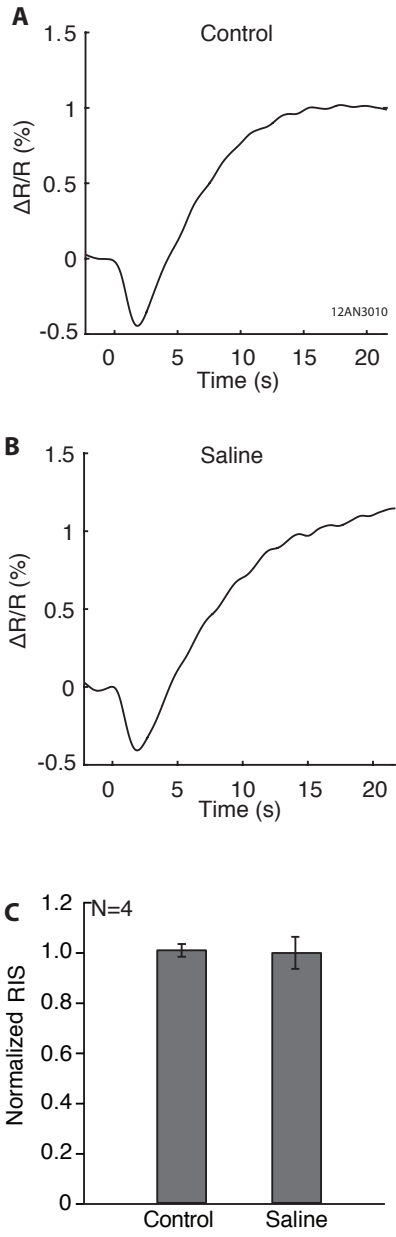


Figure 6

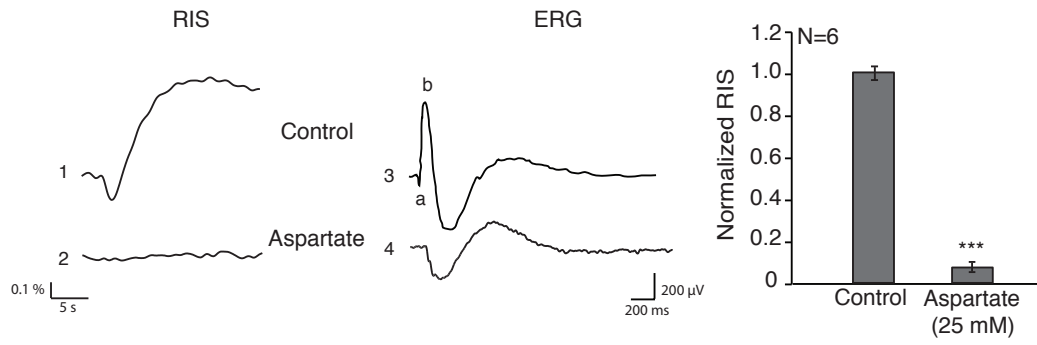
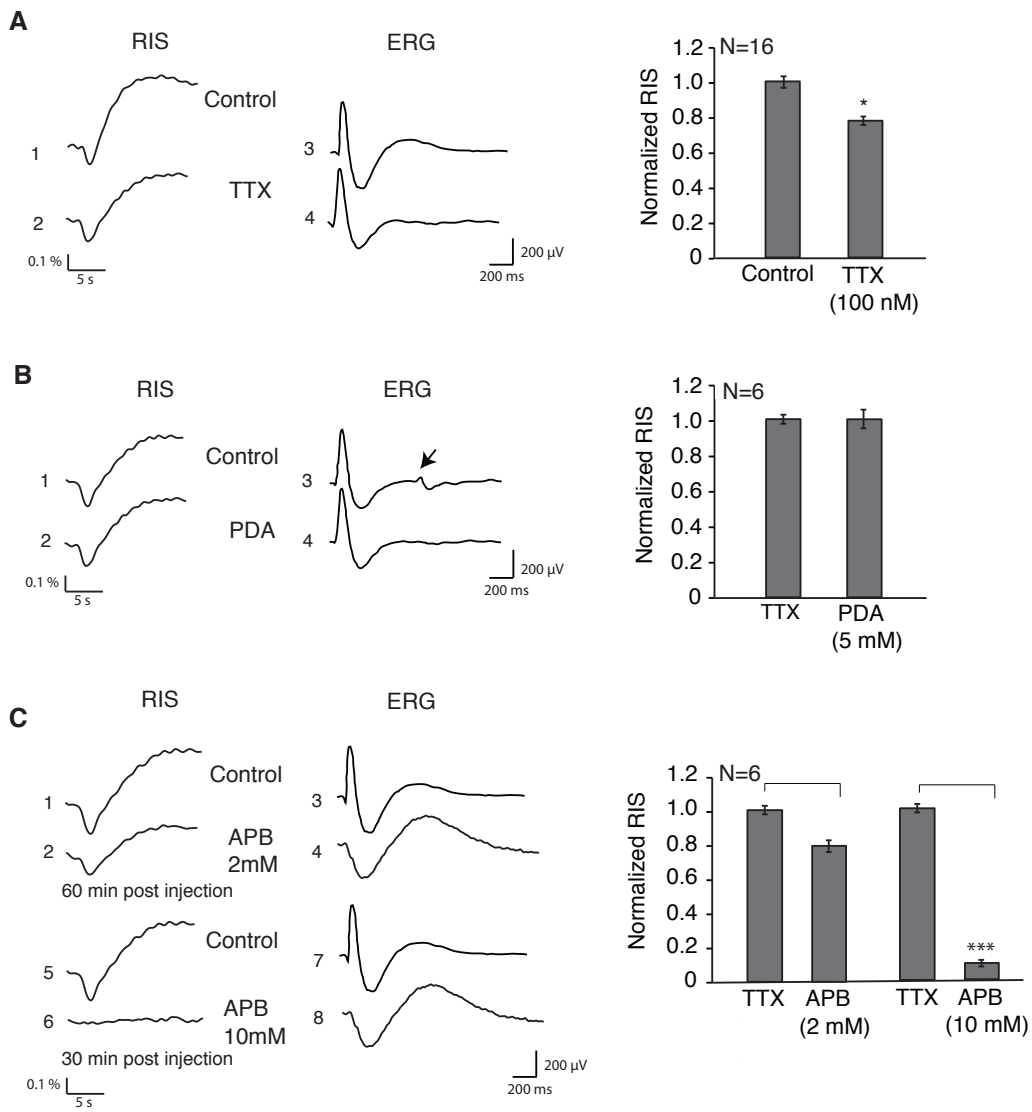
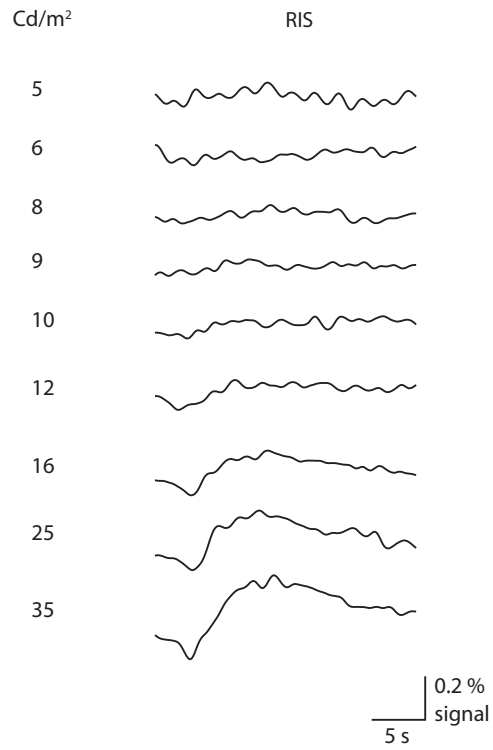


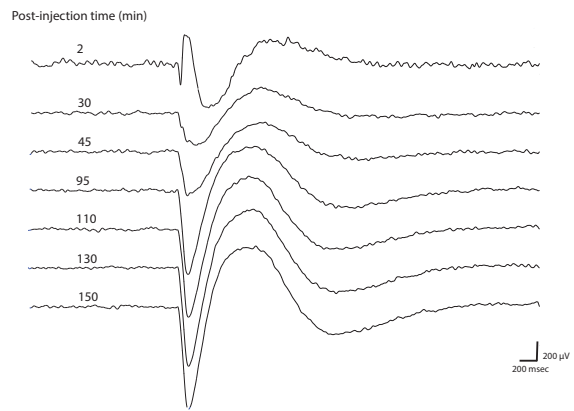
Figure 7



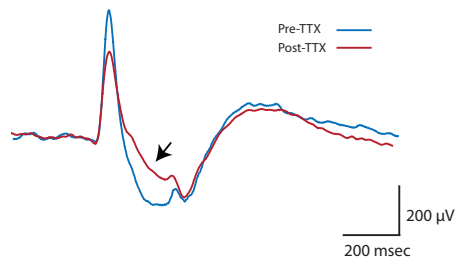


S2

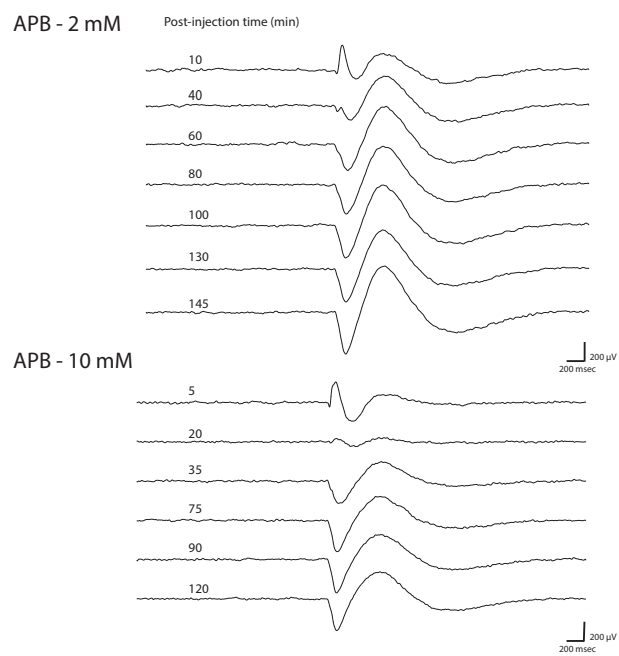
Aspartate 25mM



S3



S4



## **Chapter 3**

### **Article 2: Retinal optical imaging using intrinsic signals in rat's retina**

A. Naderian<sup>2</sup>, S. Bélanger<sup>1</sup>, B. Oliveira Ferreira de souza, F. Lesage<sup>1</sup>, C. Casanova

École d'optométrie, Université de Montréal

<sup>1</sup>Department of Electrical Engineering, École Polytechnique, Montréal

<sup>2</sup>Department of Pharmacology and physiology, Institut de Génie biomédical, Université de Montréal

**Running title:** Intrinsic signals in the retina

**Keywords:** imaging, optical design, visual evoked potential, retinal cells, b-wave.

## **Abstract**

In this study, we developed an optical imaging system to record the intrinsic signal for the rat's retina. Optical imaging of intrinsic signals has been widely used in cerebral imaging, but there are fewer studies in using this technique for retinal imaging. Although the rat is an animal model used widely in ophthalmic research, no studies are demonstrating in vivo retinal optical imaging of intrinsic signals in the rat's retina. Our imaging system was tested on control animals as well as on animals receiving intravitreal injections of aspartate. Results validate the functionality of the optical imaging system, as well as the existence of the intrinsic signals in the rat's retina following the light stimulus.

## **1. Introduction**

The retina is part of the central nervous system (CNS) that has the advantage of being accessible through the transparent media of the eye compared to the other part of the CNS. With optical access, different imaging methods can be used to study its structure and function. Ophthalmic imaging has significantly improved over the last decades: from traditional methods such as fundus drawings, fundus photography and fluorescence angiography (Bennett & Barry, 2009) to the development of novel imaging methods such as scanning laser ophthalmoscopy (SLO) (Webb & Hughes, 1981) and optical coherent tomography (OCT) (Costa et al., 2006; Fercher, 2010). Recent advances in imaging techniques such as OCT and SLO have allowed the investigation of the structure of the retina with high spatial resolution. The functional imaging of the retina has the potential

to contribute to the understanding of retinal cell functions during the processing of visual signals. It may also help provide diagnosis during the first stages of retinal diseases such as Glaucoma or Retinitis Pigmentosa (PR). In this regard, different methods of electroretinography (ERG), such as flash ERG, pattern ERG, and multifocal ERG have been widely used in clinics and laboratories (Heckenlively & Arden, 2006). ERG techniques have high temporal resolution since they measure the neuronal activity directly but their spatial resolution remains limited since they record the activity of an ensemble of neurons. Optical imaging of intrinsic signals, based on hemodynamics, is a functional imaging that has the potential to reveal the activity of retinal cells with a higher spatial resolution (Hanazono et al., 2008; Hanazono et al., 2007; Inomata et al., 2008; Tsunoda et al., 2004; Zepeda et al., 2004).

Optical imaging of intrinsic signals is an imaging technique that studies the intrinsic changes of optical properties of neuronal tissue during their activation. It was originally used to investigate the functional architecture of the cortex (Grinvald et al., 1986) where different wavelengths (between 480-940nm) were used to visualize the cortical functional architecture (Frostig et al., 1990). Depending on the illumination wavelength utilized for the imaging, various hemodynamic components of intrinsic signals can be measured which also have different time courses (Zepeda et al., 2004).

The use of optical imaging of intrinsic signals for retinal imaging demonstrated the presence of intrinsic signals during retinal activity (Hanazono et al., 2008; Hanazono et al., 2007; Inomata et al., 2008; J. B. Schallek et al., 2012; J. Schallek, Li, et al., 2009; J.

Schallek & Ts'o, 2011; D. Ts'o et al., 2009; Tsunoda et al., 2004). The functional optical imaging of intrinsic retinal signals has been shown both in vivo and in vitro, and in different animal species, i.e. monkey (Hanazono et al., 2008; Hanazono et al., 2007; Inomata et al., 2008; Tsunoda et al., 2004), cat (J. B. Schallek et al., 2012; J. Schallek, Li, et al., 2009; J. Schallek & Ts'o, 2011; D. Ts'o et al., 2009), frog (Y. C. Li et al., 2010) and mouse (Y. C. Li et al., 2012). Until now, most studies aimed to confirm the existence of intrinsic signals in the retina and to explore the characteristics and origins of these signals. With the perspective of using this imaging technique in clinics for the diagnosis of different eye pathologies, a complete characterization of the signal in pathological conditions is needed. In this regard, the rat represents an important model in studies applied to eye diseases due to their low cost, and the availability of targeted genetic manipulation.

Rats have a well-developed retinal vascular system, as with humans, with arteries and veins emerging radially from the optic disc. Its retinal structure is also similar to that of humans and is used in studies in retinal diseases, e.g., glaucoma (Johnson, Guo, Cepurna, & Morrison, 2009; Vidal-Sanz et al., 2012), and Retinopathy of prematurity (ROP) (Akula et al., 2010; Barnett, Yanni, & Penn, 2010; Cringle & Yu, 2010).

While optical imaging of intrinsic signal was used in different animal species, this technique has not been developed on the rat's retina to study the function of the retina of the rat in-vivo. In this study, we aimed to design an imaging system to stimulate and record the retinal intrinsic signal in the rat's retina. This system is based on a classic design of a fundus camera and is adapted for small eyes as seen in the rat. We validated

its function by measuring the intrinsic response of the rat retina with and without injection of aspartate.

## 2. Results

### 2.1 Part 1: Optical design of the fundus optical imager of intrinsic signals

The retinal optical imager of intrinsic signal that is developed in this study is a modified fundus camera illuminating the retina using near-infrared light. Using the near-infrared light for imaging allows us to image the rat's retina without being stimulated by the illumination light. Furthermore, the studies of the optical imaging of intrinsic signals in brain determine at least three physiological parameters affecting light reflection during neuronal activity: 1) Change in blood volume 2) The oximetry component (change in oxy/ deoxyhemoglobin ratio) and 3) Light scattering (Frostig et al., 1990; Malonek et al., 1997; Malonek & Grinvald, 1996). The first two factors rely on the increase in metabolic demand of the active tissue. Modern imaging techniques have demonstrated that there is a strong coupling between neuronal activity, local metabolic activity and blood flow (Vanzetta & Grinvald, 2008). The third factor determines the surface reflectance changes due to ionic and/ or water movement due to membrane conformation changes during neuronal activation (D. Ts'o et al., 2009; Zepeda et al., 2004). In the near-infrared region, the difference of light absorption and reflection of oxygenated blood and deoxygenated

*Fig 1-3  
near here*

blood is more pronounced, as is shown in figure 1-3. So the change of the oxygen level in hemoglobin during neuronal activity can be monitored in near-infrared light.

For developing the retinal optical imager, we followed standard optical designs of fundus cameras that have been described in the literature (DeHoog & Schwiegerling, 2009). The retina is illuminated by an illumination source, which is imaged onto the pupil. A camera, through a separate imaging pathway, captures the reflection from the retina. In the literature, the fundus cameras can have two optical designs, which are only different in the implementation of the optical layout: the internal illumination and external illumination (DeHoog & Schwiegerling, 2009). We used an internal illumination design, where the illumination and imaging paths share the objective lens since the results of the study of Dehoog et al. (DeHoog & Schwiegerling, 2009) showed this model to have comparable performance while using less optical components than an external illumination design.

*Fig 2-3  
near here*

### **2.1.1 Zemax simulation**

Zemax software was used for optical design and optimization. The optical paths for illumination and imaging were designed separately, and both in sequential mode. The Zemax design of illumination pathway and imaging pathway, as well as the spot diagram of each pathway, are illustrated in figure 2-3. In the illumination pathway, the first surface is positioned at the source of light, and the last surface is the position at which the cornea will be placed. The holed mirror in the illumination pathway is simulated as a simple mirror, and the central obscuration is simulated as an aperture with a central

circular obscuration. In the imaging pathway, the first surface is placed at the retina of the rat. Although the system is optimized in Zemax to have the minimum aberration, in the spot diagram of the image we observe the existence of spherical aberration of the order of 14  $\mu\text{m}$ . This aberration was not eliminated because of the curvature of the optical elements. It was although deemed acceptable since, for an optical system with  $f/2$  and a wavelength 0.78  $\mu\text{m}$ , the spherical aberration allowances corresponding to one Rayleigh limit ( $\text{OPD} = \lambda/4$ ) is equal to  $4\lambda/\text{NA}$  (Formula 15.16.b from the book of modern optical engineering) [117]. The value for this system is about 12.4  $\mu\text{m}$ , close to the value obtained by simulation.

To have a realistic design of the functional optical imager of intrinsic signals for imaging the retina of the rat, we needed to also integrate the optical characteristics of the rat eye in our simulations. For this aim, we followed the guidelines used to model the human's eye in Zemax: (<http://www.zemax.com/support/knowledgebase/how-to-model-the-human-eye-in-zemax>.) and we changed the parameters of the human eye characteristic by the rat's eye characteristics described in Hughes, and Chaudhuri et al. (Chaudhuri, Hallett, & Parker, 1983; Hughes, 1979). The holed mirror in the imaging pathway was simulated by an aperture having a central opening of 5 mm in diameter. The last surface of the imaging pathway is the detector of the camera.

### 2.1.2 Optical system assembly

Figure 2-3 shows the optical system of the camera. For illuminating the retina, a LED of 780nm was used (M780L2- Thorlabs). This LED was placed at the focal point of a biconvex lens (LB1757- Thorlabs-  $f=30$  mm). The illumination was then relayed to an optical window with a central obscuration (central obscurer in figure 2-3). The second lens of focal 30 mm was then used to image this central obscuration on the holed mirror (element M1 in figure 2-3), which combines the illumination and detection pathway. This mirror reflects the image of the illumination source to the objective lens, which makes an image of the illumination source on the cornea. The same objective lens forms an intermediate image of the retina, which passes through the holed mirror. In the imaging pathway, after the holed mirror, a canon macro lens (EF-S 60mm  $f/2.8$ ) was used to transfer the intermediate image of the retina to the camera. In our setup, the aperture was adjusted to  $f/2$ . This large aperture was desirable because it allows more light in and makes it possible to capture images in low light conditions as well as tissues. The images were captured with a 16-bit scientific CMOS (sCMOS) camera (Pco.edge 5.5) with a pixel size of  $6.5 \mu\text{m}$  and full resolution of  $2560 \times 2160$ . The exposure time of the camera was set to 90ms and the frame rate capture to 10 Hz. The whole optical setup was mounted on an optical breadboard (Thorlabs).

The imaging aperture was set to be the pupil diameter of the rat in full-dilated condition, considered to be 2mm. A second illumination pathway, displayed in green, was used for stimulation. This stimulation light was a full field illumination of the retina by using a

green LED (green LED, 720-LTCN5MGAHB251Z, Mouser Electronics). This illumination is transferred to the retina via a cold mirror (M2) (DMLP605-Thorlabs).

The illumination by infrared light at the cornea should have an annular form, having a central part (corneal window (CW)) reserved for the reflected light from the retina (Pomerantzeff et al. (Mariani, 1981)). Any specular reflection of illumination light in the CW from the cornea should be minimized since it can have a direct influence on the image quality captured from the retina. The use of an appropriate size for the central hole (5 mm) in the holed mirror, and also the use of a central obscurer in the illumination pathway, provided an annular illumination with an internal corneal window of 1 mm, appropriate for the pupil size of 2 mm. A picture of the annular illumination is shown in figure 3-3a while an image of the fundus in Infrared illumination is shown in figure 3-3b.

### **2.1.3 Optical system characterization**

The resolution of the system was measured using the USAF 1951 microscope target (R3L3S1N, Thorlabs, Newton NJ) with the same parameters used in the animal experiments (illumination wavelength of 780nm). The smallest element distinguishable was element 6 of group 3. Using ImageJ software, the resolution, which is measured as the full-width at half maximum (FWHM), was 3 pixels (35  $\mu$ m).

To measure the spatial signal to noise ratio of the imaging system the different parts the image were considered as the region of interests and the intensity of the signal was analyzed from each. The average intensity of the signal and standard error was then calculated. The SNR was calculated then by dividing the average signal measure on its standard error (J. L. Prince & Links, 2006). This value was 20 dB in our system.

*Fig 3-3  
near here*

## **2.2 Part 2: Validation of the optical system**

The second part is dedicated to verifying the validation of the developed retinal optical imager of intrinsic signals in experiments with the rat. There are two series of tests considered for validation of the retinal functional optical imager. At the first set of experiments, the developed retinal functional imager is used to detect the retinal intrinsic signals in the anesthetized rat. The second round of trials is considered with intravitreal injection of a pharmacological agent (aspartate) to verify if the change in the retinal intrinsic signal is detectable by our developed retinal functional imager.

### **2.2.1 Experimental setups and procedure**

All procedures were performed by the directives of the Canadian Council on Animal Care and the ethics review board of the Université de Montréal (CDEA).

### **2.2.2 Animal preparation for in-vivo imaging**

All experiments were done with Long Evans rats (n= 21, 300-400 grams). The rats were anesthetized in the induction chamber with 5% Isoflurane. In order to maintain a stable position of the animal during the experiments with minimal movement as well as to view the eye from different angles with ease, we adopted a model of a head post that was initially designed as a cranial window for imaging in awake rodents (Goldey et al., 2014). The head-post was fixed on the skull bone of the rat using two screws and dental cement. Once it is set on the skull, it can be held one side at a time and then, the rat is placed on a custom stereotaxic frame designed to hold the animal in a stable position and facilitate access to the eye. The designed stereotaxic table provided movement in 3-dimensions to adjust the position of the eye in front of the camera for better visualization. The pupil of the eye was dilated using eye drops (1% atropine) and the cornea was protected against dryness by using artificial eye drops during the experiment. Body temperature was maintained at 37-39 ° C using a heating blanket (homeothermic Blanket, Harvard Apparatus Ltd., England, UK). Electrocardiograms (ECG) were recorded using two electrodes inserted subcutaneous near to the animal chest. To keep the animal under anesthesia during the experiment, it received an intramuscular injections of ketamine (80mg/kg) and xylazine (10mg/kg) during the experiment. ECGs were controlled all the time during the experiment to be sure that the heart rate is stable during the experiments

and also to check the depth of the anaesthesia of the animal by pinching its rear toe and check if there is a change in heart rate as a reflex to this stimulation during the experiment.

### **2.2.3 Intravitreal injection**

Pharmacological experiments were done using aspartate as the pharmacological agent injected into the rats' vitreous. Aspartate is an excitatory amino acid, which is effective in blocking synaptic transmission in the OPL, thereby isolating the photoreceptors from inner retinal cells (Levinger et al., 2012). Our previous study on the rabbit showed the inner retina as the origin of the intrinsic signal in the rabbit's retina, and so the intrinsic signal disappeared after the injection of aspartate (Naderian, Bussieres, Thomas, Lesage, & Casanova, 2017). For injection, a needle (30-G) was inserted perpendicular to the eye surface the most posteriorly possible to the limbus. As soon as the needle penetrated the eyeball, it was angled toward the center of the vitreous humor to ensure the delivery of the drug as close as possible to the retina while avoiding the lens. The procedure was validated by post hoc visual inspection of the lens integrity, and no lens injury was found. After a slow and controlled delivery of the injection volume (2  $\mu$ L), the needle was kept in place for about 10 seconds before its removal. To estimate the final drug concentrations the vitreous volume was established at 52.4  $\mu$ l (Sha & Kwong, 2007). In agreement with a previously published study, the pharmacological agent (aspartate) was dissolved in saline solution (Ward, Jobling, Kalloniatis, & Fletcher, 2005), and the final vitreous concentration was 0.37 mmol. Before each injection, control levels of retinal intrinsic signal were acquired. Subsequently, the injection was performed and the

imaging resumed shortly afterward (approximately 5 min) for about 1.5 hours, on average, after injection.

#### **2.2.4 Electroretinograms (ERGs) recordings**

In order to have control over the effect of the pharmacological agent we use, concurrently with retinal intrinsic imaging, ERGs were recorded using DTL electrodes positioned onto the cornea. The reference electrode was put under the tongue and the ground electrode was put in the tail. The ERG signal was amplified 10,000 times and band-pass filtered from 1 to 1000 Hz using an AC amplifier (P511 series AC amplifier, GRASS, Astro-Med, Inc.). The amplified signal was recorded with a signal acquisition and analyzer processor 1401, controlled by Signal 3.10 software (Cambridge Electronic Design, Cambridge, UK). Components of the ERG were measured: The a-wave amplitude was measured from the baseline and the b-wave was measured from the a-wave minimum to the b-wave peak. The d-wave amplitude is also measured from the baseline (McCulloch et al., 2015). The a-wave mainly reflects the activity of photoreceptors. The b-wave is known to show the activity of bipolar cells and the d-wave considered to reveal the activity of OFF bipolar cells (Heckenlively & Arden, 2006).

#### **2.2.5 Imaging protocol**

The imaging protocol consisted of 300 frames taken in 30 seconds at a rate of 10 frames per second. The protocol had 2 seconds of pre-stimulation imaging, to record the basal activity of the retina, then a green flash of light is presented for 1 second and the stimulus followed by 27 seconds of post stimulation imaging.

### 2.2.6 Imaging results and analyses

Each block of stimulation consisted of 300 frames (10 frames per second). We averaged the intensity of the images over each frame and then followed changes in intensity during the imaging sequence (pre-stimulation, during stimulation and post stimulation).

The average intensity calculated pre-stimulation is showing the basal activity of the retina. Then the stimulus was presented, and the intensity changes after the stimulation were considered to be the intrinsic response of the retina due to the stimulation. To remove the slow drift in the response, we normalized the response post stimulus compared to the response pre-stimulus.

So the intrinsic changes in light reflection ( $\Delta R/R$ ) were calculated as follows: individual data frames ( $R$ ) were first subtracted, pixel by pixel, with the average image from the pre-stimulus period ( $R_{\text{baseline}}$ ) and further normalized by  $R_{\text{baseline}}$  to measure percent-change as shown in the following equation:

$$\Delta R/R \% = (R - R_{\text{baseline}}) / R_{\text{baseline}} \times 100$$

The result of these analyses is shown in figure 4-3 for one block of stimulation as an example.

*Fig 4-3  
near here*

### **2.2.7 Imaging of control retina and aspartate injected retina with the retinal functional imager**

We first wanted to verify the capability of our developed retinal functional imager to capture the retinal intrinsic signal and also to test the existence and repeatability of the intrinsic signal in the rat retina. In this regard, a group of 12 animals' eyes was tested.

Intravitreal injections of aspartate were made on a group of 8 animals to determine if the change in the retinal intrinsic signals is detectable by the rat retinal functional imager. The ERG signals were concomitantly recorder along with the retinal intrinsic signal imaging. It allows us to have a control of the retinal activity due to the stimulation as well as to have a control for the effectiveness of our intravitreal injections.

Figure 5-3 shows the fundamentals of the retinal intrinsic signal captured with retinal functional imager as well as the ERG recordings. Figure 5-3A shows the average retinal intrinsic signal of the group of 12 animals' eyes. The error bars indicate the standard error in 4 points during the registration time course. In this figure, we observe a brief negative peak (decrease in light reflection) following by a positive peak (increase in light reflectance) after the stimulation. This positive phase lasts for 10 seconds ( $10 \pm 1s$ ) on average. This pattern was observed for all animals' eye tested ( $N=12$ ). Figure 5-3B shows the average intrinsic signal of a group of 8 animals' eye receiving intravitreal injection of aspartate. The error bars here also show the standard error. As it is shown in this figure, the intrinsic signal diminished significantly for the  $N = 8$  retinas that were injected with aspartate.

*Fig 5-3  
near here*

The effect of the aspartate injection was controlled by ERG registration. A typical ERG for the control retina is shown in figure 5-3C. After injection of aspartate, the isolation of the photoreceptors is proved by the disappearance of the b-wave in ERG. Figure 5-3D shows an example of the ERG wave after the injection of the aspartate. The results presented here confirm the existence of the intrinsic signal in the rat's retina and also establish the sensitivity of our imaging system in capturing this signal.

### **3. Discussion**

This article is a methodological article describing in detail the method of developing the retinal functional imager of the intrinsic signal for the rat. The retinal imaging of intrinsic signal was used to study the retinal function in vivo in other animal species including cats (J. Schallek, Kardon, et al., 2009; J. Schallek, Li, et al., 2009), monkeys (Hanazono et al., 2007; Tsunoda et al., 2009) and rabbit (Naderian et al., 2017) but this technique was not developed for rat's in-vivo retinal imaging. Using the experiments with rats (intact eyes, as well as intravitreally, injected eye) validates the functionality of the retinal functional imager.

The comparable imaging system is the retinal functional imager, RFI, (Optical Imaging Ltd, Rehovot, Israel), which is used in our former study to explore the retina of rabbit (Naderian et al., 2017). The RFI is designed for human eyes, so its optical design is not suitable to be used with small size eye animal as the rat. Rats have a developed retinal vasculature system and retinal structural organization analogous to human (LeVere, 1978), and so they are one of the animal models used in ophthalmology (A.Tsonics, 2008).

Fundus imaging of the rat has the difficulties in dealing with the refractive properties of the curved cornea and also the poor quality of the rat's lens. These features make it hard to deliver and receive light to the retina and so to generate a high-quality image of the retina. For capturing the intrinsic signal of the retina, the camera should be sensitive to capture the light reflection change of less than 1%. To achieve this goal it requires

complicated and time-consuming alignment of the optical components in the imaging system.

To have the optical elements of the fundus imager aligned; the optics of the eye should also be taken into account. To simulate the rat's eye at first, we have used a gradient index (GRIN) lens as is explained by Goncharov et al. (Goncharov & Dainty, 2007). This essay was not successful because of the difficulty we had to keep the GRIN lens align with the optical axis of the system. The second way was to dissect the rat's eye post-mortem. Although this was a perfect model as we had the exact optics of the rat's eye integrated into our optical imaging system, the cornea of the dissected eye has the limitation of becoming dry and opaque very soon. So we had an insufficient time to control and do the alignment of our optical system with each rat's dissected eye. The size of the eye of the rat is small compared to other animals used for this method of imaging. It, in turn, leads to limitations in the optical design, since everything should be adapted for the small size eye.

One of the limitations is the high curvature of the cornea of the rat when compared to animals with bigger eye size. Using a high power aspheric objective, which is usually utilized in the fundus cameras with rat cornea provides a small field of view in focus and significant spherical aberrations in the periphery of the retinal image. To solve this problem, we changed our objective to a biconvex lens having less curvature to decrease the spherical aberration.

In fundus images, a clear image was seen from most angles, but a small central part of the image was saturated. It is due to specular reflection from the central part of the surface of the cornea. A holed mirror was used to prevent this specular reflection. The high

curvature of the cornea combined with the small depth of field of the imaging system limits the correction. If we change the position of the animal so that the central saturation of reflected light diminishes, the image of the retina also decreases in quality since it will not be in focus. Saturating this central part, we preserved high-quality retinal images outside of the specular region. All the analysis of the post-stimulation was then performed on the parts of the retina has no saturation.

The stimulation flash was presented full field to stimulate the entire retina. So, for the post-stimulation analyses, the response of the whole retina was used (except the saturated part). The intrinsic signal of a smaller region of interest (ROI) limited to the vascular part of the retina, as well as an ROI of non-vascular part of the retina was also analyzed, and the results of all these regions followed the same response shape and time course.

The result of the injection of aspartate to separate the outer retina from the inner retina is in agreement with our other study on the rabbit (Naderian et al., 2017). After the injection of aspartate in both species, the intrinsic signal diminished completely, and these results suggest an origin of inner retinal layers for the intrinsic signals in the retina. We need further experiments to study the exact source of the intrinsic signals in the rat's retina.

A comparable fundus imaging system that is designed for rat's fundus imaging is by using an endoscope (Hernandez et al., 2012). In this imaging system, a GRIN lens is used to be placed over the cornea so that the refractive error reduces. The light is delivered to the retina by the fiber optics built into the endoscope in a ring-shaped structure and the reflected light from the retina is detected from the central circle of this illuminated ring. This system is however insufficient for stimulating the retina, on the contrary to our system that gives us a broad choice of using different stimuli and so to

study the intrinsic response of the retina to the stimuli. In our imaging system, we have used a green light to stimulate the retina but the stimulus can be easily changed, and the retina can be stimulated by different patterns by just replacing the green LED by another stimulus. An LCD can be used for projecting the pattern stimuli on the eye.

**Acknowledgments:** This work was supported by a NSERC grant to Dr. Christian Casanova. We thank Dr. Sébastien Thomas for his scientific advises and Geneviève Cyr for her technical help.

## References

- A.Tsonics, Panagiotis. (2008). *Animal models in eye research*: Academic press.
- Akula, J. D., Favazza, T. L., Mocko, J. A., Benador, I. Y., Asturias, A. L., Kleinman, M. S., . . . Fulton, A. B. (2010). The anatomy of the rat eye with oxygen-induced retinopathy. *Doc Ophthalmol*, *120*(1), 41-50. doi: 10.1007/s10633-009-9198-1
- Barnett, J. M., Yanni, S. E., & Penn, J. S. (2010). The development of the rat model of retinopathy of prematurity. *Doc Ophthalmol*, *120*(1), 3-12. doi: 10.1007/s10633-009-9180-y
- Bennett, T. J., & Barry, C. J. (2009). Ophthalmic imaging today: an ophthalmic photographer's viewpoint - a review. *Clin Experiment Ophthalmol*, *37*(1), 2-13. doi: 10.1111/j.1442-9071.2008.01812.x
- Chaudhuri, A., Hallett, P. E., & Parker, J. A. (1983). Aspheric curvatures, refractive indices and chromatic aberration for the rat eye. *Vision Res*, *23*(12), 1351-1363.
- Costa, R. A., Skaf, M., Melo, L. A., Jr., Calucci, D., Cardillo, J. A., Castro, J. C., . . . Wojtkowski, M. (2006). Retinal assessment using optical coherence tomography. *Prog Retin Eye Res*, *25*(3), 325-353. doi: 10.1016/j.preteyeres.2006.03.001
- Cringle, S. J., & Yu, D. Y. (2010). Oxygen supply and consumption in the retina: implications for studies of retinopathy of prematurity. *Doc Ophthalmol*, *120*(1), 99-109. doi: 10.1007/s10633-009-9197-2
- DeHoog, E., & Schwiegerling, J. (2009). Fundus camera systems: a comparative analysis. *Appl Opt*, *48*(2), 221-228.
- Fercher, A. F. (2010). Optical coherence tomography - development, principles, applications. *Z Med Phys*, *20*(4), 251-276. doi: 10.1016/j.zemedi.2009.11.002
- Frostig, R. D., Lieke, E. E., Ts'o, D. Y., & Grinvald, A. (1990). Cortical functional architecture and local coupling between neuronal activity and the microcirculation revealed by in vivo high-resolution optical imaging of intrinsic signals. *Proc Natl Acad Sci U S A*, *87*(16), 6082-6086.
- Goldey, G. J., Roumis, D. K., Glickfeld, L. L., Kerlin, A. M., Reid, R. C., Bonin, V., . . . Andermann, M. L. (2014). Removable cranial windows for long-term imaging in awake mice. *Nat Protoc*, *9*(11), 2515-2538. doi: 10.1038/nprot.2014.165
- Goncharov, A. V., & Dainty, C. (2007). Wide-field schematic eye models with gradient-index lens. *J Opt Soc Am A Opt Image Sci Vis*, *24*(8), 2157-2174.
- Grinvald, A., Lieke, E., Frostig, R. D., Gilbert, C. D., & Wiesel, T. N. (1986). Functional architecture of cortex revealed by optical imaging of intrinsic signals. *Nature*, *324*(6095), 361-364. doi: 10.1038/324361a0
- Hanazono, G., Tsunoda, K., Kazato, Y., Tsubota, K., & Tanifuji, M. (2008). Evaluating neural activity of retinal ganglion cells by flash-evoked intrinsic signal

- imaging in macaque retina. *Invest Ophthalmol Vis Sci*, 49(10), 4655-4663. doi: 10.1167/iovs.08-1936
- Hanazono, G., Tsunoda, K., Shinoda, K., Tsubota, K., Miyake, Y., & Tanifuji, M. (2007). Intrinsic signal imaging in macaque retina reveals different types of flash-induced light reflectance changes of different origins. *Invest Ophthalmol Vis Sci*, 48(6), 2903-2912. doi: 10.1167/iovs.06-1294
- Heckenlively, John R., & Arden, Geoffrey B. (2006). Origins of slow electrophysiological components *Principle and practice of clinical electrophysiology of vision* (pp. 121-234): MIT press.
- Hernandez, V., Albin, T., Lee, W., Rowaan, C., Nankivil, D., Arrieta, E., & Parel, J. M. (2012). A portable, contact animal fundus imaging system based on Rol's GRIN lenses. *Vet Ophthalmol*, 15(3), 141-144. doi: 10.1111/j.1463-5224.2011.00935.x
- Hughes, A. (1979). A schematic eye for the rat. *Vision Res*, 19(5), 569-588.
- Inomata, K., Tsunoda, K., Hanazono, G., Kazato, Y., Shinoda, K., Yuzawa, M., . . . Miyake, Y. (2008). Distribution of retinal responses evoked by transscleral electrical stimulation detected by intrinsic signal imaging in macaque monkeys. *Invest Ophthalmol Vis Sci*, 49(5), 2193-2200. doi: 10.1167/iovs.07-0727
- Johnson, E. C., Guo, Y., Cepurna, W. O., & Morrison, J. C. (2009). Neurotrophin roles in retinal ganglion cell survival: lessons from rat glaucoma models. *Exp Eye Res*, 88(4), 808-815. doi: 10.1016/j.exer.2009.02.004
- LeVere, T. E. (1978). The primary visual system of the rat: A primer of its anatomy. *Physiological Psychology*, 6( 2), 142-169. doi: 10.3758/BF03326707
- Levinger, E., Zemel, E., & Perlman, I. (2012). The effects of excitatory amino acids and their transporters on function and structure of the distal retina in albino rabbits. *Doc Ophthalmol*. doi: 10.1007/s10633-012-9354-x
- Li, Y. C., Luo, J. M., Lu, R. W., Liu, K. M., Levy, A. M., & Yao, X. C. (2012). Dynamic intrinsic optical signal monitoring of electrically stimulated inner retinal neural response. *J Mod Opt*, 59(11). doi: 10.1080/09500340.2012.687464
- Li, Y. C., Strang, C., Amthor, F. R., Liu, L., Li, Y. G., Zhang, Q. X., . . . Yao, X. C. (2010). Parallel optical monitoring of visual signal propagation from the photoreceptors to the inner retina layers. *Opt Lett*, 35(11), 1810-1812. doi: 10.1364/OL.35.001810
- Malonek, D., Dirnagl, U., Lindauer, U., Yamada, K., Kanno, I., & Grinvald, A. (1997). Vascular imprints of neuronal activity: relationships between the dynamics of cortical blood flow, oxygenation, and volume changes following sensory stimulation. *Proc Natl Acad Sci U S A*, 94(26), 14826-14831.
- Malonek, D., & Grinvald, A. (1996). Interactions between electrical activity and cortical microcirculation revealed by imaging spectroscopy: implications for functional brain mapping. *Science*, 272(5261), 551-554.
- Mariani, A. P. (1981). A diffuse, invaginating cone bipolar cell in primate retina. *J Comp Neurol*, 197(4), 661-671. doi: 10.1002/cne.901970408
- McCulloch, D. L., Marmor, M. F., Brigell, M. G., Hamilton, R., Holder, G. E., Tzekov, R., & Bach, M. (2015). ISCEV Standard for full-field clinical electroretinography

- (2015 update). *Doc Ophthalmol*, 130(1), 1-12. doi: 10.1007/s10633-014-9473-7
- Naderian, A., Bussieres, L., Thomas, S., Lesage, F., & Casanova, C. (2017). Cellular origin of intrinsic optical signals in the rabbit retina. *Vision Res*, 137, 40-49. doi: 10.1016/j.visres.2017.04.015
- Prince, Jerry L., & Links, Jonathan M. (2006). *Medical imaging signals and systems*: Pearson Education, Inc. .
- Schallek, J. B., McLellan, G. J., Viswanathan, S., & Ts'o, D. Y. (2012). Retinal intrinsic optical signals in a cat model of primary congenital glaucoma. *Invest Ophthalmol Vis Sci*, 53(4), 1971-1981. doi: 10.1167/iovs.11-8299
- Schallek, J., Kardon, R., Kwon, Y., Abramoff, M., Soliz, P., & Ts'o, D. (2009). Stimulus-evoked intrinsic optical signals in the retina: pharmacologic dissection reveals outer retinal origins. *Invest Ophthalmol Vis Sci*, 50(10), 4873-4880. doi: 10.1167/iovs.08-3291
- Schallek, J., Li, H., Kardon, R., Kwon, Y., Abramoff, M., Soliz, P., & Ts'o, D. (2009). Stimulus-evoked intrinsic optical signals in the retina: spatial and temporal characteristics. *Invest Ophthalmol Vis Sci*, 50(10), 4865-4872. doi: 10.1167/iovs.08-3290
- Schallek, J., & Ts'o, D. (2011). Blood contrast agents enhance intrinsic signals in the retina: evidence for an underlying blood volume component. *Invest Ophthalmol Vis Sci*, 52(3), 1325-1335. doi: 10.1167/iovs.10-5215
- Sha, O., & Kwong, W.H. (2007). Postnatal Developmental Changes of Vitreous and Lens Volumes in Sprague-Dawley Rats. *Neuroembryology and Aging*, 4(4), 183-188. doi: 10.1159/000118928
- Ts'o, D., Schallek, J., Kwon, Y., Kardon, R., Abramoff, M., & Soliz, P. (2009). Noninvasive functional imaging of the retina reveals outer retinal and hemodynamic intrinsic optical signal origins. *Jpn J Ophthalmol*, 53(4), 334-344. doi: 10.1007/s10384-009-0687-2
- Tsunoda, K., Hanazono, G., Inomata, K., Kazato, Y., Suzuki, W., & Tanifuji, M. (2009). Origins of retinal intrinsic signals: a series of experiments on retinas of macaque monkeys. *Jpn J Ophthalmol*, 53(4), 297-314. doi: 10.1007/s10384-009-0686-3
- Tsunoda, K., Oguchi, Y., Hanazono, G., & Tanifuji, M. (2004). Mapping cone- and rod-induced retinal responsiveness in macaque retina by optical imaging. *Invest Ophthalmol Vis Sci*, 45(10), 3820-3826. doi: 10.1167/iovs.04-0394
- Vanzetta, I., & Grinvald, A. (2008). Coupling between neuronal activity and microcirculation: implications for functional brain imaging. *HFSP J*, 2(2), 79-98. doi: 10.2976/1.2889618
- Vidal-Sanz, M., Salinas-Navarro, M., Nadal-Nicolas, F. M., Alarcon-Martinez, L., Valiente-Soriano, F. J., de Imperial, J. M., . . . Villegas-Perez, M. P. (2012). Understanding glaucomatous damage: anatomical and functional data from ocular hypertensive rodent retinas. *Prog Retin Eye Res*, 31(1), 1-27. doi: 10.1016/j.preteyeres.2011.08.001
- Ward, M. M., Jobling, A. I., Kalloniatis, M., & Fletcher, E. L. (2005). Glutamate uptake in retinal glial cells during diabetes. *Diabetologia*, 48(2), 351-360. doi: 10.1007/s00125-004-1639-5

- Webb, R. H., & Hughes, G. W. (1981). Scanning laser ophthalmoscope. *IEEE Trans Biomed Eng*, 28(7), 488-492. doi: 10.1109/TBME.1981.324734
- Zepeda, A., Arias, C., & Sengpiel, F. (2004). Optical imaging of intrinsic signals: recent developments in the methodology and its applications. *J Neurosci Methods*, 136(1), 1-21. doi: 10.1016/j.jneumeth.2004.02.025

## Figures

Figure 1-3: the optical absorption spectra of oxyhemoglobin in blue and deoxyhemoglobin in red. The figure adapted from <http://omlc.org/spectra/hemoglobin/>

Figure 2-3: The Optical design of the fundus camera: (A) A schematic of the retinal optical imager of intrinsic signals. Red tracing shows the illumination pathway, green tracing shows the stimulation pathway and the black tracing shows the imaging pathway. M1 is the holed mirror and M2 a cold mirror. (B) The spot diagram of the illumination pathway design from Zemax simulation. The scale bar value is in  $\mu\text{m}$ . (C) The spot diagram of the imaging pathway design from Zemax simulation. The scale bar value is in  $\mu\text{m}$ .

Figure 3-3: (A) The annular illumination on the target. (B) The fundus image of the rat in infrared illumination. The white part of the picture is the part of the picture, which is saturated by the high intensity of the light reflection.

Figure 4-3: An example of one block of stimulation. The normalized intrinsic signal of the rat's eye due to a stimulus of 1 second. The figure shows the average intensity changes in the image of the fundus during the 30 seconds of imaging. The x-axis indicates the time in seconds, and the y-axis shows the percentage of the intensity change value of the image. The green light stimulus is presented between the second and third seconds. After the stimulation, it appears a very brief negative peak, following by a positive peak, which lasts 10 seconds (from the moment 5 to 15). After this intense response, the intrinsic signal fluctuates around the basic level. The error bars show the standard error at 4 points in time.

Figure 5-3: The intrinsic signal of the rat's retina. (A) The average of the normalized retinal intrinsic signal in the 12 animal's eye. The error bars show the standard error at 4 points in time. (B) The intrinsic retinal signal of 8 animal's eye, intravitreally injected with the aspartate. (C) An example of the ERG wave of the control eye. The a-wave, b-wave, and d-wave measures are shown in red traces. (D) An example of the ERG wave following the aspartate injection, only the a-wave is preserved.

Figure 1-3

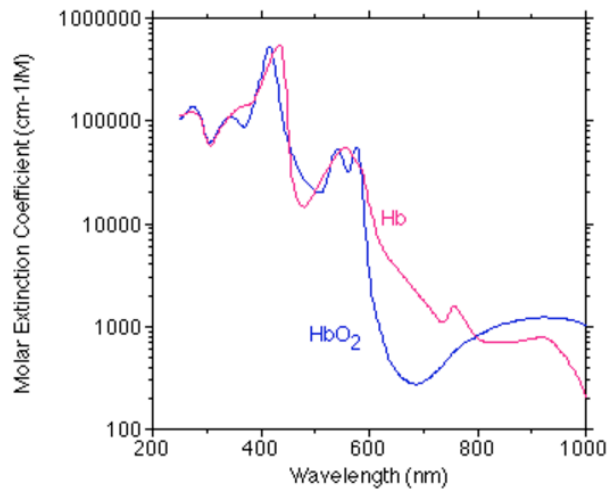


Figure 2-3

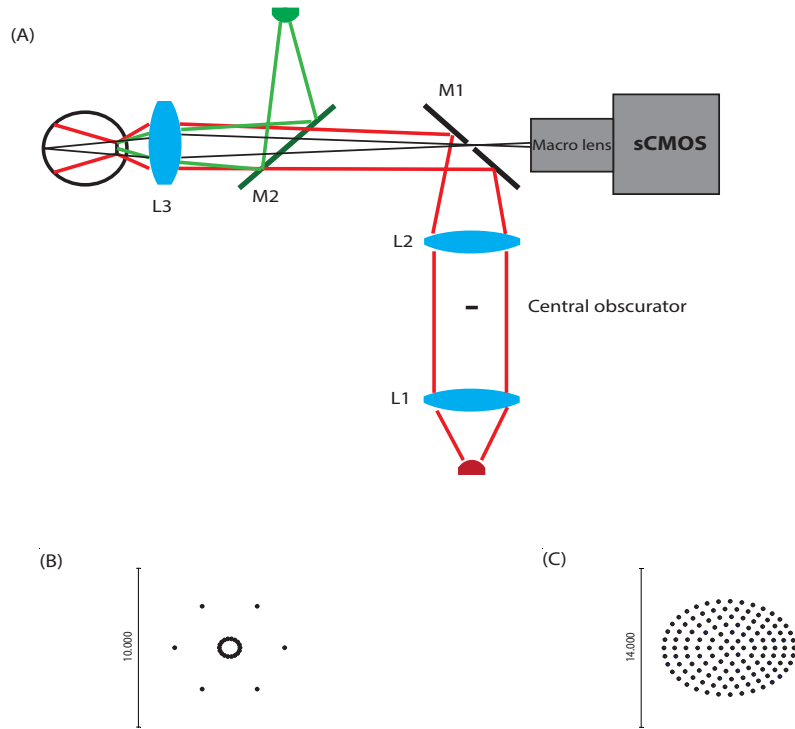
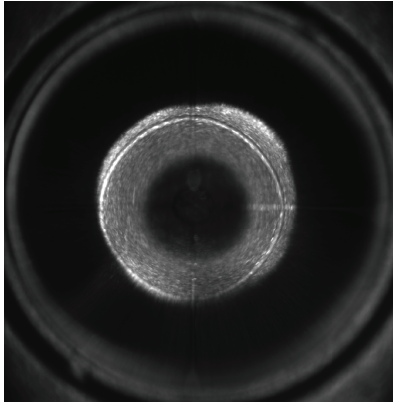


Figure 3-3

(A)



(B)



Figure 4-3

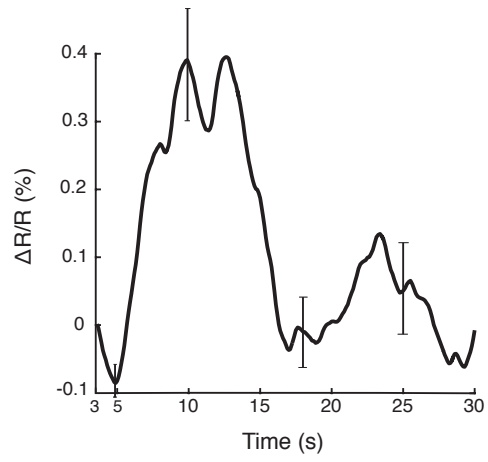
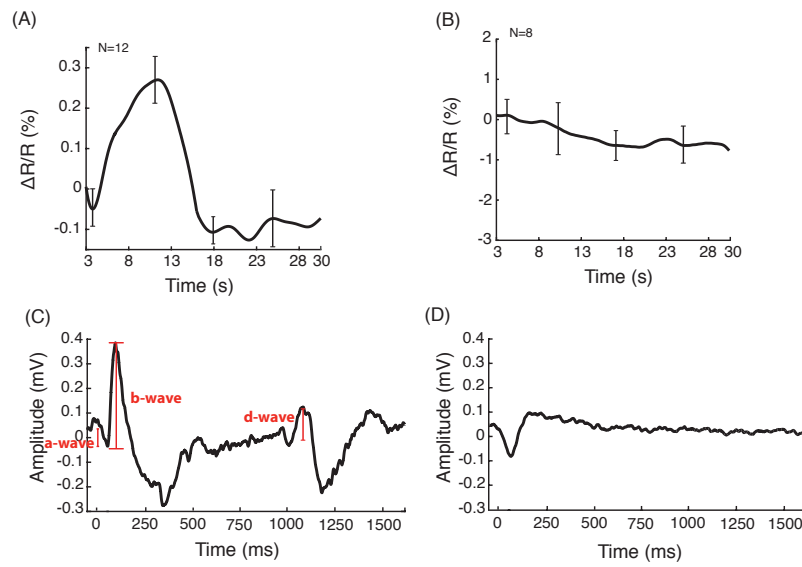


Figure 5-3



## Chapter 4

### 1. Discussion

Optical imaging of intrinsic signals was first developed for mapping the cortical activity (Grinvald et al., 1986). This method of imaging employs the change of optical properties in the brain such as blood flow/oxygenation, cellular volume change, or refractive index change during neuronal activation using near-infrared light to study cortical activity. Optical imaging of intrinsic signals using infrared light is also used to investigate the neuronal function of the retina (Hanazono et al., 2007; J. Schallek, Li, et al., 2009; Tsunoda et al., 2009). The intrinsic signals are studied in-vivo (Hanazono et al., 2008; Hanazono et al., 2007; Inomata et al., 2008; Mihashi et al., 2011; J. B. Schallek et al., 2012; J. Schallek, Li, et al., 2009; J. Schallek & Ts'o, 2011; D. Ts'o et al., 2009; Tsunoda et al., 2004) and in-vitro (Y. C. Li et al., 2010) in the retina of different animal species. Despite the agreement on the presence of the retinal intrinsic signals in different animal species, there is yet no consensus regarding the anatomical origins of these signals. Once the character and anatomical source of the retinal intrinsic signals are completely understood, this functional imaging method can be used for retinal studies, characterization of the retinal diseases and for monitoring the therapeutic effects.

Our study focused on the retinal optical imaging of intrinsic signals following two aims: The first was to explore and characterize the retinal intrinsic signal using retinal functional imager (RFI). Since RFI is designed for human eyes, we chose rabbit as our animal model, having big eyes close to the human's eye size.

The second aim was to design and develop a retinal functional imager of the intrinsic signal for small size eye animals like rats. We chose rat since they are widely used in ophthalmology, and they are available in genetically mutant models. Having this functional imager adapted for rat's retina would open the door to the future studies on models of retinal diseases.

### **1.1 Summary of results**

Our results using RFI on rabbit's retina demonstrate that rabbit's retinal intrinsic signals (RIS), stimulating from a stimulus of 200 msec, are biphasic. The first negative phase arising very quickly and reaching its maximum within a second of stimulation onset and the positive peak which follows it reaches its maximum approximately 10 seconds after stimulus onset. Our data indicate that retinal intrinsic signals are spatially restricted to the stimulated retinal segments. They couldn't be observed in all the retinal loci. Although a strong RIS was always detected in the visual streak, we haven't register RIS at the optic nerve head, the myelinated region of the nerve fibers or the vascular part of the retina. We examined the stimulus-dependency of the intrinsic signals, and the results show that RIS increased as a function of light intensity for a limited range of intensities (from 12-25cd.m<sup>-2</sup>).

ERG signals were recorded along with the RIS imaging, allowing a direct comparison between the two functional recordings. A strong correlation between RIS and ERG b-wave suggest a common cellular origin of the ON-bipolar cells in rabbit retina. Using pharmacological agents to determine the contribution of the different retinal cells in the

genesis of RIS confirms that the RIS arise from the activity of the inner retina with a dominant contribution from ON bipolar cells.

The second study was to develop a functional retinal imager, and the majority of the resulting paper includes the methodology used to develop the retinal functional imager. This functional imager is validating by using rat's experiments. The results of RIS from 12 eye tested show the presence and repeatability of the response. Using intravitreal injection of aspartate in 8 eyes diminished the retinal intrinsic signal.

## **1.2 Compare & Contrast**

This study was the first, which examined the intrinsic signal of rabbit retina through optical imaging. The comparable studies were done on other animal species. The results of these studies indicate that the characteristics of RIS and its cellular origins are subject to significant inter-species differences (Y. G. Li, Zhang, Liu, Amthor, & Yao, 2010; D. Ts'o et al., 2009; Tsunoda et al., 2009; Yao, 2009). Several studies are questioning the retinal intrinsic signal using OCT imaging (Akhlagh Moayed, Hariri, Choh, & Bizheva, 2012; Srinivasan, Wojtkowski, Fujimoto, & Duker, 2006; Wang & Yao, 2016). Among the different studies on the retinal intrinsic signal, there are mostly the studies of two groups, Schalleck et al. on cats and Hanazono et al. on macaque that have a comparable experimental paradigm to our studies so I will get more into detail about these studies and compare their results with ours.

The study of optical intrinsic signals in cat's retina shows two predominant signals after presenting a bar of stimulation ( $7.7 \text{ cd}\cdot\text{m}^{-2}$ ) for 3 seconds. A negative signal, which

corresponds to a relative decrease in reflectance co-localized with the stimulated region and the second signal with positive polarity, which appears adjacent and only on one side of the negative signal. This positive signal is although not observed in all of their results. Both of these signals have the same time course. They appear within the 500 ms of stimulus onset, they both increase monophasically with opposing polarity during the 3 seconds of stimulation, and they both decrease slowly towards baseline after the stimulus turned off (J. Schallek, Li, et al., 2009; D. Ts'o et al., 2009).

They declare that the biophysical mechanism of the observed intrinsic signal in the cat eyes is because of the changes in blood volume (J. Schallek & Ts'o, 2011). They examined the intrinsic signal characteristic before and after the injection of blood contrast agents (nigrosin and indocyanine green), and their results demonstrate that the injection of these agents effectively increased the functional intrinsic signal strength. They conclude that this enhancement of the intrinsic signal suggests that the changes in blood volume in response to the visual stimulation is a component of the retinal intrinsic optical signal in the cat's retina (J. Schallek & Ts'o, 2011).

To identify the contribution from specific retinal layers on the intrinsic retinal signal of the cat, schallek et al. (J. Schallek, Kardon, et al., 2009) injected intravitreally three pharmacological agents (TTX, APB, and PDA). They have examined the intrinsic signal characteristics before and after the drug application. Their results show the persistence of the intrinsic signals after the injection of all the drugs. They concluded that the dominant intrinsic signals arise from the outer retina (J. Schallek, Kardon, et al., 2009; D. Ts'o et al., 2009).

The study on macaque's retina using a xenon flash of 1 ms, given to the entire posterior pole of the ocular fundus with a maximum intensity of 308 cd.s/m<sup>2</sup>, shows the existence of two different group of intrinsic signals (Hanazono et al., 2007). Both of the signals appear 500 ms after the initiation of data acquisition. A fast signal with the peak after 100 ms was observed in the fovea and a slow signal with the maximum peak after 5-6 seconds was recorded from the optic disc and non-foveal posterior retina. To find out the mechanism underneath these two retinal intrinsic signal, Hanazono et al. have measured the flash evoked retinal blood flow changes by laser Doppler flowmetry. The results show that the blood flow at the optic disc gradually increase and reached a peak at 7.5 seconds following the stimulus flash. This time course is similar to the time course of slow RIS, and so they concluded that the slow intrinsic signal reflects the blood flow changes following stimulation. They have also observed the change in blood volume, and they couldn't find any correlation between the flash stimulus intrinsic signals and blood volume changes. They also couldn't see any change in the blood flow evoked by stimulus flash in the foveal area. They conclude that the fast signal at the fovea results from the scattering changes from the structural changed in photoreceptor layer (Tsunoda et al., 2009). To determine what triggers the blood flow increase and so to find the anatomical origin for the slow signals they have injected TTX intravitreally. After the injection of the TTX, the slow signal abolished so they concluded that the RGCs are the primary triggers of the flashed induced blood flow change and the cellular origin of the slow intrinsic signal in the macaque retina (Hanazono et al., 2007; Tsunoda et al., 2009).

Comparing the form and time course of the intrinsic signal in the rabbit with the studies on cat and macaque, we conclude that the kinetics of RIS responses in rabbits is

comparable to the ones reported in cats and primates models (D. Ts'o et al., 2009; Tsunoda et al., 2009). In contrast, the form of the negative and positive response is different in rabbit and cat. Our results demonstrate that rabbit RIS are biphasic and that both phases of the signal (negative and positive) are co-localized and reflect with high spatial fidelity the retinal stimulation site. The negative peak of RIS rose very quickly, within a second of stimulation onset, whereas the positive peak reached its maximum approximately 10 seconds after stimulus onset, only to get back to baseline levels after 60 seconds. In contrast, negative and positive phases of cat RIS are spatially separated. The RIS negative phase is confined to the stimulated retinal region, whereas signals with a positive phase are only found on the periphery of the stimulation site (J. Schallek, Li, et al., 2009; D. Ts'o et al., 2009). In primates, RIS signals are mainly negative, and their kinetics depend on the retinal region being stimulated (Hanazono et al., 2007; Ivo Vanzetta, 2014). The time course of the RIS in our study with rabbit was comparable to the RIS describes in cats and slow RIS in primates (Hanazono et al., 2007; D. Ts'o et al., 2009; Tsunoda et al., 2009).

In the study of the retinal intrinsic signal on macaque, Hanazono et al. (Hanazono et al., 2007) have reported different intrinsic signal depending on the retinal site of stimulation. In our data, when images were divided into multiple ROIs, we did not find any regional specificity in RIS waveforms, but we have not done a systematic study on this. What we found, however, is that optical signals were absent at the optic nerve head (ONH) location, in the nearby myelinated optic fibers, and in the vascularized regions. The reliable and robust responses were always located along the visual streak area, i.e., the avascular part of the retina. This result is at odds with results described in the macaque

monkey where functional responses are also observed in the blood-vessel-rich optic nerve (Ivo Vanzetta, 2014). In agreement with our result schalleck et al. also were unable to find any evidence of a spatial relationship between the signals and the retinal vasculature (D. Ts'o et al., 2009). The reason for this discrepancy can be probably because of the inter-species differences and the difference in mechanisms underneath the retinal intrinsic signals in different species.

Our data from pharmacological dissection of the retina suggest that, in rabbits, RIS arise from the activity of the inner retina. This result is in contrast to the cat finding showing a principal role of the photoreceptors in the genesis of intrinsic signals (J. Schalleck, Kardon, et al., 2009; D. Ts'o et al., 2009).

The exact cellular mechanism at the origin of retinal intrinsic signals is still poorly understood, and there is still not an agreement between the results of experiments on different animal species. In primates, slow RIS is thought to be controlled by retinal ganglion cells that trigger blood flow changes in vessels and capillaries (Tsunoda et al., 2009). While we cannot rule out the contribution of ganglion cells in rabbits, we suggest, based on the weak effect of the TTX injections, that part of RIS originated from the activity of retinal amacrine cells. The mechanism at the origin of rabbit RIS likely consists of cellular mechanisms such as hyperpolarisation-induced changes in light scattering, osmotic changes in cytoplasmic volume, or the oxygenation change in neuroglobins (Burmester, Weich, Reinhardt, & Hankeln, 2000; Zepeda et al., 2004) because of the rabbit retina's poor irrigation (Yu & Cringle, 2004) and the major role played by bipolar cells in RIS generation. Neuroglobins are respiratory protein, which is discovered to exist in the retina in a high concentration (Schmidt et al., 2003). Our data

also indicate that ON bipolar cells' activity plays a major role in RIS under mesopic conditions in rabbits, with a possible small contribution of amacrine cells.

The second part of our research studied the imaging on rat retina. This study is valuable because of the methodological details of the retinal functional optical imager, which is adapted for rat retina. The experimental results with rat validate the functionality of developed functional imager. The intrinsic signal in the rat retina needs more investigation to be comparable with the studies of retinal intrinsic signals on other animal species. A comparison of the preliminary results of the intrinsic signals in rat with our results on rabbit shows comparable results.

Our data demonstrate that after a stimulus of 1 second of green light we observed a decrease in light reflection that peak 2 seconds after the stimulus offset. This initial dip was followed by an increase in light reflectance. This positive response peaked at 10 seconds following stimulus onset. Comparing the rat and rabbit retinal intrinsic signals, both show a biphasic form of response. The intrinsic signal of a smaller region of interest (ROI) limited to the vascular part of the retina, as well as an ROI of non-vascular part of the retina was also analyzed and the results suggest no specific spatial relationship between the signals and the retinal vasculature.

The result of the injection of aspartate to separate the outer retina from the inner retina is in agreement with our other study on the rabbit. After the injection of aspartate in both species, the intrinsic signal diminished completely at the same time as ERG b-wave. These results suggest an origin of inner retinal layers for the intrinsic signals in the retina. Although we need further experiments to study the exact source of the intrinsic signals in

the rat's retina, both systems indicate the existence of the intrinsic signal in the retina and both are in agreement for the inner retinal origin of the intrinsic signal.

A comparable fundus imaging system that is designed for rat's fundus imaging is by using an endoscope (Hernandez et al., 2012). In this imaging system, a GRIN lens is used to be placed over the cornea so that the refractive error reduces. The light is delivered to the retina by the fiber optics built into the endoscope in a ring-shaped structure and the reflected light from the retina is detected from the central circle of this illuminated ring. This system is however insufficient for stimulating the retina, on the contrary to our system that gives us a broad choice of using different stimuli and so to study the intrinsic response of the retina to the stimuli. In our imaging system, we have used a green light to stimulate the retina but the stimulus can be easily changed, and the retina can be stimulated by different patterns by just replacing the green LED by another stimulus. An LCD can be used for projecting the pattern stimuli on the eye.

There is a study that compares the two prototype of the miniaturized fundus camera. One with the graded refractive index (GRIN)-based optics, and the other with conventional optics. Their results indicate that although with using the GRIN lens the diameter of the contact lens can be minimal, the conventional optics perform better concerning image quality (Gliss, Parel, Flynn, Pratisto, & Niederer, 2004).

### **1.3 Technical difficulties**

In our experiments using RFI for rabbit retina, we had some limitations regarding the duration of the stimulation. The maximum duration that we could achieve with RFI was limited to one second, and this restriction was from the conventional fundus camera.

Another limitation of this study was to integrate an LCD to the RFI to stimulate the retina with pattern stimuli. The LCD was imaged to the rabbit's eye by using a convex lens. Our attempts to replace the integrated green flashing light and replace it with an LCD were not successful.

The intrinsic signals are the reflection change of the active tissue of less than 1%. To capture these signals, we need a sensitive imaging system having an excellent optical quality. Designing of a retinal functional imager for rat's retina has the difficulties in dealing with the refractive properties of the curved cornea and also the poor quality of the rat's lens. These features make it hard to deliver and receive light to the retina and so to generate a high-quality image of the retina. To achieve a retinal functional imager for rat retina it requires complicated and time-consuming alignment of the optical components in the imaging system.

Another difficulty in this regard was to integrate the optic of the rat's eye in our optical design and implementation. The first approach that we had for this aim was to use a gradient index (GRIN) lens having the similar diameter size to the rat's pupil and try to capture an image that was contacted at the other surface of the GRIN lens. Using a GRIN lens as a model for the eye is explained by Goncharov et al. (Goncharov & Dainty, 2007). This approach was not successful because of the difficulties we had to hold the GRIN lens align with the optical axis of the functional imager system. The second method was to use the dissected eye of the rat. The cornea of the dissected eye has the limitation of becoming dry and opaque very soon. So we had an insufficient time to control and do the alignment of our optical system with each rat's dissected eye.

Another limitation was to use a high power aspheric objective, which is usually employed in the fundus cameras, with rat cornea. Because of the high curvature of the cornea of the rat, this objective lens provides a small field of view in focus and significant spherical aberrations in the periphery of the retinal image. To solve this problem, we changed our objective lens to a biconvex lens having less curvature to decrease the spherical aberration. The high curvature of the cornea also limited us in preventing the specular reflection from the cornea. Changing the position of the animal so that the central saturation of reflected light diminishes, the image of the retina also decrease in quality since it will not be in focus. Saturating this central part, we preserved high-quality retinal images outside of the specular region. All the analysis of the post-stimulation was then performed on the parts of the retina has no saturation.

## **2. Prospective**

The existence of the intrinsic signals in the retina is shown in different species (Hanazono et al., 2007; Hirohara et al., 2013; J. Schallek, Kardon, et al., 2009; J. Schallek, Li, et al., 2009; D. Ts'o et al., 2009; Tsunoda et al., 2009), there are however discrepancies in the origin of intrinsic signals reported by these studies on various species.

More studies can be done to surmount this gap. One part of this difference can be because of the differences in the animal species or the experimental protocol used in different studies. Comparative studies can be done using one experimental paradigm on various species, and also to use the different experimental model presented in related studies on one animal species. These comparative studies would help to better understand the role of the experimental paradigm and different species on the intrinsic signals. Also, the result of these comparative studies can contribute to having a general conclusion regardless of the animal species used.

Another aspect of the retinal intrinsic signal which is not completely understood is the temporal and spatial character of these signals. The retinal intrinsic signal can be studied and characterized by using different stimuli from simple flashes to more complex stimuli. The different duration of flashes can be tested to examine its influence on intrinsic signals. Also, more complex stimuli as bars of black and white can be presented with a different spatial presentation of the bright part and study its influence on the intrinsic

signal.

Another study in this field can be a comparative study of the retinal intrinsic signal and cortical intrinsic signal that are revealed by the same stimulation. In this regard, the temporal relationship between these two signals can be studied. Also, this kind of studies can be used to investigate the influence of different pharmacological agents on the visual pathway, from the retina to the visual cortex.

The retinal optical imager of the intrinsic signal which is adapted for the rat's retina also can be of great use in all the studies indicated above. Since this retinal functional imager is not yet thoroughly studied and characterized, there is the need for more studies to find the anatomical origin of the intrinsic signal by using different pharmacological agents as it is used for cat and rabbit (Naderian et al., 2017; J. Schallek, Kardon, et al., 2009).

The retinal functional imager can also be used in various clinical studies.

## References

- A.Tsonics, Panagiotis. (2008). *Animal models in eye research*: Academic press.
- Akhlagh Moayed, A., Hariri, S., Choh, V., & Bizheva, K. (2012). Correlation of visually evoked intrinsic optical signals and electroretinograms recorded from chicken retina with a combined functional optical coherence tomography and electroretinography system. *J Biomed Opt*, 17(1), 016011. doi: 10.1117/1.JBO.17.1.016011
- Akula, J. D., Favazza, T. L., Mocko, J. A., Benador, I. Y., Asturias, A. L., Kleinman, M. S., . . . Fulton, A. B. (2010). The anatomy of the rat eye with oxygen-induced retinopathy. *Doc Ophthalmol*, 120(1), 41-50. doi: 10.1007/s10633-009-9198-1
- Alm, A., & Bill, A. (1973). Ocular and optic nerve blood flow at normal and increased intraocular pressures in monkeys (*Macaca irus*): a study with radioactively labelled microspheres including flow determinations in brain and some other tissues. *Exp Eye Res*, 15(1), 15-29.
- Ames, A., 3rd. (1992). Energy requirements of CNS cells as related to their function and to their vulnerability to ischemia: a commentary based on studies on retina. *Can J Physiol Pharmacol*, 70 Suppl, S158-164.
- Barnett, J. M., Yanni, S. E., & Penn, J. S. (2010). The development of the rat model of retinopathy of prematurity. *Doc Ophthalmol*, 120(1), 3-12. doi: 10.1007/s10633-009-9180-y
- Bennett, T. J., & Barry, C. J. (2009). Ophthalmic imaging today: an ophthalmic photographer's viewpoint - a review. *Clin Experiment Ophthalmol*, 37(1), 2-13. doi: 10.1111/j.1442-9071.2008.01812.x
- Bloomfield, S. A., & Dowling, J. E. (1985). Roles of aspartate and glutamate in synaptic transmission in rabbit retina. I. Outer plexiform layer. *J Neurophysiol*, 53(3), 699-713.
- Botir T. Sagdullaev, Tomomi Ichinose, Erika D. Eggers, and Peter D. Lukasiewicz. (2008). Visual Signal Processing in the Inner Re. In a. C. J. B. Joyce Tombran-Tink (Ed.), *Visual Transduction and Non-Visual Light Perception*: humana press.
- Boycott, B. B., & Wassle, H. (1974). The morphological types of ganglion cells of the domestic cat's retina. *J Physiol*, 240(2), 397-419.
- Burmester, T., Weich, B., Reinhardt, S., & Hankeln, T. (2000). A vertebrate globin expressed in the brain. *Nature*, 407(6803), 520-523. doi: 10.1038/35035093
- Caldwell, J. H., & Daw, N. W. (1978). New properties of rabbit retinal ganglion cells. *J Physiol*, 276, 257-276.
- Chaudhuri, A., Hallett, P. E., & Parker, J. A. (1983). Aspheric curvatures, refractive indices and chromatic aberration for the rat eye. *Vision Res*, 23(12), 1351-1363.
- Chen, T. C., Cense, B., Pierce, M. C., Nassif, N., Park, B. H., Yun, S. H., . . . de Boer, J. F. (2005). Spectral domain optical coherence tomography: ultra-high speed, ultra-

- high resolution ophthalmic imaging. *Arch Ophthalmol*, 123(12), 1715-1720. doi: 10.1001/archophth.123.12.1715
- Cohen, L. B. (1973). Changes in neuron structure during action potential propagation and synaptic transmission. *Physiol Rev*, 53(2), 373-418.
- Connaughton, V. (1995). Glutamate and Glutamate Receptors in the Vertebrate Retina. In H. Kolb, E. Fernandez & R. Nelson (Eds.), *Webvision: The Organization of the Retina and Visual System*. Salt Lake City (UT).
- Costa, R. A., Skaf, M., Melo, L. A., Jr., Calucci, D., Cardillo, J. A., Castro, J. C., . . . Wojtkowski, M. (2006). Retinal assessment using optical coherence tomography. *Prog Retin Eye Res*, 25(3), 325-353. doi: 10.1016/j.preteyeres.2006.03.001
- Cringle, S. J., & Yu, D. Y. (2010). Oxygen supply and consumption in the retina: implications for studies of retinopathy of prematurity. *Doc Ophthalmol*, 120(1), 99-109. doi: 10.1007/s10633-009-9197-2
- Dacey, D. M. (1993). The mosaic of midget ganglion cells in the human retina. *J Neurosci*, 13(12), 5334-5355.
- De Schaepdrijver, L., Simoons, P., Lauwers, H., & De Geest, J. P. (1989). Retinal vascular patterns in domestic animals. *Res Vet Sci*, 47(1), 34-42.
- DeHoog, E., & Schwiegerling, J. (2009). Fundus camera systems: a comparative analysis. *Appl Opt*, 48(2), 221-228.
- Delaey, C., & Van De Voorde, J. (2000). Regulatory mechanisms in the retinal and choroidal circulation. *Ophthalmic Res*, 32(6), 249-256. doi: 55622
- DeRouck, A. F. (2006). History of the Electroretinogram. In J. R. Heckenlively & G. B. Arden (Eds.), *Principle and practice of clinical electrophysiology of vision* (pp. 3-10): MIT press.
- Dong, C. J., Agey, P., & Hare, W. A. (2004). Origins of the electroretinogram oscillatory potentials in the rabbit retina. *Vis Neurosci*, 21(4), 533-543. doi: 10.1017/S0952523804214043
- Dowling, J. E., & Boycott, B. B. (1966). Organization of the primate retina: electron microscopy. *Proc R Soc Lond B Biol Sci*, 166(1002), 80-111.
- Dumskyj, M. J., Eriksen, J. E., Dore, C. J., & Kohner, E. M. (1996). Autoregulation in the human retinal circulation: assessment using isometric exercise, laser Doppler velocimetry, and computer-assisted image analysis. *Microvasc Res*, 51(3), 378-392. doi: 10.1006/mvre.1996.0034
- Falk, Gertrude, & Shiells, Richard. (2006). Synaptic Transmission: Sensitivity Control Mechanisms. In J. R. Heckenlively & G. B. Arden (Eds.), *Principle and practice of clinical electrophysiology of vision* (pp. 79-92): MIT press.
- Fercher, A. F. (2010). Optical coherence tomography - development, principles, applications. *Z Med Phys*, 20(4), 251-276. doi: 10.1016/j.zemedi.2009.11.002
- Frishman, Laura J. (2006). Origins of the Electroretinogram. In J. R. Heckenlively & G. B. Arden (Eds.), *Principles and practice of clinical electrophysiology of vision* (2 ed., pp. 139-184): MIT press.
- Frostig, R. D., Lieke, E. E., Ts'o, D. Y., & Grinvald, A. (1990). Cortical functional architecture and local coupling between neuronal activity and the

- microcirculation revealed by in vivo high-resolution optical imaging of intrinsic signals. *Proc Natl Acad Sci U S A*, 87(16), 6082-6086.
- Fu, Y. (1995). Phototransduction in Rods and Cones. In H. Kolb, E. Fernandez & R. Nelson (Eds.), *Webvision: The Organization of the Retina and Visual System*. Salt Lake City (UT).
- Gallego, A. (1971). Horizontal and amacrine cells in the mammal's retina. *Vision Res, Suppl 3*, 33-50.
- Gliss, C., Parel, J. M., Flynn, J. T., Pratisto, H., & Niederer, P. (2004). Toward a miniaturized fundus camera. *J Biomed Opt*, 9(1), 126-131. doi: 10.1117/1.1631313
- Goldey, G. J., Roumis, D. K., Glickfeld, L. L., Kerlin, A. M., Reid, R. C., Bonin, V., . . . Andermann, M. L. (2014). Removable cranial windows for long-term imaging in awake mice. *Nat Protoc*, 9(11), 2515-2538. doi: 10.1038/nprot.2014.165
- Goncharov, A. V., & Dainty, C. (2007). Wide-field schematic eye models with gradient-index lens. *J Opt Soc Am A Opt Image Sci Vis*, 24(8), 2157-2174.
- Grinvald, A., Bonhoeffer, T., Vanzetta, I., Pollack, A., Aloni, E., Ofri, R., & Nelson, D. (2004). High-resolution functional optical imaging: from the neocortex to the eye. *Ophthalmol Clin North Am*, 17(1), 53-67. doi: 10.1016/j.ohc.2003.12.003
- Grinvald, A., Frostig, R. D., Lieke, E., & Hildesheim, R. (1988). Optical imaging of neuronal activity. *Physiol Rev*, 68(4), 1285-1366.
- Grinvald, A., Frostig, R. D., Siegel, R. M., & Bartfeld, E. (1991). High-resolution optical imaging of functional brain architecture in the awake monkey. *Proc Natl Acad Sci U S A*, 88(24), 11559-11563.
- Grinvald, A., Lieke, E., Frostig, R. D., Gilbert, C. D., & Wiesel, T. N. (1986). Functional architecture of cortex revealed by optical imaging of intrinsic signals. *Nature*, 324(6095), 361-364. doi: 10.1038/324361a0
- Grunert, Paul R. Martin and Ulrike. (2003). Ganglion Cells in Mammalian Retinae. In J. S. W. Leo M. Chalupa (Ed.), *The Visual Neurosciences*.
- Guite, P., & Lachapelle, P. (1990). The effect of 2-amino-4-phosphonobutyric acid on the oscillatory potentials of the electroretinogram. *Doc Ophthalmol*, 75(2), 125-133.
- Hanazono, G., Tsunoda, K., Kazato, Y., Tsubota, K., & Tanifuji, M. (2008). Evaluating neural activity of retinal ganglion cells by flash-evoked intrinsic signal imaging in macaque retina. *Invest Ophthalmol Vis Sci*, 49(10), 4655-4663. doi: 10.1167/iovs.08-1936
- Hanazono, G., Tsunoda, K., Shinoda, K., Tsubota, K., Miyake, Y., & Tanifuji, M. (2007). Intrinsic signal imaging in macaque retina reveals different types of flash-induced light reflectance changes of different origins. *Invest Ophthalmol Vis Sci*, 48(6), 2903-2912. doi: 10.1167/iovs.06-1294
- Hare, W. A., & Ton, H. (2002). Effects of APB, PDA, and TTX on ERG responses recorded using both multifocal and conventional methods in monkey. Effects of APB, PDA, and TTX on monkey ERG responses. *Doc Ophthalmol*, 105(2), 189-222.
- Heckenlively, John R., & Arden, Geoffrey B. (2006). Origins of slow electrophysiological components *Principle and practice of clinical electrophysiology of vision* (pp. 121-234): MIT press.

- Hernandez, V., Albin, T., Lee, W., Rowan, C., Nankivil, D., Arrieta, E., & Parel, J. M. (2012). A portable, contact animal fundus imaging system based on RoI's GRIN lenses. *Vet Ophthalmol*, *15*(3), 141-144. doi: 10.1111/j.1463-5224.2011.00935.x
- Hillman, E. M. (2014). Coupling mechanism and significance of the BOLD signal: a status report. *Annu Rev Neurosci*, *37*, 161-181. doi: 10.1146/annurev-neuro-071013-014111
- Hirohara, Y., Mihashi, T., Kanda, H., Morimoto, T., Miyoshi, T., Wolffsohn, J. S., & Fujikado, T. (2013). Optical imaging of retina in response to grating stimuli in cats. *Exp Eye Res*, *109*, 1-7. doi: 10.1016/j.exer.2013.01.007
- Hood, D. C., Bach, M., Brigell, M., Keating, D., Kondo, M., Lyons, J. S., . . . International Society For Clinical Electrophysiology of, Vision. (2012). ISCEV standard for clinical multifocal electroretinography (mfERG) (2011 edition). *Doc Ophthalmol*, *124*(1), 1-13. doi: 10.1007/s10633-011-9296-8
- Hood, D. C., Odel, J. G., Chen, C. S., & Winn, B. J. (2003). The multifocal electroretinogram. *J Neuroophthalmol*, *23*(3), 225-235.
- Horiguchi, M., Suzuki, S., Kondo, M., Tanikawa, A., & Miyake, Y. (1998). Effect of glutamate analogues and inhibitory neurotransmitters on the electroretinograms elicited by random sequence stimuli in rabbits. *Invest Ophthalmol Vis Sci*, *39*(11), 2171-2176.
- Hughes, A. (1971). Topographical relationships between the anatomy and physiology of the rabbit visual system. *Doc Ophthalmol*, *30*, 33-159.
- Hughes, A. (1979). A schematic eye for the rat. *Vision Res*, *19*(5), 569-588.
- Inomata, K., Tsunoda, K., Hanazono, G., Kazato, Y., Shinoda, K., Yuzawa, M., . . . Miyake, Y. (2008). Distribution of retinal responses evoked by transscleral electrical stimulation detected by intrinsic signal imaging in macaque monkeys. *Invest Ophthalmol Vis Sci*, *49*(5), 2193-2200. doi: 10.1167/iovs.07-0727
- Ivo Vanzetta, Thomas Deneux, Amiram Grinvald. (2014). High-Resolution Wide-Field Optical Imaging of Microvascular Characteristics: From the Neocortex to the Eye. In H. M. Mingrui Zhao, Theodore H. Schwartz (Ed.), *Neurovascular Coupling Methods* (Vol. 88, pp. 123-159): Springer New York.
- Izhaky, D., Nelson, D. A., Burgansky-Eliash, Z., & Grinvald, A. (2009). Functional imaging using the retinal function imager: direct imaging of blood velocity, achieving fluorescein angiography-like images without any contrast agent, qualitative oximetry, and functional metabolic signals. *Jpn J Ophthalmol*, *53*(4), 345-351. doi: 10.1007/s10384-009-0689-0
- Johnson, E. C., Guo, Y., Cepurna, W. O., & Morrison, J. C. (2009). Neurotrophin roles in retinal ganglion cell survival: lessons from rat glaucoma models. *Exp Eye Res*, *88*(4), 808-815. doi: 10.1016/j.exer.2009.02.004
- Kiernan, D. F., Mieler, W. F., & Hariprasad, S. M. (2010). Spectral-domain optical coherence tomography: a comparison of modern high-resolution retinal imaging systems. *Am J Ophthalmol*, *149*(1), 18-31. doi: 10.1016/j.ajo.2009.08.037
- Knapp, A. G., & Schiller, P. H. (1984). The contribution of on-bipolar cells to the electroretinogram of rabbits and monkeys. A study using 2-amino-4-phosphonobutyrate (APB). *Vision Res*, *24*(12), 1841-1846.

- Kolb, H. (1970). Organization of the outer plexiform layer of the primate retina: electron microscopy of Golgi-impregnated cells. *Philos Trans R Soc Lond B Biol Sci*, 258(823), 261-283.
- Kolb, H. (1995a). Inner Plexiform Layer. In H. Kolb, E. Fernandez & R. Nelson (Eds.), *Webvision: The Organization of the Retina and Visual System*. Salt Lake City (UT).
- Kolb, H. (1995b). Neurotransmitters in the Retina. In H. Kolb, E. Fernandez & R. Nelson (Eds.), *Webvision: The Organization of the Retina and Visual System*. Salt Lake City (UT).
- Kolb, H. (1995c). Photoreceptors. In H. Kolb, E. Fernandez & R. Nelson (Eds.), *Webvision: The Organization of the Retina and Visual System*. Salt Lake City (UT).
- Kolb, H. (1995d). Roles of Amacrine Cells. In H. Kolb, E. Fernandez & R. Nelson (Eds.), *Webvision: The Organization of the Retina and Visual System*. Salt Lake City (UT).
- Kolb, H., Nelson, R., & Mariani, A. (1981). Amacrine cells, bipolar cells and ganglion cells of the cat retina: a Golgi study. *Vision Res*, 21(7), 1081-1114.
- Lamb, Marie E. Burns and Trevor D. (2003). Visual Transduction by Rod and Cone Photoreceptors. In J. S. W. Leo M. Chalupa (Ed.), *The Visual Neurosciences* (Vol. 1).
- Leure-Dupree, A. E. (1974). Observations on the synaptic organization of the retina of the albino rat: a light and electron microscopic study. *J Comp Neurol*, 153(2), 149-178. doi: 10.1002/cne.901530203
- LeVere, T. E. (1978). The primary visual system of the rat: A primer of its anatomy. *Physiological Psychology*, 6( 2), 142–169. doi: 10.3758/BF03326707
- Levinger, E., Zemel, E., & Perlman, I. (2012). The effects of excitatory amino acids and their transporters on function and structure of the distal retina in albino rabbits. *Doc Ophthalmol*. doi: 10.1007/s10633-012-9354-x
- Li, Y. C., Luo, J. M., Lu, R. W., Liu, K. M., Levy, A. M., & Yao, X. C. (2012). Dynamic intrinsic optical signal monitoring of electrically stimulated inner retinal neural response. *J Mod Opt*, 59(11). doi: 10.1080/09500340.2012.687464
- Li, Y. C., Strang, C., Amthor, F. R., Liu, L., Li, Y. G., Zhang, Q. X., . . . Yao, X. C. (2010). Parallel optical monitoring of visual signal propagation from the photoreceptors to the inner retina layers. *Opt Lett*, 35(11), 1810-1812. doi: 10.1364/OL.35.001810
- Li, Y. G., Zhang, Q. X., Liu, L., Amthor, F. R., & Yao, X. C. (2010). High spatiotemporal resolution imaging of fast intrinsic optical signals activated by retinal flicker stimulation. *Opt Express*, 18(7), 7210-7218. doi: 10.1364/OE.18.007210
- Lindauer, U., Leithner, C., Kaasch, H., Rohrer, B., Foddis, M., Fuchtemeier, M., . . . Dirnagl, U. (2010). Neurovascular coupling in rat brain operates independent of hemoglobin deoxygenation. *J Cereb Blood Flow Metab*, 30(4), 757-768. doi: 10.1038/jcbfm.2009.259
- MacNeil, M. A., & Masland, R. H. (1998). Extreme diversity among amacrine cells: implications for function. *Neuron*, 20(5), 971-982.
- Malonek, D., Dirnagl, U., Lindauer, U., Yamada, K., Kanno, I., & Grinvald, A. (1997). Vascular imprints of neuronal activity: relationships between the dynamics of

- cortical blood flow, oxygenation, and volume changes following sensory stimulation. *Proc Natl Acad Sci U S A*, 94(26), 14826-14831.
- Malonek, D., & Grinvald, A. (1996). Interactions between electrical activity and cortical microcirculation revealed by imaging spectroscopy: implications for functional brain mapping. *Science*, 272(5261), 551-554.
- Mariani, A. P. (1981). A diffuse, invaginating cone bipolar cell in primate retina. *J Comp Neurol*, 197(4), 661-671. doi: 10.1002/cne.901970408
- Mariani, A. P. (1984). Bipolar cells in monkey retina selective for the cones likely to be blue-sensitive. *Nature*, 308(5955), 184-186.
- Martin, C., Martindale, J., Berwick, J., & Mayhew, J. (2006). Investigating neural-hemodynamic coupling and the hemodynamic response function in the awake rat. *Neuroimage*, 32(1), 33-48. doi: 10.1016/j.neuroimage.2006.02.021
- Masland, R. H. (2012). The tasks of amacrine cells. *Vis Neurosci*, 29(1), 3-9.
- Massey, S. C., & Miller, R. F. (1988). Glutamate receptors of ganglion cells in the rabbit retina: evidence for glutamate as a bipolar cell transmitter. *J Physiol*, 405, 635-655.
- Massey, S. C., Redburn, D. A., & Crawford, M. L. (1983). The effects of 2-amino-4-phosphonobutyric acid (APB) on the ERG and ganglion cell discharge of rabbit retina. *Vision Res*, 23(12), 1607-1613.
- McCulloch, D. L., Marmor, M. F., Brigell, M. G., Hamilton, R., Holder, G. E., Tzekov, R., & Bach, M. (2015). ISCEV Standard for full-field clinical electroretinography (2015 update). *Doc Ophthalmol*, 130(1), 1-12. doi: 10.1007/s10633-014-9473-7
- Mihashi, T., Okawa, Y., Miyoshi, T., Kitaguchi, Y., Hirohara, Y., & Fujikado, T. (2011). Comparing retinal reflectance changes elicited by transcorneal electrical retinal stimulation with those of optic chiasma stimulation in cats. *Jpn J Ophthalmol*, 55(1), 49-56. doi: 10.1007/s10384-010-0906-x
- Mosinger, J. L., & Altschuler, R. A. (1985). Aspartate aminotransferase-like immunoreactivity in the guinea pig and monkey retinas. *J Comp Neurol*, 233(2), 255-268. doi: 10.1002/cne.902330207
- Naderian, A., Bussieres, L., Thomas, S., Lesage, F., & Casanova, C. (2017). Cellular origin of intrinsic optical signals in the rabbit retina. *Vision Res*, 137, 40-49. doi: 10.1016/j.visres.2017.04.015
- Narahashi, T., Moore, J. W., & Scott, W. R. (1964). Tetrodotoxin Blockage of Sodium Conductance Increase in Lobster Giant Axons. *J Gen Physiol*, 47, 965-974.
- Nelson, D. A., Krupsky, S., Pollack, A., Aloni, E., Belkin, M., Vanzetta, I., . . . Grinvald, A. (2005). Special report: Noninvasive multi-parameter functional optical imaging of the eye. *Ophthalmic Surg Lasers Imaging*, 36(1), 57-66.
- Nelson, R. (1995). Visual Responses of Ganglion Cells. In H. Kolb, E. Fernandez & R. Nelson (Eds.), *Webvision: The Organization of the Retina and Visual System*. Salt Lake City (UT).
- Nelson, R., & Connaughton, V. (1995). Bipolar Cell Pathways in the Vertebrate Retina. In H. Kolb, E. Fernandez & R. Nelson (Eds.), *Webvision: The Organization of the Retina and Visual System*. Salt Lake City (UT).

- Noell, W. K. (1954). The origin of the electroretinogram. *Am J Ophthalmol*, 38(1:2), 78-90.
- Perlman, I. (1995). The Electroretinogram: ERG. In H. Kolb, E. Fernandez & R. Nelson (Eds.), *Webvision: The Organization of the Retina and Visual System*. Salt Lake City (UT).
- Perlman, Ido, Kolb, Helga, & Nelson, Ralph. (2003). Anatomy, Circuitry, and Physiology of Vertebrate Horizontal Cells. In J. S. W. Leo M. Chalupa (Ed.), *The Visual Neurosciences*.
- Prince, Jack H. (1964). *The Rabbit in Eye Research* (J. H. Prince Ed.).
- Prince, Jerry L., & Links, Jonathan M. (2006). *Medical imaging signals and systems*: Pearson Education, Inc. .
- Purves D, Augustine GJ, Fitzpatrick D, et al. (2001). Neuroscience. In S. (MA) (Ed.), (2nd edition ed.): Sinauer Associates.
- Roe, A. W. (2007). Long-term optical imaging of intrinsic signals in anesthetized and awake monkeys. *Appl Opt*, 46(10), 1872-1880.
- Schallek, J. B., McLellan, G. J., Viswanathan, S., & Ts'o, D. Y. (2012). Retinal intrinsic optical signals in a cat model of primary congenital glaucoma. *Invest Ophthalmol Vis Sci*, 53(4), 1971-1981. doi: 10.1167/iops.11-8299
- Schallek, J., Kardon, R., Kwon, Y., Abramoff, M., Soliz, P., & Ts'o, D. (2009). Stimulus-evoked intrinsic optical signals in the retina: pharmacologic dissection reveals outer retinal origins. *Invest Ophthalmol Vis Sci*, 50(10), 4873-4880. doi: 10.1167/iops.08-3291
- Schallek, J., Li, H., Kardon, R., Kwon, Y., Abramoff, M., Soliz, P., & Ts'o, D. (2009). Stimulus-evoked intrinsic optical signals in the retina: spatial and temporal characteristics. *Invest Ophthalmol Vis Sci*, 50(10), 4865-4872. doi: 10.1167/iops.08-3290
- Schallek, J., & Ts'o, D. (2011). Blood contrast agents enhance intrinsic signals in the retina: evidence for an underlying blood volume component. *Invest Ophthalmol Vis Sci*, 52(3), 1325-1335. doi: 10.1167/iops.10-5215
- Schiller, P. H., Sandell, J. H., & Maunsell, J. H. (1986). Functions of the ON and OFF channels of the visual system. *Nature*, 322(6082), 824-825. doi: 10.1038/322824a0
- Schmidt, M., Giessl, A., Laufs, T., Hankeln, T., Wolfrum, U., & Burmester, T. (2003). How does the eye breathe? Evidence for neuroglobin-mediated oxygen supply in the mammalian retina. *J Biol Chem*, 278(3), 1932-1935. doi: 10.1074/jbc.M209909200
- Sha, O., & Kwong, W.H. (2007). Postnatal Developmental Changes of Vitreous and Lens Volumes in Sprague-Dawley Rats. *Neuroembryology and Aging*, 4(4), 183-188. doi: 10.1159/000118928
- Sharp, P. F., & Manivannan, A. (1997). The scanning laser ophthalmoscope. *Phys Med Biol*, 42(5), 951-966.
- Sieving, Paul A. (2006). Electrical Signals of the Retina and Visual Cortex. In T. D. Duane, W. Tasman & E. A. Jaeger (Eds.), *Duane's ophthalmology*.

- Sillman, A. J., Ito, H., & Tomita, T. (1969). Studies on the mass receptor potential of the isolated frog retina. II. On the basis of the ionic mechanism. *Vision Res*, 9(12), 1443-1451.
- Slaughter, M. M., & Miller, R. F. (1981). 2-amino-4-phosphonobutyric acid: a new pharmacological tool for retina research. *Science*, 211(4478), 182-185.
- Srinivasan, V. J., Wojtkowski, M., Fujimoto, J. G., & Duker, J. S. (2006). In vivo measurement of retinal physiology with high-speed ultrahigh-resolution optical coherence tomography. *Opt Lett*, 31(15), 2308-2310.
- Stepnoski, R. A., LaPorta, A., Racchia-Behling, F., Blonder, G. E., Slusher, R. E., & Kleinfeld, D. (1991). Noninvasive detection of changes in membrane potential in cultured neurons by light scattering. *Proc Natl Acad Sci U S A*, 88(21), 9382-9386.
- Sugiyama, K., Bacon, D. R., Morrison, J. C., & Van Buskirk, E. M. (1992). Optic nerve head microvasculature of the rabbit eye. *Invest Ophthalmol Vis Sci*, 33(7), 2251-2261.
- Thoreson, W. B., & Witkovsky, P. (1999). Glutamate receptors and circuits in the vertebrate retina. *Prog Retin Eye Res*, 18(6), 765-810.
- Tornquist, P., & Alm, A. (1979). Retinal and choroidal contribution to retinal metabolism in vivo. A study in pigs. *Acta Physiol Scand*, 106(3), 351-357. doi: 10.1111/j.1748-1716.1979.tb06409.x
- Trenholm, S., Borowska, J., Zhang, J., Hoggarth, A., Johnson, K., Barnes, S., . . . Awatramani, G. B. (2012). Intrinsic oscillatory activity arising within the electrically coupled All amacrine-ON cone bipolar cell network is driven by voltage-gated Na<sup>+</sup> channels. *J Physiol*, 590(10), 2501-2517. doi: 10.1113/jphysiol.2011.225060
- Ts'o, D., Schallek, J., Kwon, Y., Kardon, R., Abramoff, M., & Soliz, P. (2009). Noninvasive functional imaging of the retina reveals outer retinal and hemodynamic intrinsic optical signal origins. *Jpn J Ophthalmol*, 53(4), 334-344. doi: 10.1007/s10384-009-0687-2
- Ts'o, D. Y., Frostig, R. D., Lieke, E. E., & Grinvald, A. (1990). Functional organization of primate visual cortex revealed by high resolution optical imaging. *Science*, 249(4967), 417-420.
- Tsunoda, K., Hanazono, G., Inomata, K., Kazato, Y., Suzuki, W., & Tanifuji, M. (2009). Origins of retinal intrinsic signals: a series of experiments on retinas of macaque monkeys. *Jpn J Ophthalmol*, 53(4), 297-314. doi: 10.1007/s10384-009-0686-3
- Tsunoda, K., Oguchi, Y., Hanazono, G., & Tanifuji, M. (2004). Mapping cone- and rod-induced retinal responsiveness in macaque retina by optical imaging. *Invest Ophthalmol Vis Sci*, 45(10), 3820-3826. doi: 10.1167/iovs.04-0394
- Vanzetta, I., & Grinvald, A. (2008). Coupling between neuronal activity and microcirculation: implications for functional brain imaging. *HFSP J*, 2(2), 79-98. doi: 10.2976/1.2889618
- Vidal-Sanz, M., Salinas-Navarro, M., Nadal-Nicolas, F. M., Alarcon-Martinez, L., Valiente-Soriano, F. J., de Imperial, J. M., . . . Villegas-Perez, M. P. (2012). Understanding glaucomatous damage: anatomical and functional data from ocular hypertensive rodent retinas. *Prog Retin Eye Res*, 31(1), 1-27. doi: 10.1016/j.preteyeres.2011.08.001

- Wang, B., & Yao, X. (2016). In vivo intrinsic optical signal imaging of mouse retinas. *Proc SPIE Int Soc Opt Eng*, 9693. doi: 10.1117/12.2212810
- Wangsa-Wirawan, N. D., & Linsenmeier, R. A. (2003). Retinal oxygen: fundamental and clinical aspects. *Arch Ophthalmol*, 121(4), 547-557. doi: 10.1001/archophth.121.4.547
- Ward, M. M., Jobling, A. I., Kalloniatis, M., & Fletcher, E. L. (2005). Glutamate uptake in retinal glial cells during diabetes. *Diabetologia*, 48(2), 351-360. doi: 10.1007/s00125-004-1639-5
- Webb, R. H., & Hughes, G. W. (1981). Scanning laser ophthalmoscope. *IEEE Trans Biomed Eng*, 28(7), 488-492. doi: 10.1109/TBME.1981.324734
- Yamada, E. (1969). Some structural features of the fovea centralis in the human retina. *Arch Ophthalmol*, 82(2), 151-159.
- Yannuzzi, L. A., Ober, M. D., Slakter, J. S., Spaide, R. F., Fisher, Y. L., Flower, R. W., & Rosen, R. (2004). Ophthalmic fundus imaging: today and beyond. *Am J Ophthalmol*, 137(3), 511-524. doi: 10.1016/j.ajo.2003.12.035
- Yao, X. C. (2009). Intrinsic optical signal imaging of retinal activation. *Jpn J Ophthalmol*, 53(4), 327-333. doi: 10.1007/s10384-009-0685-4
- Yu, D. Y., & Cringle, S. J. (2004). Low oxygen consumption in the inner retina of the visual streak of the rabbit. *Am J Physiol Heart Circ Physiol*, 286(1), H419-423. doi: 10.1152/ajpheart.00643.2003
- Zepeda, A., Arias, C., & Sengpiel, F. (2004). Optical imaging of intrinsic signals: recent developments in the methodology and its applications. *J Neurosci Methods*, 136(1), 1-21. doi: 10.1016/j.jneumeth.2004.02.025
- Zhang, Q. X., Zhang, Y., Lu, R. W., Li, Y. C., Pittler, S. J., Kraft, T. W., & Yao, X. C. (2012). Comparative intrinsic optical signal imaging of wild-type and mutant mouse retinas. *Opt Express*, 20(7), 7646-7654. doi: 10.1364/OE.20.007646